TAMPEREEN TEKNILLINEN YLIOPISTO
TAMPERE UNIVERSITY OF TECHNOLOGY

Jussi Turkka

Aspects of Knowledge Mining on Minimizing Drive Tests in Self-organizing Cellular Networks

Julkaisu 1229 • Publication 1229

Tampere 2014

Tampereen teknillinen yliopisto. Julkaisu 1229
Tampere University of Technology. Publication 1229

Jussi Turkka

Aspects of Knowledge Mining on Minimizing Drive Tests in Self-organizing Cellular Networks

Thesis for the degree of Doctor of Science in Technology to be presented with due permission for public examination and criticism in Tietotalo Building, Auditorium TB109, at Tampere University of Technology, on the 22nd of August 2014, at 12 noon.

Tampereen teknillinen yliopisto - Tampere University of Technology
Tampere 2014

ISBN 978-952-15-3332-7 (printed)
ISBN 978-952-15-3401-0 (PDF)
ISSN 1459-2045

Doctoral advisor

Professor Jukka Lempiäinen

Department of Communications Engineering

Tampere University of Technology

Tampere, Finland

Second advisor

Professor Tapani Ristaniemi

Department of Mathematical Information Technology

University of Jyväskylä

Jyväskylä, Finland

Pre-examiner

Assistant Director, Ph.D. Seppo Hämäläinen

Ooredoo Group

Doha, Qatar

Pre-examiner and opponent

Head of the Institute, Professor Petri Mähönen

Institute for Networked Systems

RWTH Aachen University

Aachen, Germany

Opponent

Head of Department, Professor Riku Jäntti

Department of Communications and Networking

Aalto University

Helsinki, Finland

Abstract

The demand for mobile data traffic is about to explode and this drives operators to find ways to further increase the offered capacity in their networks. If networks are deployed in the traditional way, this traffic explosion will be addressed by increasing the number of network elements significantly. This is expected to increase the costs and the complexity of planning, operating and optimizing the networks. To ensure effective and cost-efficient operations, a higher degree of automation and self-organization is needed in the next generation networks. For this reason, the concept of self-organizing networks was introduced in LTE covering multitude of use cases. This was specifically done in the areas of self-configuration, self-optimization and self-healing of networks. From an operator's perspective, automated collection and analysis of field measurements while complementing the traditional drive test campaigns is one of the top use cases that can provide significant cost savings in self-organizing networks.

This thesis studies the Minimization of Drive Tests in self-organizing cellular networks from three different aspects. The first aspect is network operations, and particularly the network fault management process, as the traditional drive tests are often conducted for troubleshooting purposes. The second aspect is network functionality, and particularly the technical details about the specified measurement and signaling procedures in different network elements that are needed for automating the collection of the field measurement data. The third aspect concerns the analysis of the measurement databases that is a process used for increasing the degree of automation and self-awareness in the networks, and particularly the mathematical means for autonomously finding meaningful patterns of knowledge from huge amounts of data. Although the above mentioned technical areas have been widely discussed in previous literature, it has been done separately and only a few papers discuss how for example, knowledge mining is employed for processing field measurement data in a way that minimizes the drive tests in self-organizing LTE networks.

The objective of the thesis is to use well known knowledge mining principles to develop novel self-healing and self-optimization algorithms. These algorithms analyze MDT databases to detect coverage holes, sleeping cells and other geographical areas of anomalous network behavior. The results of the research suggest that by employing knowledge mining in processing the MDT databases, one can acquire knowledge for discriminating between different network problems and detecting anomalous network behavior. For example, downlink coverage optimization is enhanced by classifying RLF reports into coverage, interference and handover problems. Moreover, by incorporating a normalized power headroom report with the MDT

reports, better discrimination between uplink coverage problems and the parameterization problems is obtained. Knowledge mining is also used to detect sleeping cells by means of supervised and unsupervised learning. The detection framework is based on a novel approach where diffusion mapping is used to learn about network behavior in its healthy state. The sleeping cells are detected by observing an increase in the number of anomalous reports associated with a certain cell. The association is formed by correlating the geographical location of anomalous reports with the estimated dominance areas of the cells.

Moreover, RF fingerprint positioning of the MDT reports is studied and the results suggest that RF fingerprinting can provide a quite detailed location estimation in dense heterogeneous networks. In addition, self-optimization of the mobility state estimation parameters is studied in heterogeneous LTE networks and the results suggest that by gathering MDT measurements and constructing statistical velocity profiles, MSE parameters can be adjusted autonomously, thus resulting in reasonably good classification accuracy.

The overall outcome of the thesis is as follows. By automating the classification of the measurement reports between certain problems, network engineers can acquire knowledge about the root causes of the performance degradation in the networks. This saves time and resources and results in a faster decision making process. Due to the faster decision making process the duration of network breaks become shorter and the quality of the network is improved. By taking into account the geographical locations of the anomalous field measurements in the network performance analysis, finer granularity for estimating the location of the problem areas can be achieved. This can further improve the operational decision making that guides the corresponding actions for example, where to start the network optimization. Moreover, by automating the time and resource consuming task of tuning the mobility state estimation parameters, operators can enhance the mobility performance of the high velocity UEs in heterogeneous radio networks in a cost-efficient and backward compatible manner.

Preface

The research work for the thesis was done during between 2009 and 2013 when I had an opportunity to work at Magister Solutions Ltd. Honestly speaking, without the encouraging and innovative working environment, I would not have had the dedication and energy for accomplishing this scientific excursion alongside my daily duties. I would like to thank all my Magister colleagues at Tampere, Jyväskylä and Helsinki, and especially Dr. Janne Kurjenniemi (CEO), Dr. Timo Nihtilä, Dr. Jani Puttonen and Dr. Kari Aho.

I would like to express my sincere appreciation to my doctoral advisors, Professor Jukka Lempiäinen from the Department of Communications Engineering at Tampere University of Technology and Professor Tapani Ristaniemi from the Department of Mathematical Information Technology at the University of Jyväskylä, for the opportunity to work under their guidance. I want to dedicate special thanks to Professor Amir Averbuch from the School of Computer Science at Tel-Aviv University and Dr. Gil David for introducing me to the concept of anomaly detection. Moreover, I would also like to thank all of my co-authors, Dr. Olli Alanen, Mr. Tero Henttonen, Mr. Fedor Chernogorov, Mr. Kimmo Brigatti and Mr. Andreas Lobinger, for making valuable contributions to the publications that this thesis is compiled from.

In addition to the support from the Department of Communications Engineering (Thank You Prof. Mikko Valkama and Prof. Markku Renfors), the work was financially supported by the University of Jyväskylä, the Tampere Doctoral Program in Information Science and Engineering (TISE), Tekniikan edistämissäätiö (TES), Elektroniikka Insinöörien Seura (EIS) and the Ulla Tuominen Foundation.

Moreover, I want to thank the doctors and former members of the Radio Network Group at Tampere University of Technology, Dr. Jarno Niemelä, Dr. Jakub Borkowski, Dr. Panu Lähdekorpi, Dr. Tero Isotalo, Mr. Muhammed Ushan Sheik and Mr. Teemu Pesu, for all the innovative discussions, feedback and criticism that they gave me when it was needed and seen appropriate. In addition, I want to thank Mr. Jaakko Penttinen for his views and hands-on experience about manual drive tests in the field of network troubleshooting. I am also grateful for the various informal tea-table discussions with Mr. Jukka Talvitie, Mr. Toni Levanen, Mr. Tero Kuosmanen, Mr. Kari Hämäläinen, and many former co-workers, senior co-workers and line managers at Nokia, Nokia Siemens Networks and Renesas Mobile Europe Ltd.

I want to thank my parents Tuomo and Ulla, and my brothers, Jaakko, Joonas and Jesse, for their support and the time we have spent together at Jurkkola over the years. Family is the most important thing that one can have throughout life time. Finally, I want to thank my beloved wife Orvokki for all the love and care at home, and our young offspring Ossi, for spontaneously re-organizing my papers and my thoughts from time to time while I was writing the thesis. It has been fun.

Tampere, Finland
August 2014.

Jussi Taneli Turkka

Table of Contents

List of Publications

This thesis is a compilation of the following publications

[P1] Turkka J. and Lobinger A., "Non-regular Layout for Cellular Network System Simulations", published in *Proceeding of 21st IEEE International Symposium on Personal, Indoor and Mobile Radio Communications (PIMRC)*, September 2010, Istanbul, Turkey.

[P2] Puttonen J., Turkka J., Alanen O. and Kurjenniemi, "Coverage Optimization for Minimization of Drive Tests in LTE with Extended RLF Reporting", published in *Proceeding of 21st IEEE International Symposium on Personal, Indoor and Mobile Radio Communications (PIMRC)*, September 2010, Istanbul, Turkey.

[P3] Turkka J. and Puttonen J., "Using LTE Power Headroom Report for Coverage Optimization", published in *Proceeding of 72nd IEEE Vehicular Technology Conference (VTC-fall)*, September 2011, San Francisco, United States.

[P4] Chernogorov F., Turkka J., Ristaniemi T. and Averbuch A.," Detection of Sleeping Cells in LTE Networks Using Diffusion Maps", published in *Proceeding of International Workshop on Self-Organizing Networks (IWSON)*, May 2011, Budapest, Hungary.

[P5] Turkka J., Chernogorov F., Brigatti K., Ristaniemi T. and Lempiäinen J., "An Approach for Network Outage Detection from Drive Testing Databases", published in *Journal of Computer Networks and Communications*, vol. 2012, Article ID: 163184, 13 pages, December 2012, doi:10.1155/2012/163184.

[P6] Mondal R., Turkka J., Ristaniemi T. and Henttonen T, "Positioning in Heterogeneous Small Cell Networks using MDT RF Fingerprints", published in *Proceedings of the First IEEE International Black Sea Conference on Communications and Networking*, July 2013, Batumi, Georgia.

[P7] Mondal R., Turkka J., Ristaniemi T. and Henttonen T., "Performance Evaluation of MDT Assisted LTE RF Fingerprinting Framework", published in *Proceedings of 7th International Conference on Mobile Computing and Ubiquitous Networking (ICMU2014)*, January 2014, Singapore.

[P8] Turkka J., Henttonen T. and Ristaniemi T., "Self-optimization of LTE Mobility State Estimation Thresholds", published in *Proceeding of IEEE International Conference on Wireless Communications and Networking, Workshop on Self-Organizing Networks (SONET)*, April 2014, Istanbul, Turkey.

List of Abbreviations

5G	5th Generation of Mobile Networks
3GPP	Third Generation Partnership Project
ANR	Automatic Neighbor Relations
ARPU	Average Revenue Per User
BS	Base Station
BSC	Base Station Controller
CAPEX	Capital Expenditures
CART	Classification And Regression Trees
CCO	Coverage and Capacity Optimization
CGI	Cell Global Identification
CN	Core Network
CRS	Cell-specific Reference Symbols
CS	Circuit Switched
DM	Diffusion Map
eNB	Evolved NodeB
EPC	Evolved Packet Core
E-UTRAN	Evolved Universal Terrestrial Radio Access Network
FM	Fault Management
GNSS	Global Navigation Satellite System
GSM	Global System for Mobile communications
HOF	Handover Failure
HSPA	High Speed Packet Access
ICIC	Inter-Cell Interference Coordination
IMEI SV	International Mobile Equipment Identifier and Software Version
IMS	Internet Multimedia Services
IMSI	International Mobile Subscriber Identifier
IP	Internet Protocol
IPEX	Investment Expenditures
KLD	Kullback-Leibler Divergence
KNN	k-Nearest Neighbors
KPI	Key Performance Indicators
LTE	Long Term Evolution
LTE-A	LTE Advanced
MAD	Mahalanobis Distance
MDT	Minimization of Drive Tests
MIMO	Multi-Input Multi-Output
MLB	Mobility Load Balancing
MRO	Mobility Robustness Optimization
MSE	Mobility State Estimation
NB	UTRAN NodeB
NGMN	Next Generation Mobile Networks

OAM	Operations, Administration and Maintenance architecture
OFDM	Orthogonal Frequency-Division Multiplexing
OPEX	Operational Expenditures
PCI	Physical Cell Identifier
PHR	Power Headroom Report
PM	Performance Management
PRB	Physical Resource Block
PS	Packet Switched
QCI	QoS Class Identifier
QoS	Quality of Service
RACH	Random Access Channel
RAN	Radio Access Network
RAT	Radio Access Technologies
RF	Radio Frequency
RLF	Radio Link Failure
RNC	Radio Network Controller
RSRP	Reference Symbol Received Power
RSRQ	Reference Symbol Received Quality
RSSI	Received Signal Strength Indicator
RRC	Radio Resource Control
RRM	Radio Resource Management
RXP	Received Power
SINR	Signal to Interference and Noise Ratio
SON	Self-Organizing Networks
TCO	Total Cost of Ownership
UL	Uplink
UL-SCH	Uplink Shared Channel for data transmission in LTE
UMTS	Universal Mobile Telecommunication System
UTRAN	Universal Terrestrial Radio Access Network
VoIP	Voice over IP
WCQI	Wideband Channel Quality Indictor
WLAN	Wireless Local Area Network

List of Symbols

$(.)^T$	Transpose operation
$tr(.)$	Trace operation
$(.)^{-1}$	Matrix inverse operation
$\|.\|$	Absolute value of a real number or a determinant operation of a matrix
$\mathbf{\Sigma_p}$	Covariance matrix for training data
$\mathbf{\Sigma_q}$	Covariance matrix for testing data
$\mathbf{p}$	Column vector of training data
$\mathbf{q}$	Column vector of testing data
d_e	Euclidean distance
d_m	Mahalanobis distance
d_{kl}	Kullback-Leibler divergence
$\mathbf{I}$	Identity matrix
ρ_m	Density metric for mth data sample
η_m	Number of samples inside k-dimensional ball for mth data sample
z_i	Anomaly score for eNB i
x_i	Number of outage samples associated with eNB i
μ_L	Sample mean of outage samples observed in set of eNBs
σ_L	Sample deviation of outage samples observed in set of eNBs
ψ_l	The lth Eigen vector of decomposed Markov's transition matrix
$\psi_l(x_i)$	The lth entry of the right eigenvector for point x_i
λ_l	Eigenvalue of the lth eigenvector ψ_l
$D_t^2(.)$	Diffusion distance operation between two points
Ψ_t	A matrix of diffusion coordinates
$\Psi_t(x_i)$	The ith row of Ψ_t providing the diffusion coordinates of x_i
P_{CMAX}	UE Nominal Maximum Transmission Power
$M_{PUSCH}(i)$	UL-SCH PRB allocation for ith subframe
$P_{0\_PUSCH}(j)$	Minimum transmission power level per PRB
$\alpha(j)$	Fractional pathloss compensation factor
$\Delta_{TF}(i)$	Modulation and coding scheme dependent constant offset
$f(i)$	Correction function to the UL power control mechanism
N_{CR}	Number of handovers and reselections during T_{CRmax}
T_{CRmax}	Time duration for sliding time window
N_{CR_M}	N_{CR} threshold between normal and medium mobility categories
N_{CR_H}	N_{CR} threshold between medium and high mobility categories
X_1	Distribution of N_{CR} samples belonging to lower mobility category
X_2	Distribution of N_{CR} samples belonging to higher mobility category
μ_1	Mean N_{CR} value of distribution X_1
σ_1	Standard deviation of distribution X_1
μ_2	Mean value of distribution X_2
σ_2	Standard deviation of distribution X_2
N_{TH}	Threshold between distributions X_1 and X_2

$\hat{E}s$	Energy per symbol
Iot	Interference over thermal noise
l_e^{iu}	Radio link between eNB i and UE u for one resource element $e_{s,sc}$
$e_{s,sc}$	Resource element indexed by subcarrier sc and OFDM symbol s
s	Index for certain OFDM symbol in LTE transmission
sc	Index for certain subcarrier in LTE transmission
$pl_i(.)$	Distance d_{iu} dependent pathloss model
d_{iu}	Distance between eNB i and UE u.
$sf_{iu}(.)$	Log-normal slow fading factor
$\|ff_{iu}(.)\|^2$	Average power of complex fast fading factor
$g_i(.)$	Antenna gain factor
φ_{iu},	Angular difference between eNB i antenna and UE in horizontal plane
θ_{iu}	Angular difference between eNB i antenna and UE in vertical plane
rx_e^{iu}	Received power per resource element
tx_e^{i}	Transmitted power per resource element
$rsrp(t)$	Instantaneous RSRP
S	A set of indexes of OFDM symbols transmitting reference symbols
RS_s^N	A set of subcarrier indexes transmitting CRS symbols during s
Ns	Number of OFDM symbols transmitting reference symbols
Nrs_N	Number of subcarriers transmitting CRS symbols on measurement bandwidth
$rsrp_{L1}$	Layer one RSRP measurement
Nw	Number of instantaneous RSRP samples
w	Sampling index in sliding time window
Δt	Sampling period for instantaneous measurements
$rsrp_{L3}$	Layer three RSRP measurement
$rsrp_{L3\_prev}$	Previous layer three RSRP measurement
a	L3 filtering variable
k	Configurable filter coefficient
$rsrq(t)$	Instantaneous RSRQ
$rssi(t)$	Instantaneous RSSI
SC^N	A set of indexes of all subcarrier on measurement bandwidth
Ntx	Number of radio links to eNBs
RS_s^W	A set of subcarriers indexes of transmitting reference symbols during s in whole transmission bandwidth
Nrs_W	Number of subcarriers per OFDM symbol transmitting CRS symbols in whole transmission bandwidth
$wcqi(t)$	Instantaneous wideband CQI

List of Figures

"*It is not the strongest of the species that survives, nor the most intelligent that survives. It is the one that is the most adaptable to change."* – Charles Darwin

1. Introduction

It was year 2012 and a small, light-weight and stylish cordless mobile phone is the *de-facto* item that we all carry with us in all times. More than 21 years has passed since the first official GSM (Global System for Mobile communications) call was made on Radiolinja's network in 1991 and now we have more than 8.9 million mobile subscribers in Finland. In 2011, Finnish mobile subscribers made more than 5.1 billion calls, sent more than 4.5 billion text messages and transmitted more than 60 000 terabytes of data [1]. The technological success of the mobile phones is unquestionable and life without one would be challenging, if not impossible. The mobile business segment is becoming more and more popular and is growing every year. New technologies, new applications and new services are offered to data hungry subscribers. Two decades ago we had GSM, ten years ago we had UMTS (Universal Mobile Telecommunication System) and today we have LTE (Long Term Evolution) and now, we are already paving the road for the 5th generation (5G) technologies and the Internet of Things. Although the mobile phones are the most visible evidence of this new technology, the high quality services with seamless mobility performance always require the deployment of a sophisticated cellular network infrastructure in the background. The popularity of the different mobile applications, services and the rapid growth of the network usage create new challenges for service providers and operators [2]. How do we provide the capacity that is needed to satisfy the increasing data demands of subscribers while still maintaining the profitability of the mobile business?

1.1 Background and Motivation

For decades there have been three main design principles for increasing the capacity of wireless systems. The principles are widening the system bandwidth, improving the spectral efficiency and shortening the frequency reuse distance. The total system bandwidth and signal to noise conditions define the upper bound for total system capacity according to the Shannon–Hartley theorem. Therefore, the trend has been to increase the bandwidth when introducing new generation of radio technologies. The maximum bandwidth in LTE is four times wider than the bandwidth in UMTS. By aggregating carriers in LTE Advanced (LTE-A), even larger system bandwidths can be achieved. Spectral efficiency on the other hand refers to the means to enhance bandwidth usage by increasing the number of transmitted bits per second per unit of bandwidth. Recent improvements in LTE spectral efficiency have been related to advanced multi antenna transceivers for example, multi-input multi-output (MIMO) transceivers. These transceivers provide remarkable capacity gains [3]. However, the whole concept of cellular networks relies on reusing frequencies since only it allows deployment of continuous coverage for nationwide areas

with limited frequency resources. In principle, two base stations can use the same frequencies simultaneously if they are isolated. One way to ensure this isolation is to have a large enough separation distance between the base stations. By shortening the distance, the capacity and frequency reuse rate increases, but the interference increases as well. If the interference can be mitigated for example, by using higher frequencies; adjusting transmission power; optimizing antenna configurations; or using advanced transceivers; then more base stations per unit area can be deployed, thus increasing the total capacity. For the next generation of cellular networks, dense small cell networks are envisioned to be one of the potential deployment strategies for addressing the capacity crunch [4]. However, cell densification and the co-existence of several radio access networks for example, GSM, UMTS and LTE, poses challenges for network vendors and operators. In particular, it will be difficult to manage their complex network infrastructures in a cost efficient way by using traditional methods while maintaining a good grade of service.

A fundamental planning principle of any radio network is to fulfill coverage, capacity and quality targets as cost efficiently as possible [5], [6]. Traditionally, the cost-efficiency goal is fulfilled by using the minimum number of base station sites because this minimizes the total cost of the network. Cell densification means that capacity is increased by deploying a hundred or a thousand times more small base stations. Hence, one of the challenges from an operator point of view will be to ensure efficient operation and optimization of the all co-existing networks with limited cost constraints. Even if the purchase cost of a small base station is reduced to the minimum, the total cost of small cell networks can reach an unacceptable level if implementation and operational expenditures (OPEX) cannot be reduced significantly. For this reason, the concept of Self-Organizing Networks (SON) has been introduced in LTE [7].

The goal of the SON concept is to increase the degree of automation in the network planning, configuration and optimization processes in order to increase efficiency while reducing the costs of operating the networks. The cost savings in Capital Expenditures (CAPEX) are related to better utilization of the network resources when increasing coverage, capacity and quality. If this allows for new investments to be postponed, then the return of the investments in the existing equipment improves and results in CAPEX savings. The OPEX savings are related to increasing the productivity of the operator's staff, for example by reducing the amount of repetitive and time consuming optimization tasks. Although self-organization can reduce the amount of manual intervention needed to carry out the optimization tasks, it also poses new challenges. It is expected that the automation of complex network procedures that have intricate interdependencies will require more feedback data to assist with the autonomous decision making with regards to the network elements. In particular, the autonomous collection of the radio measurements for network coverage monitoring and verification is anticipated to be a data intensive process. Hence, efficient

means are needed to process and analyze this data. In this thesis, different aspects of knowledge mining are studied as a way to support self-organizing cellular networks.

1.2 Scope and Objectives of the Thesis

From an operator's perspective, automated collection of radio measurements that complements the manual drive test campaigns is one of the top use cases in self-organizing radio networks. It is foreseen that such automation can provide significant cost savings [7]. However, it also requires an extensive number of measurements and is likely to lead to big databases. The objective of the thesis is to study the challenges of network operation and optimization that arise due to the increased complexity of modern radio networks and to subsequently develop knowledge mining assisted self-healing and self-optimization algorithms that can reduce an operator's need to conduct expensive and time consuming manual drive tests. The purpose of knowledge mining is to learn from the measurement data and detect hidden patterns that can improve network optimization and troubleshooting while proving additional value to the self-organization of the network. In short, the thesis focuses on:

- Modeling and simulating irregularities and anomalies in cellular radio networks;
- Studying the feasibility of using RF fingerprints for positioning the radio measurement reports in heterogeneous LTE networks;
- Designing self-healing algorithms for detecting coverage problems and anomalous network behavior by using the means of machine learning and advanced knowledge mining;
- Designing a self-optimization algorithm for enhancing the classification accuracy of UE mobility state estimation in LTE by learning statistical velocity profiles from drive test data.

The scope of the thesis is limited to designing self-healing and self-optimization algorithms which rely on standardized measurements and interfaces introduced in the 3GPP Release 10 and Release 11 specifications for minimizing drive tests in LTE and UMTS. The concept of *Minimization of Drive Tests* (MDT) provides an automated framework for gathering user reported location-aware radio measurements from commercial mobile phones. The validation of the designed algorithms is done by conducting system simulations with a state-of-the-art dynamic LTE system simulator (see Appendix A). In most of the studied cases, simulations are first used for building an MDT database and learning network behavior in its functional stage. Later, the knowledge acquired during normal operation is used to detect coverage problems, anomalous sleeping base stations or self-optimizing network parameters. In the MDT concept, RF fingerprinting can be used to estimate the location of radio measurements in case the accurate location is not available. The location information plays an important role both in the sleeping

cell detection and the optimization of mobility state estimation. Hence, the feasibility of using RF fingerprinting in location estimation is studied to understand its impact on the designed self-healing and self-optimization algorithms. Throughout the thesis, the target has not only been to design and verify the self-healing and self-optimization algorithms, but also to consider their impact on the network planning, optimization and operation work flows. Since the automated collection of drive test measurements is likely to lead to huge databases, a common framework is needed for understanding how this data should be processed and analyzed. In this thesis, knowledge mining is used for this purpose. Knowledge mining focuses on learning based approaches in data clustering, data classification, anomaly detection and dimensionality reduction, to support efficient processing and analysis of MDT data, which in turn results in more efficient network operation and optimization process.

1.3 Main Results of the Thesis

The main results of the thesis are a set of knowledge mining assisted self-healing and self-optimization algorithms that aim for a more automated network troubleshooting and optimization processes. First, radio network irregularities were analyzed in [P1] where a synthetic irregular layout known as a *Non-regular Springwald* layout, was defined by giving a description and a mathematical definition for the placement of irregular base station site locations and antenna directions. The Springwald layout helps to determine the site locations in a simple and simulator-friendly manner by reflecting the realistic network deployments. The layout was used later in several other simulation campaigns, for example in [P2], where extended Radio Link Failure (RLF) reports are used to classify network problems into three categories that are downlink coverage, interference and handover problems. Based on the results, the coverage, interference and handover problems can be differentiated by using the RLF reports containing Radio Frequency (RF) measurements from both the serving and neighboring cells. In [P3], an enhancement for triggering the MDT measurement reporting procedure and for detecting uplink coverage problems is described. It is concluded that by normalizing LTE power headroom reports (PHR), the classification between coverage-based and parameterization-based uplink problems can be improved. Moreover, the normalization also results in a lower false alarm rate for triggering the MDT measurements that are used to detect uplink coverage problems.

In [P4], the Diffusion Maps method was applied for both pre-processing MDT and extended RLF reports to assist with the detection of coverage problems and anomalous network elements by means of clustering. Moreover, the work in [P4] was continued in [P5] by including the classification of the periodical MDT measurements in the analysis. It was observed that by using the periodical measurements, more anomalous samples indicating outage are detected, thus improving the reliability of sleeping cell detection. The research results of [P4] and [P5] provide

a comprehensive set of knowledge mining tools that can be used for analyzing and post-processing the large MDT databases whereas with 3rd generation partnership project (3GPP) specifications, only the means to collect the measurements are discussed.

In [P6] and [P7], a grid-based RF fingerprint positioning framework is introduced for evaluating the positioning accuracy of MDT RF fingerprints in LTE networks. The results suggest that fingerprint matching based on Kullback-Leibler Divergence can provide a good way of locating MDT reports in dense small cell networks. In [P8], self-optimization of the mobility state estimation (MSE) parameters is done in heterogeneous LTE networks. The findings suggest that by gathering the field measurements and constructing statistical UE velocity profiles, the network parameters used for estimating UE mobility state can be optimized autonomously, thus resulting in reasonably good overall classification accuracy. By self-optimizing the MSE thresholds, operators can improve the mobility performance of the high velocity UEs in heterogeneous network topologies in a cost-efficient and a backward compatible manner whereas the majority of the other MSE enhancements discussed in 3GPP are not backward compatible.

The overall outcome of the main results is that by having tools to automatically learn and classify measurements for certain problems or to detect anomalous behavior in network elements, the network engineers can acquire more knowledge about the root causes of the performance degradation. This will result in a faster decision making process that shortens the duration of the network breaks and the time needed to adapt to the changed network conditions. Therefore, autonomous learning can improve network quality and the grade of service. Moreover, by using the detailed or estimated geographical location of the measurements in the performance analysis, finer granularity for estimating the location of problematic or anomalous network areas can be achieved. This can further improve the decision making with regards to how the network should be optimized and re-planned.

It is also worth highlighting that in addition to the novel ideas presented in the publications, some of the research results have been contributed to 3GPP specifications, for example, 3GPP TR 36.805 and 3GPP TS 36.839. Moreover, during the research work, three patent applications related to the results in this thesis were filed. For example:

- US2013/0005381, *Terminal Mobility State Detection*

The author of this thesis is an inventor of the aforementioned process, thus highlighting the applicability and the unique value of this work for the telecom industry.

1.4 Author's Original Contribution

This section describes the author's original contribution to the publications compiled to this thesis. The research work was conducted between 2009 and 2013 while the author was working at Magister Solutions Ltd. The research work was supervised by Prof. Jukka Lempiäinen at the

Department of Communication Engineering at Tampere University of Technology. Co-supervision was given by Prof. Tapani Ristaniemi at the Department of Mathematical Information Technology at the University of Jyväskylä. Moreover, informal discussions between the author and the co-authors from Nokia, Nokia Siemens Networks, Renesas Mobile Europe and Magister Solutions have contributed to the thesis in various ways concerning for example, different aspects of self-organizing networks.

In publication [P1], Mr. Andreas Lobinger defined the site positions and antenna directions for the Springwald layout, and the author was responsible for implementing the Springwald in the system simulator, for analyzing the simulation results and for writing the publication. Publication [P2] was mainly done by Dr. Jani Puttonen. This included simulations, analysis and writing. The author's contribution to [P2] was limited to providing Springwald simulation scenario and participating in brainstorming about the discrimination of RLF reports. Simulations and analysis of PHR based uplink coverage optimization in [P3] was mainly done by the author, whereas the co-author took part in improving the text of the publication. The clustering and the classification frameworks described in [P4] and [P5] were defined mostly by the author. The author was also responsible for simulating the MDT data for the performance evaluations. The Diffusion Maps program used for dimensionality reduction was developed by Dr. Gil David. Moreover, Mr. Fedor Chernogorov contributed significantly to [P4] by writing a Matlab program for the clustering framework; he also took part in the performance analysis and writing process of the publication. In addition, Mr. Kimmo Brigatti contributed to [P5] by writing a Matlab program for classification and by taking part in the performance analysis whereas the author is responsible of analyzing the results and writing the journal article. In [P6] and [P7], the research problem, the evaluation methodology and the simulation data were provided by the author whereas a Matlab program used for RF fingerprinting was written by Mr. Riaz Uddin Mondal. In [P8], the framework for self-optimizing the mobility state estimation parameters using the MDT measurements was done. The design of the framework and the verification simulations were done solely by the author whereas the co-authors provided additional knowledge about the LTE system and the related 3GPP specifications.

1.5 Organization of the Thesis

The thesis is organized into six chapters. Chapter 1 provides the introduction, scope and objectives of the thesis. It also gathers the main results of the publications and discusses the author's original contribution to the results. Chapter 2 describes the principles of operating modern radio networks by focusing on planning, operation, optimization and troubleshooting processes. The purpose is to elaborate on how networks are operated nowadays and identify how automation and self-organization can be introduced into network processes. In Chapter 3, the concept of self-

organizing networks is described with a focus on different functionalities such as self-configuration, self-optimization, self-healing. In addition, a detailed description of the concept of Minimization of Drive Tests is given.

Chapter 4 focuses on the essential principles of knowledge mining because the majority of the proposed algorithms rely on the methods of extracting knowledge from large measurement databases. The knowledge mining principles such as anomaly detection, dimensionality reduction, classification and clustering are the tools that were used in the publications that this thesis is composed of. Chapter 5 gathers the main results of the novel self-healing and self-organizing algorithms in [P1]-[P8]. The algorithms are related to discriminating between different coverage problems, detecting anomalous base stations and enhancing UE mobility state estimation by processing the minimization of drive test measurement databases. Finally, Chapter 6 concludes the research results and discusses the future work. In Appendix A, a system simulator software is briefly discussed, specifically from the MDT simulation point of view. In the end, seven internationally reviewed conference articles and one journal article are included to give a detailed compilation that summarizes the contribution and the work conducted for this thesis.

2. Operation of Modern Cellular Radio Network

This chapter provides an overview of operating and optimizing modern radio networks. First the economic aspects of radio networks are discussed. In later sections, an overview of cellular network architecture is given with an introduction to radio network planning, operation and optimization processes. Since this chapter focuses on the architecture and the operational aspects of the networks, readers who are keen for more details about LTE radio access technology are asked to take look at an excellent guidebook that is edited by Sesia, Toufik and Baker [8].

2.1 The Economics of the Radio Networks

It is anticipated that demand for data traffic will increase dramatically in the future and that growth will be linked with new types of services, applications and devices that rely on Device-To-Device (D2D) communication and Machine Type Connectivity (MTC). The forecast for traffic demand that is shown in Figure 1 indicates that by 2020, typical mobile traffic demand per user is expected to grow by a factor of 30 from 0.5 GB to 15 GB per month [2]. Such growth will set rigid requirements on the capacity improvements in mobile networks. In order to be able to provide the required capacity, operators will eventually have to invest in their networks and use the all of the available spectrum. Since the amount of usable spectrum is limited and the improvements in spectral efficiency are marginal compared with the growth of the demand, operators will have to deploy new base stations on a large scale in order to increase the offered capacity. On one hand, network *densification* (higher base station density) increases the offered capacity per area, but it may also increase the costs for the operator as well.

The foundations of analyzing the economic aspects of cellular networks were laid in [9] by introducing a model for analyzing major components of both costs and revenue of the networks. Typically, the total cost of ownership (TCO) of the radio network is divided into capital expenditures (CAPEX) and operational expenditures (OPEX). The CAPEX includes the license fees and hardware equipment costs, for example the purchase cost of new network elements. In addition, implementation expenditures (IPEX) related to site preparation and network equipment installation that occur only once are part of the CAPEX. The OPEX consists of running costs such as site and transmission line rental costs, electricity and heating costs, and network optimization and maintenance costs. In [10] and [11], an analytical model for estimating the infrastructure costs in macro, micro and pico networks was given. Particularly in [10], the model predicted that when site density increases, the operation and the transmission costs tend to dominate the total costs, rather than the radio equipment and the site costs.

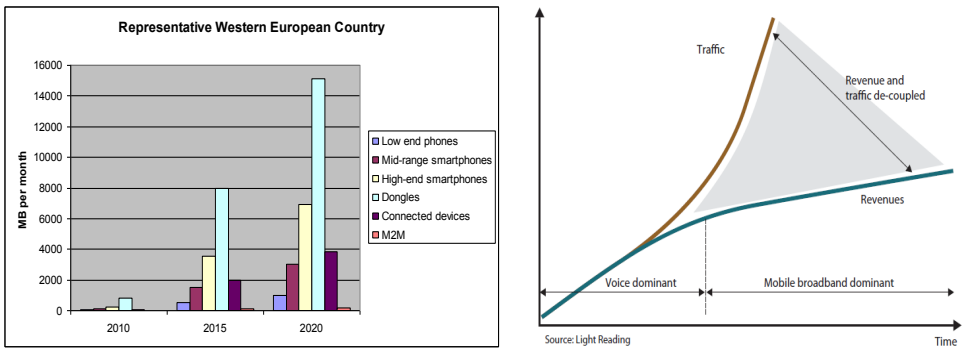

a.) Monthly traffic per device in western Europe [2] *b.) Revenue de-coupling in radio networks [13]*

Figure 1: Trend for traffic and revenue in radio networks

Hence, the densification and the co-existence of several radio technologies creates challenges for operators with regards to cost efficiently managing complex networks with a good grade of service. On one hand, the TCO must be kept under control, but on the other, revenue must also be secured. Nowadays, revenue is typically generated by voice, data and Short Message Services (SMS) that are based on a variety of different pricing models. The average revenue generation in 2010 in Europe came from the following sources: 77% voice, 10% SMS and 13% data. At the same time, more than 75% of the traffic was broadband data [12]. In the future, if the traffic per user increases quickly while the average revenue per user (ARPU) stagnates, then the operators are expected to face a *scissor effect* where traffic de-couples from revenue. This happens because revenues are not keeping up with the traffic growth [13]. The scissor effect depicted in Figure 1 may occur if for example, the bandwidth usage of customers increases rapidly while revenue is based on flat rate pricing, or if the customers start to replace voice and SMS services with value added data applications such as *Skype* and *WhatsApp*, thus reducing the revenue generated by the traditional services.

In [12], the profitability of cellular network operation was analyzed for moderate and high traffic growth scenarios. In the case of moderate growth, the profit margin remains positive, but deteriorates. In the case of high growth, the network has limited capacity and the operator has to aggressively increase the number of sites in order to meet the increased demand. This results in higher OPEX and a rapid decrease in profit margin [12]. Hence, it is foreseen that flat rate pricing for data services cannot last forever, and it will likely be replaced by pricing models that depend on the amount or type of usage. However, this also motivates subscribers to seek and use alternative access methods for data services. It is worth noting that the increase in costs is not equal to the increase in data demand [13]. However, rapid traffic growth forces operators to rethink their revenue and business models and there is a clear need for identifying new innovative

added-value services that increase revenue per transmitted bit while reducing total costs of network ownership. The cost reductions of operating dense and complex network infrastructure are one of the biggest motivations for introducing automation and self-organization into cellular networks.

2.2 Radio Network Architecture

The architecture of cellular radio networks has evolved during the past few years and nowadays modern networks are multi-layer and multi-RAT networks that support equipment from several vendors. An illustration of 3GPP network architecture is shown in Figure 2. Network architecture is split into a radio access network (RAN) part and a core network (CN) part. RAN consists of mobile devices and geographically distributed base station sites. One base station site is often divided into cells and each cell provides radio access service to mobile devices in the geographical area that the cell is covering. Such cellular infrastructure allows for the construction of continuous coverage and efficient usage of the frequency resources. Hence, RAN is responsible for radio related functions. For example: Radio Resource Management (RRM) and providing wireless access to the network [14]. On the other hand, CN is responsible for the overall control of User Equipment (UE) and the establishment of the end-to-end communication services [14]. A common requirement for a modern radio network is the inter-operability of an operator's existing GSM and Universal Terrestrial Radio Access Network (UTRAN) radio access networks. Such inter-operability is needed to ensure seamless mobility, service continuity, and flexible spectrum management. This is especially important during the early deployment phase of the next generation networks that only have partial coverage. Older radio access networks based on GSM and UTRAN consist of several different types of network elements (NE) in RAN and they have different functional splits [5]. In GSM, Base Stations (BS) are controlled by Base Station Controllers (BSC) whereas in UTRAN, the base station is known as NodeB (NB) and it is controlled by Radio Network Controllers (RNC) which connect a UTRAN network to the circuit switched (CS) and packet switched (PS) parts of the core network.

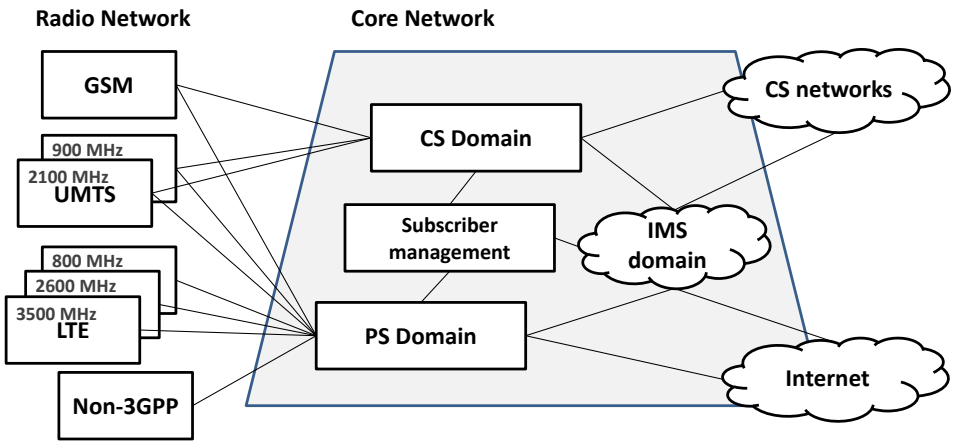

Figure 2: Illustration of 3GPP radio network architecture

In Evolved Universal Terrestrial Radio Access Network (E-UTRAN), the radio access network architecture is a *flat architecture* consisting of only E-UTRAN NodeB's (eNB) which are connected to the Evolved Packet Core (EPC) network. In addition to the inter-operability between the RATs, coordination between different frequency layers on the same RAT is needed. Coverage in UTRAN and E-UTRAN can be provided by using lower frequencies, for example by deploying UMTS on the 900MHz frequency band and LTE on the 800 MHz frequency band, whereas additional capacity is provided by using higher frequency bands. On one hand, network deployment with different frequency bands increases the overall capacity of the system, but it will also increase the number of co-existing RAT service layers, thus making the radio network architecture more complex to operate and optimize.

A core network consists of various subscriber management databases, CS domain and PS domain network elements. The subscriber management databases contain data storages and functionality that is needed to assist subscriber related functions like for example, authentication, security, roaming, service policies and charging, between and within CS, PS and Internet Multimedia Services (IMS) domains [14]. Network elements in the CS domain have been used in GSM and UTRAN to deliver circuit switched services between CS networks, for example with voice calls, whereas elements in the PS domain are used to provide packet connectivity, for example Internet Protocol (IP) connectivity, to the Internet. Since EPC architecture is converging towards all-IP architecture, the IMS domain contains functions that provide support for multimedia sessions that utilize the IP connectivity from the PS domain, for example Voice over IP (VoIP). In addition, E-UTRAN and EPC supports interworking with non-3GPP radio access technologies, thus allowing operators to provide service continuity and mobility between 3GPP and non-3GPP radio access technologies, for example between 3GPP and Wireless Local Area Network (WLAN).

2.3 Operating the Radio Network

Operating a radio network is a continuous process where network performance is constantly monitored and optimized to achieve the best return of investment. Nowadays, the operation and management process is based on centralized Operation. In particular, it is based on Administration and Maintenance (OAM) architecture that is used to centrally coordinate operational tasks from the Operations and Maintenance Center [15]. Operational tasks can be divided into planning, deployment, monitoring, optimization and fault management task. Although the different operational domains are managed centrally and are interconnected in Figure 3, network planning and operation domains are actually rather independent because they use different tools for their internal procedures, and therefore, they require expert-driven supervision in overall task management [15].

2.3.1 Radio Network Planning

The radio network planning process starts with the definition of the policies for network coverage, capacity and quality that are used to guide the planning. The rule of thumb in planning is to find the minimum number of base stations that can satisfy the coverage, capacity and quality of service requirements [5], [6], [29]. It is expected that by minimizing the number of base stations, an operator can reduce their capital and operational expenditures; CAPEX and OPEX are proportional to the amount of radio network equipment. Hence, by minimizing the number of base stations, one can minimize the economic constraints of operating the network [16]. The planning process consists of different phases, for example the dimensioning phase, the detailed planning phase and the re-planning phase. In the dimensioning phase, an estimate of the network layout and the number of network elements is determined whereas in the detailed planning phase, a radio access dependent configuration, topology and parameterization are set up. After the detailed planning, the radio network is deployed according to the plan. The deployment can be a full-scale rollout of thousands of base stations or just the addition or replacement of a single base station. The deployment is tested before it is taken in commercial use. In commissioning and acceptance testing, the deployment is validated by collecting, for example with drive test measurements of Key Performance Indicators (KPI) that are related to coverage, capacity and network functionality such as network accessibility, retainability and mobility [17], [18]. In network accessibility testing, the functionality needed for establishing calls or connections is tested. In network retainability testing, connection failures are analyzed, whereas in mobility testing, handover performance is verified. The need for re-planning in commercial networks is usually triggered either by network alarms indicating failures or by performance indicators suggesting that optimization is needed.

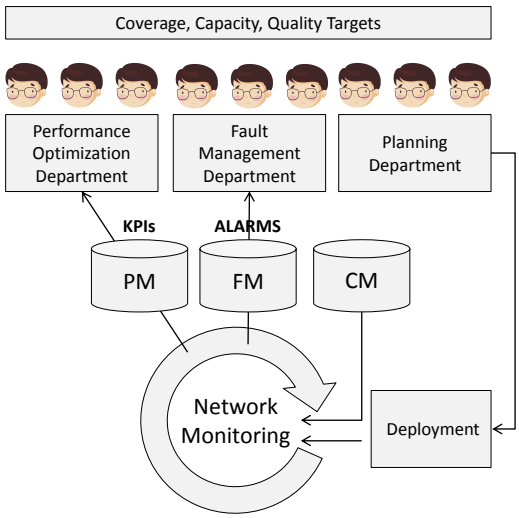

Figure 3: Procedure for operating a traditional radio network

2.3.2 Radio Network Monitoring

Radio network operation requires continuous monitoring and optimization to ensure that the target grade of service is maintained. The purpose of monitoring is to provide KPI measurements for optimization and fault management domains. KPIs are constructed from a multitude of measurements that are collected from service and network layers throughout the network life cycle. This is depicted in Figure 4. The measurements can be collected in various ways by using different tools, for example by conducting field measurements, by using mobile agents, by using real-time network protocol analyzers and probes, by analyzing network equipment logs or by analyzing records from Network Management System (NMS) databases [19].

The field measurements are typically radio interface measurements that are conducted for performance monitoring and troubleshooting. The field measurements, especially the information about radio coverage and coverage problems, are very important for network planning, network optimization and network management activities such as marketing. For these reasons, operators monitor network performance by conducting drive tests for collecting the field measurements. Field measurements prior to network planning are done for example, for signal propagation predictions that are used for assisting the network dimensioning process. During a network rollout, field measurements are collected in order to validate network coverage, quality and radio interface functionality with regards to network accessibility, retainability and mobility performance [19]. Later during the network life cycle, drive tests are typically conducted after deployment of new base stations; construction of new highways, railways and major buildings; customer complaints and network alarms [20].

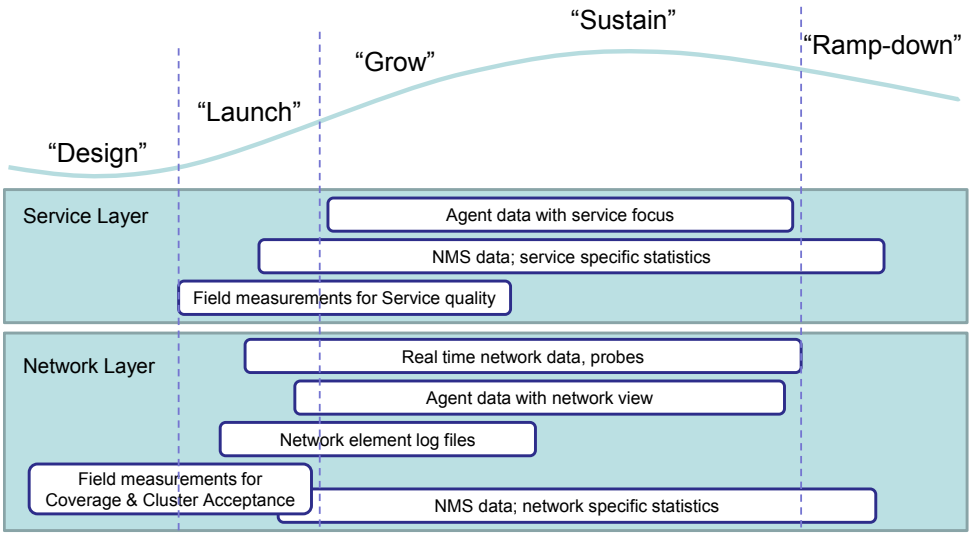

Figure 4: Network monitoring tools

Although the drive tests are performed around major buildings, they cannot be conducted after every small scale construction project that may have an effect on radio propagation. Therefore, operators also perform periodical drive tests to monitor coverage and network grade of service. Periodical drive tests are also conducted for marketing purposes. This is done by benchmarking other operators since coverage or lack of it is something that customers can easily notice through a device out-of-service area indicator or via noticeable network events such as call drops or connection problems [20]. Hence, coverage is a major criterion for customers (and marketing) to consider when they compare service provided by different operators.

Mobile agents are applications that are installed on the mobile phones that are capable of collecting measurements related to end user behavior, service usage and service quality together with radio interface details and positioning information [19]. In addition, 3GPP has specific Subscriber and Equipment Tracing functionality that is based on features from field measurements and mobile agents [21]. Tracing can log data from several interfaces at the call level for a specific UE, mobile type, or service initiated by a user. Thus, it allows for the collection of data from the end-user that is based on QoS per call, the correlation between protocol messages and RF measurements, or interoperability with specific mobile vendors. Trace functionality is also used for configuring MDT measurements that replenish data for traditional drive test measurements.

Real-time protocol data, network element logs and records from NMS are collected from core network elements. The real-time protocol data is collected by using various probes that monitor the interfaces between the network elements. The probes can provide detailed information that is suitable for troubleshooting and root cause analysis [19]. The network element

logs, for example eNB logs in LTE or RNC logs in UMTS, can be used to obtain additional details about vendor specific logged data from the elements and the interfaces to which the network element is connected. This helps to understand the behavior of the network elements in case of hardware and the software problems whereas NMS data is typically aggregated from a large number of network elements [19]. Since NMS data is typically collected from all cells in the network, the amount of data is huge, and thus reported data is typically averaged in terms of network elements, time or measurement content, thus NSM is ideally used for performance monitoring when the network is fully operational [19].

2.3.3 Radio Network Optimization

The goal of the radio network optimization process is to determine how network performance can be improved by optimizing the configuration or parameterization of the deployed network elements through the re-planning process [5], [6]. As depicted in Figure 3, KPIs are the input in the manual optimization process. The KPIs are used to detect the need for network re-planning and to validate that earlier optimization decisions are affecting to the network performance as expected. After deciding that optimization is needed, the network is re-planned and deployment is changed accordingly, for example by changing site configurations, base station parameterizations or by deploying new base stations. Optimization is always followed by a verification phase where network performance is validated, thus resulting in a continuous network monitoring and optimization loop. The need for continuous optimization is based on two facts:

- the initial radio network plan is never perfect because planning is always based on insufficient knowledge and abstract modeling of propagation and radio access network behavior in the real environment.
- environmental developments such as the construction of new highways, railways or residential areas affects radio propagation and may change network characteristics.

On one hand, operators can improve the coverage, capacity and quality of the network by optimizing it. This can postpone additional investments in network coverage and capacity, thus increasing the profitability and the return of the earlier investments. On the other hand, optimization can be time consuming and require significant amount of manual human involvement which increases OPEX. Thus, the optimization in practice is bound by economic constraints and after a certain point the benefits of it are lost. This means that gains in CAPEX become smaller than the cost of optimizations in OPEX. As discussed later in Chapter 3, by automating the optimization process one can reduce the OPEX related to the optimization tasks. This is expected to be a mandatory feature in next generation radio networks.

2.3.4 Radio Network Fault Management

Radio network fault management (or troubleshooting), is a crucial part of the radio network operation process. Its purpose is to ensure high reliability and constant availability of the networks. The aim of troubleshooting is to react to network degradation and correct faults in its behavior. In many cases, an operator's troubleshooting can be divided into reactive and proactive fault management. This is depicted in Figure 5 [22]. The fault management process consists of three steps. In the first step, network faults are detected by monitoring network alarms, customer complaints and KPI statistics. Network alarms are raised when severe network degradation is detected. In the second step, root cause analysis is carried out to figure out what is causing the problem and determine how it should be fixed. The root cause analysis often requires extensive analysis of KPI statistics, site visits and drive tests for collecting the field measurements for troubleshooting. This step can be iterative, time consuming and can require a high degree of expert knowledge, thus it potentially increases OPEX. In the third step, the problem is fixed for example by adjusting network parameters remotely, by rebooting base stations, or by repairing or replacing hardware equipment on-site. Reactive fault management is straightforward in the sense that the need for troubleshooting is triggered by network alarms or customer complaints. Proactive fault management can be a more complex process because there are no alarms and problems are triggered either by finding suspicious KPI statistics that indicate performance degradation or by analyzing unresolved fault management tasks known as trouble tickets.

One aspect of fault management (and its automation) is determining when to trigger alarms based on KPI statistics that imply performance degradation. Often the triggering is done by making observations on KPI statistics that exceed thresholds [18]. However, defining good thresholds is not a trivial process. In fact, the thresholds must be adjusted carefully to ensure that alarms are triggering properly. Here are two key things to consider:

- On one hand, alarms need to be triggered early enough so that corrective actions can be taken without prolonging the duration of network breaks.
- On the other hand, a false alarm rate must be kept as low as possible to avoid alarm avalanches, unnecessary troubleshooting and the related costs.

Nevertheless, operators are often faced with alarm floods that are caused by single incidents, poor alarm prioritization, misleading alarm descriptions, and an incomplete maintenance manual for repair actions [7]. Reacting to alarm floods is laborious unless it is ignored completely, and for these reasons special emphasis should be put on both the quantity and quality of the alarms. Specifically, a mostly automated and efficient fault management processes should be implemented in future networks. In such process, the number of iterations should be minimized and the relevant root causes should be identified quickly.

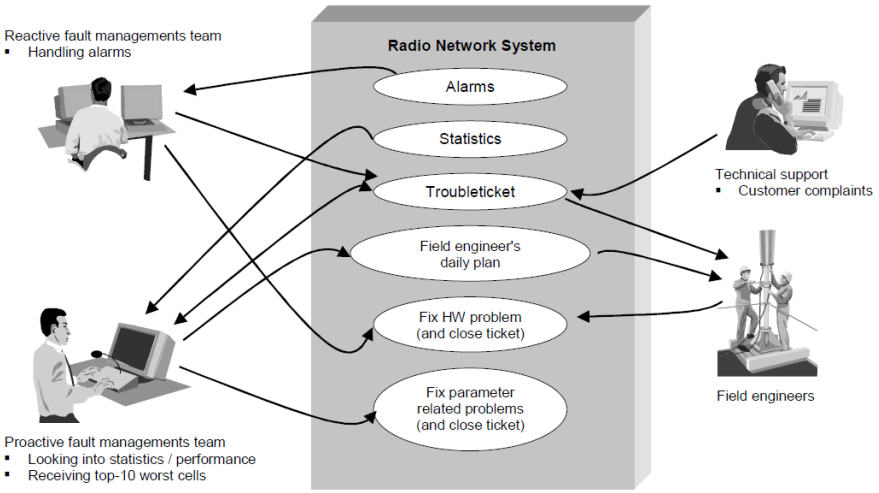

Figure 5: Manual network fault management process [22]

2.4 Operation and Management Vision for Future Radio Networks

The overall process of understanding radio network imperfections and addressing them with the correct solutions is time consuming, expensive and complicated. Nowadays, this process requires a high degree of expert knowledge, special tools and manual human involvement in planning, optimization and troubleshooting tasks. The increasing complexity of the radio network infrastructure, due to the densification and the seamless interoperability of several access networks, is making the operation of such networks challenging. If the costs of operating a network increase to an intolerable level while the revenue per user per transmitted megabit decreases, then cost-efficient operation of the networks while maintaining a good grade of service becomes impossible.

It is envisioned that by integrating the network planning, configuration and optimization into one mostly automated process, the overall network performance will be improved while the network operational costs can be reduced [23]. Radio network automation itself is not a new topic and it has been widely discussed before, for example in several publications [24], [25]; in research projects MOMENTUM [26], GANDALF [27] and SOCRATES [28]; and in books [15], [29] that address the various topics of automated network design, planning and optimization. However, automation in cellular radio network research became a very hot topic after the concept of Self-Organizing Networks was introduced by the operator's alliance Next Generation Mobile Network (NGMN) in 2006 [30]. Later, NGMN in [7], [31] and 3GPP in [32], [33] introduced the concept requirements and the use cases for self-organization in E-UTRAN. In fact, the concept of self-organization has been one of the design principles and a part of E-UTRAN specifications since the first release of LTE technology.

3. Concept of Self-Organizing Networks

This chapter provides an overview of the concept of network self-organization. The concept consists of three functionalities: self-configuration, self-optimization and self-healing. In addition, Minimization of Drive Tests framework in E-UTRAN is introduced. Readers who are keen for more details about SON can take a look at an excellent SON guidebook edited by Hämäläinen, Sanneck and Sartori [15].

3.1 Self-Organizing Networks

The vision of Self-Organizing Networks is to enable automation in an operator's planning, deployment and operational tasks. The aim is to:

- reduce OPEX by reducing the amount of unnecessary human involvement in network operational tasks;
- improve network coverage, capacity and quality by utilizing available network resources in a more optimal way.

The cost savings in OPEX are achieved by better utilizing human resources for tasks which are repetitive, complex, granular, or require fast adaptation. These tasks are too expensive to be done manually [34]. A repetitive operational task can be learned. By automating such tasks as much as possible, time and human effort are saved, thus reducing the costs of repeating the task. Complex operational tasks are typically error-prone because incidental mistakes lead to errors which make optimization an iterative and time consuming task, thus also making it expensive. Granular tasks, for example optimizing parameters per user, per device type or per service in a dynamically changing network environment requires a lot of effort, and thus easily becomes too expensive. Moreover, since manual operation by nature is slow, optimization which requires fast reaction and adaptation to a dynamically changing network is impossible to implement without the help of automation. Automation helps to carry out operational tasks that would be too expensive to complete otherwise. This allows for further optimization of the network and results in cost savings in OPEX and CAPEX due to the better utilization of the available human and network resources [34]. This also changes the role of human involvement in operational tasks. In the future, it is anticipated that human involvement will take place on a higher level and that role will be in defining performance policies and monitoring high level KPIs, while SON algorithms do the measurements and adjust the network parameters autonomously following the given policies. Such process is depicted in Figure 6. This is different from the traditional network operation process depicted in Figure 3.

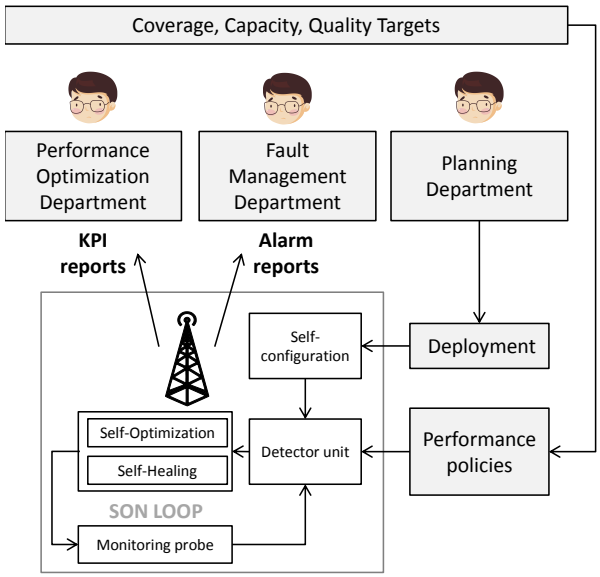

Figure 6: Operation of a Self-Organizing Network

As illustrated in Figure 6, the SON concept is integrated in the operator's network management process through three functionalities: self-configuration, self-optimization and self-healing. The purpose of the self-configuration is to automate the initial steps of the network element setup which is by nature a repetitive process [15]. After the self-configuration, network elements start continuous monitoring of feedback measurements that aims to determine if optimization is needed. Self-optimization is concentrated on monitoring network performance and automating the parameter tuning. The goal is to improve the network grade of service without compromising the robust operation [15]. If network failures or suspicious behavior is detected, self-healing tries to autonomously diagnose the root causes and compensate or recover from the malfunctioning state [15]. Although the concept of SON may look like a simple and straightforward method for achieving cost savings and improved network performance, there are several challenges facing the successful implementation of self-organization in practice [23].

The first challenge is the complexity of radio networks. Radio networks are complex infrastructures consisting of a multitude of tunable parameters and procedures that act on different time scales. In addition, there are complicated interconnections and interdependencies among the parameters and procedures. This is depicted in Figure 7. For example, network coverage and the capacity can be optimized by either jointly or independently adjusting several parameters such as transmission power, antenna configurations and resource allocations. This makes it challenging to determine what parameters or procedures should be optimized to achieve the best overall performance.

The second challenge is robust operation. Since self-organizing networks are anticipated to consist of several SON control functions that might have conflicting optimization goals, multivariable control and coordination between the algorithms is needed to ensure robust overall performance [23]. For example, one SON function may try to compensate for network outage by improving the coverage in one cell whereas another function wants to adjust the cell borders in the opposite direction to compensating for network overloading. This creates additional requirements for SON algorithms and increases the complexity of the SON architecture.

The third challenge is the tradeoff between performance and complexity. In any automated process, the feedback measurements are the foundations of automation. Hence, SON functions need data to be exchanged between various network elements in order to acquire the knowledge that is needed to autonomously make the right optimization decisions that fulfill both the performance and robustness requirements [35]. However, everything cannot be measured all the time due to practical signaling, processing and data storage limitations, and therefore device techniques for measuring and monitoring network performance are needed. On one hand, because of complexity and cost, it is necessary to determine and limit the amount of data that is signaled between the different SON functions. On the other hand, enough data must be collected in order to make good optimization decisions that result in the reliable and robust operation of self-organizing networks.

Reliable SON algorithms behave as expected; they do not fluctuate and converge towards optimal performance [35]. Robust SON algorithms tolerate missing, wrong or corrupted measurements in addition to conflicting decisions from other SON algorithms while still providing satisfying performance [35]. For example, with coverage optimization it is not enough to only measure and report the downlink signal strength of the serving cell that is received. The downlink signal strength that is received may suggest that the coverage target can be fulfilled by modifying transmission power. However, to ensure robust operation, more measurements are needed to verify that uplink coverage and downlink interference is in balance. This needs to happen before a reliable and robust optimization decision can be made leading to a satisfying grade of service in both the serving and neighboring cells.

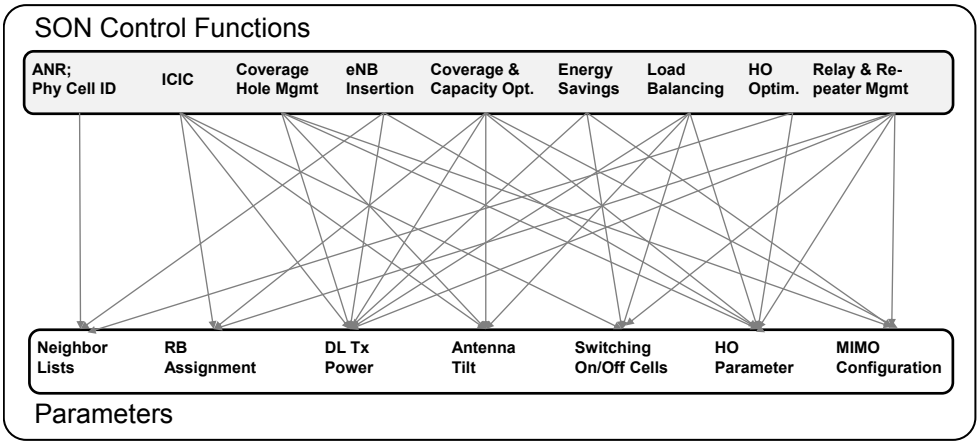

Figure 7: Illustration of parameter and process interdependencies [15]

3.1.1 Self-Configuration

The goal of self-configuration is to automate the initial steps of the network equipment installation and autonomous integration to OAM, RAN and CN to allow for secure and faster deployment of LTE networks. In LTE Release 8, such self-configuration functions were based on the *plug-and-play* functionality of eNBs where the initial configuration and the radio configuration are fetched from the network after the eNB is powered up and has established backbone connectivity. Since manual planning and the configuration of neighbor relations and Physical Cell Identifier (PCI) values is a time consuming task that needs to always be done when new eNB is deployed, automatic configuration of the cell PCI values and Automatic Neighbor Relations (ANR) were introduced in LTE Release 8.

PCI is the LTE physical layer identifier for eNB that must be carefully selected among 504 different alternatives to avoid collision and confusion between neighboring cells [8]. The self-configuration procedure for the automatic selection of PCI is based on UE measurements and information exchange between the neighboring eNBs. This ensures the proper reuse of PCI values fulfilling the collision and confusion criteria [36]. The process of self-configuring the neighbor relations uses UE measurements to help the eNB update its neighbor relations list autonomously and establish connections to neighboring eNBs. This ensures proper handover performance in LTE. The neighbor lists are used by the eNBs to tell the UEs which cells UEs should measure and report for handover management. Since the neighbor lists contain several entries and must be maintained for every eNB, manual configuration of the lists is slow and error-prone. With the ANR process, the eNB uses the UE measurement reports to update neighbor relations and establish connections to those neighbors. UE can detect these connections even though they do not yet exist in the eNB neighbor relation lists [36].

3.1.2 Self-Optimization

The goal of self-optimization is to monitor network performance, detect the need for optimization and adjust its parameters autonomously. Monitoring and self-optimization begins after network elements are in an operational state i.e. when the eNB RF interface is switched on. In LTE Release 9, several self-optimization functions were introduced to support mobility load balancing (MLB), mobility robustness optimization (MRO), Random Access channel (RACH) optimization and Inter-Cell Interference Coordination (ICIC) [34]. In LTE Release 10, new SON features were added, such as coverage and capacity optimization (CCO), enhanced ICIC (eICIC), energy savings and Minimization of Drive Tests [34]. In this section, 3 SON functions, coverage and capacity optimization, MRO and MLB, are introduced briefly whereas MDT functionality is described in more detail later in Section 3.1.4.

The purpose of self-optimization of coverage and capacity is to enhance the traditional planning methods by adjusting eNB configuration (transmission power, resource allocation and antenna parameters) autonomously for ensuring better network performance [36]. The CCO aims to improve system capacity while keeping the downlink and the uplink coverage sufficient. This usually means that certain tradeoffs between capacity and coverage must be made. Self-optimization of coverage and capacity allows the network configuration to be continuously tuned at a faster pace. This allows for a faster reaction to dynamically changing network conditions and ensures higher utilization of the deployed network elements.

The purpose of mobility robustness optimization is to self-optimize the handover parameters that are used to improve mobility between the cells. This is accomplished by reducing the number of handover problems due to poor network parameterization [36]. In cellular networks, the handover procedure is triggered by measurement events, for example Event A3[1]. To achieve optimal performance, these events can be configured differently depending on the frequency, cell or cell-pair specific parameters [58]. However, this makes manual optimization of the parameters a time consuming and expensive task. This is especially true if it is done separately for each cell-pair. The MRO algorithm monitors handover problems such as short stay handovers, handovers that happen too early, handovers that happen too late and handovers to wrong cells, and adjusts the measurement configurations so that handovers trigger faster or slower, thus avoiding handovers to poor eNB candidates [34].

The purpose of load balancing is to balance network load and resource usage between eNBs. By doing so, higher resource utilization in all cells can be ensured. In mobility load balancing, eNBs exchange load information and adjust handover parameters between the cells so that UEs from an overloaded cell are handed over to under loaded cells in a coordinated manner [37], [38].

[1]A3 Event triggers when target cell is an offset better than the serving cell.

The fundamental difference between MRO and MLB illustrates one of the challenges of the SON framework. The MRO function controls handover parameters to improve the overall mobility performance whereas MLB wants to relax the handover parameters and push UEs towards the second best serving cell candidate so that the load is balanced. This type of situation can easily lead to conflicting optimization goals.

3.1.3 Self-Healing

The goal of the self-healing process is to automate the overall fault management process in self-organizing networks [15]. As described in Section 2.3.4, manual troubleshooting is time consuming and laborious. Furthermore, it is a complicated process in complex multi-layer and multi-RAT networks. Hence, it is foreseen that reliable and robust self-healing algorithms can increase the efficiency of the fault management process while providing additional cost savings. This means automating fault detection; root cause analysis; and the process of recovering from or compensating for performance degradation.

In E-UTRAN, self-healing use cases have been mostly related to network outage management situations based on network outage detection and outage compensation procedures for example as in [34]. The aim of outage detection is to identify network areas that do not have sufficient service coverage. An outage can be caused either by poor planning or poor hardware. It can also be caused by software or parameterization failures in the network elements. In outage compensation, the network is self-optimized to compensate for the outage by improving the coverage by other means, for example extending the coverage of the neighboring cells by uptilting antennas.

In [39] and [40], a framework for cell outage management in LTE was presented. It describes the key components that are necessary for detecting and compensating for outages, as well as what is necessary for developing and evaluating the required algorithms. Moreover, in [41], an experimental self-healing framework was developed for LTE networks where detection and compensation for cell outages are evaluated in a realistic environment. The experimental framework is capable of early fault detection and executing correction tasks automatically. It was observed that the early detection and the execution of compensation tasks improves the network grade of service by reducing the number of radio link failures and by increasing the number of users being able to connect to the network. Hence, it is expected that by automating the fault detection process, operators can reduce the complexity of network troubleshooting and react faster to network failures. This is discussed in for example, [42] and [43]. In particular, the second generation of operational fault detection algorithms that was introduced in [42], describes the principles of automating fault detection in cellular network. The principles are discussed in more detail in Section 4.2.4

In the scope of this thesis, one research goal is to study self-healing algorithms that autonomously detect coverage problems such as coverage holes and sleeping cells. The coverage holes are areas that do not have sufficient service coverage whereas a sleeping cell is a cell where performance is degraded, but a network alarm is not raised. This makes sleeping cells hard to detect by just observing the traditional performance KPIs or alarms. This is also a very important aspect of autonomous fault detection because there are differences between automating the detection of known problems and autonomously detecting suspicious network behavior. The core parts of the studied self-healing algorithms consist of two enablers:

- Automated means for gathering data that is used for detecting the coverage problems;
- Means of knowledge mining for enriching that data to meaningful knowledge patterns.

These enablers allow similarities between known problems and suspicious network elements to be found. This helps to understand the root cause of a problem and guides self-optimization. Traditionally, data for coverage optimization and troubleshooting has been collected by means of manual drive tests. However, the concept of MDT that is described in Section 3.2 introduces an automated mechanism for gathering coverage data from user terminals; the concept of knowledge mining is discussed later in Chapter 4.

3.2 Minimization of Drive Tests

As discussed in Chapter 2, mobile operators need to carry out various field measurements throughout the life cycle of a network to make sure that sufficient coverage, capacity and QoS are achieved in both indoor and outdoor locations. Traditionally, drive tests have been employed for this purpose but it has two major limitations. Firstly, manual drive testing is a resource consuming task that requires time, specialized equipment and the involvement of highly qualified engineers. This has the potential to cause high OPEX. Secondly, it is difficult in practice to measure coverage completely from every geographical location with manual drive testing. This is the case because most of the UE generated traffic comes from indoor locations, while drive tests are limited mainly to the roads. This makes drive testing an expensive task that is limited in practice by cost and reachability constraints. For these reasons, the minimization of such drive tests was identified by NGMN as one of the top SON use cases that should be automated in self-organizing networks [7]. After the minimization of drive tests use case was introduced by NGMN [31], a feasibility study for the use case was started in 3GPP [20].

The goal of the feasibility study was to define solutions that reduces the need for conducting drive tests by introducing the automated collection of coverage measurements from user terminals. By collecting the measurements with the location and time stamp, a comprehensive radio environment database can be built autonomously to support network optimization. During

the feasibility study, coverage optimization, capacity optimization and QoS verification were identified as the main use cases of the MDT. The purpose of the coverage optimization use case is to support coverage mapping and detect network problems such as coverage holes, weak coverage, overshoot coverage, and issues with uplink coverage [20]. This is different from the SON coverage and capacity use case which also aims to optimize the network. Hence, there is a fundamental difference between the purpose of MDT and SON in 3GPP. After the feasibility study, 3GPP focused on defining MDT measurement and reporting schemes for LTE and HSPA [44]. The measurement and reporting schemes are known as *immediate MDT* and *logged MDT*, and configuration of these schemes relies on signaling that is reusing the functionality of Subscriber and Equipment Trace [21], [45].

It is worth noting that the collection of UE radio measurements with the location and time information is not a new concept. The problem and related work has already been addressed e.g., in the ITS-CELLO project [46], [47], [48], [49], where the goal was to develop methods for location aided network planning, handover management and mobility management. However, comprehensive usage of the location aided functionalities requires support from a wide range of UEs, and therefore, the proposed methods are not applicable until automatic collection of such measurements is supported by the standards. Research related to applications which use MDT or have a similar functionality has been discussed recently in [50], [52], [53], [54]. In [50], the detection of uplink and downlink coverage problems is studied by using MDT measurements, and the analysis is carried out in a similar way as in [P3]. In [52], layered radio environment map architecture is described along with how it is applied to an MDT coverage hole detection use case. In [53], [54], REM based automated coverage hole detection is enhanced by using spatial interpolation of radio coverage that is based on the Bayesian Kriging technique. While interpolation is found to be useful for MDT-like applications, the automated coverage hole detection approach is still based on a simple threshold comparison. This is different from [P4] and [P5], where advanced knowledge mining techniques are used to learn about network behavior and subsequently analyze network performance from high dimensional data sets.

Moreover, in [55] and [56], MDT measurements are used to verify QoS and detect sleeping cells in LTE networks. The findings in [56] suggest that MDT measurements can be used to estimate the level of QoS with high precision if the throughput metric is normalized. Without normalization the chosen scheduler in eNB significantly affects the estimation and creates poor correlation between the MDT measurements and the experienced QoS. In [55], MDT measurements are used to detect a sleeping cell which has a high RACH failure rate. Sleeping cell detection is improved based on an *n*-gram analysis of subsequent MDT events whereas in [P4] and [P5], the detection was only based on the MDT radio measurements in a different sleeping cell scenario.

3.2.1 MDT Architecture

The aim of MDT functionality is to collect UE-specific radio measurements by using an architecture based on control plane signaling in UTRAN and E-UTRAN networks. The benefit of using control plane architecture is that it allows RAN nodes (i.e. an eNB or RNC) to include additional data in UE measurements. The measurements for MDT can be configured either by using management-based or signaling-based configuration procedures [44], [45]. In signaling-based MDT, subscriber and equipment trace functionality is used to configure a specific UE based on its International Mobile Subscriber Identity (IMSI) or International Mobile Equipment Identifier and Software Version (IMEI SV) [45]. In management-based MDT, trace functionality is used to configure a specific RAN node for collecting measurements for a certain area. Configuring the management-based MDT is straight-forward because the parameters are sent directly to the RAN nodes that are responsible for selecting the UEs for MDT. This is different from signaling-based MDT which involves more core network elements.

Since this thesis is more about processing and analyzing the data collected from a set of UEs, the following sections focus on applications that employ a management-based MDT procedure. An illustration of management-based MDT architecture is depicted in Figure 8, which is based on [15], [44], [45], [50], [51]. In management-based MDT architecture, O&M or an element manager sends an MDT trace session activation request directly to the eNB or RNC. This request includes parameters for configuring MDT measurements such as Trace Reference, Trace Collecting Entity (TCE) address, area scope (i.e. a list of cells) and measurement configuration. After receiving the parameters, the eNB selects UEs that have given consent for an operator to perform the immediate or logged MDT measurements and assigns Trace Recording Session References that correspond to the selected UEs. It is worth highlighting that immediate and logged MDT measurements are configured as separate trace sessions. Immediate MDT refers to a measurement reporting mode for UEs that has an established Radio Resource Control (RRC) connection, whereas logged MDT refers to a measurement mode for UEs that are normally in an RRC idle state [44]. With immediate MDT, existing RRC measurements are used to gather the MDT measurements. For this reason, RRC measurement reporting functionality is extended to include location information that supports MDT [58]. An eNB configures RRC measurements according to MDT parameters such as reporting triggers, measurement intervals and a list of intra-frequency, inter-frequency and inter-RAT measurements. Whenever an eNB receives the RRC measurement reports from UEs, it stores the measurements in a trace record together with its additional MDT information such as time stamp, trace parameters and vendor specific data. The trace records are then forwarded to the TCE [45].

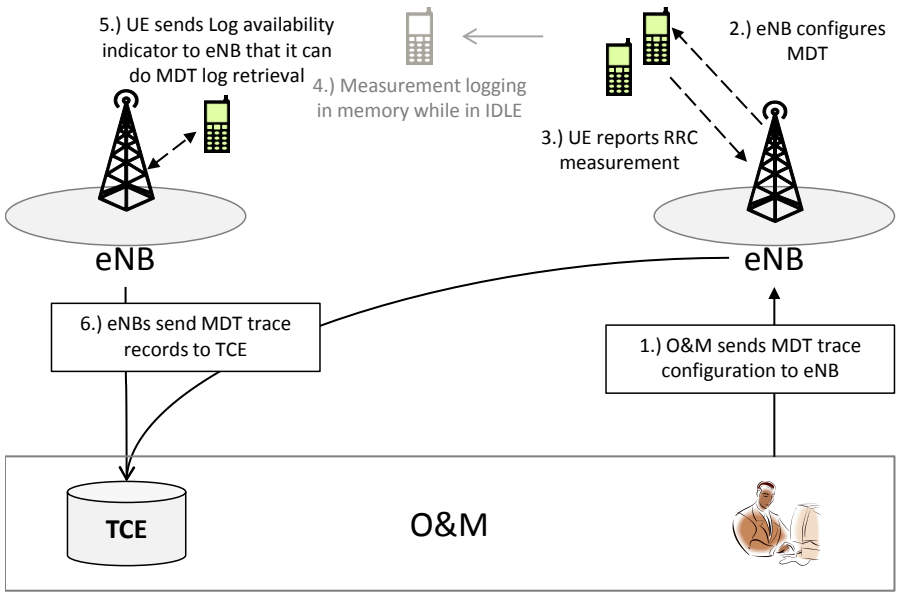

Figure 8: Overview of management-based MDT architecture

Logged MDT measurement and reporting mode allows data collection from UEs that are in an RRC idle state. The configuration for the logged MDT is provided to the UEs via dedicated RRC signaling while they are in an RRC connected state. After the UE moves to an RRC idle state, the measurement data is logged in UE memory. Later when an UE connects back to the network, it indicates that it has logged measurement data available. This allows another eNB on the same RAN to do log retrieval for MDT data and forward the logged data to the TCE.

In LTE Release 11, MDT functionality was extended with several new features that allow for gathering more detailed information, such as [57]:

- Allowing a network to make a request to UE to acquire detailed location information;
- The ability to relax the measurement anonymization level so that it includes device type information to MDT traces records;
- The ability to collect information about connection establishment failures and radio link failures in a centralized manner;
- The ability to measure downlink and uplink throughputs and data volumes.

In particular, the enhancements for gathering the measurement data together with the detailed location information was seen important, and therefore, the ability for a network to request UE to deliver MDT measurements with GNSS location was added to the MDT specifications. During LTE Release 12 research, the discussions of future enhancements of MDT have not been active in 3GPP.

3.2.3 MDT Measurements

The MDT procedure allows operators to collect radio measurements, i.e. received signal strength and quality, with UE location information and a time stamp. In immediate MDT, the measurements can be conducted either periodically or when a trigger such as a network event happens [44]. In logged MDT, the measurements are collected periodically. The MDT measurements consist of:

- The location information with the longitude and latitude (if available);
- A time stamp either from a UE or eNB depending on the MDT mode;
- The cell identification data and the radio measurements for serving cell and detected intra-frequency, inter-frequency and inter-RAT neighboring cells.

There are different mechanisms for estimating user location. The most coarse location info is the serving Cell Global Identification (CGI) and in the best case detailed location information is obtained from the Global Navigation Satellite System (GNSS). If detailed location information is obtained from GNSS, then the measurement report shall consist of latitude and longitude, and a GNSS time stamp. Depending on availability, altitude, uncertainty and confidence can be also included [44]. It is worth noting that for immediate MDT, the network can make a UE attempt to make GNSS location information available for MDT [44].

With immediate MDT, the UE does not send time stamp information as it does in the case of logged MDT. Instead the eNB is responsible for adding the time stamp to the received MDT measurement reports when saving them to the trace records. However, if GNSS was used, the GNSS time information is included as a way to validate the detailed location information [44]. It is anticipated that this will allow outdoor samples to be separated from MDT samples where location is not known. The cell identification information consists of the serving cell CGI or Physical Cell Identifications (PCI) of the detected neighboring cells. The measurements for both the serving and neighboring cells include the Reference Signal Received Power (RSRP) and Reference Signal Received Quality (RSRQ) for LTE. Similarly, common pilot channel Received Signal Code Power (RSCP) and received signal quality (EC/N0) are measured for a UTRAN system [44].

The MDT procedure can also be used to obtain a UE location for UE accessibility failure reports, for enhanced radio link failure reports, and for other network measurements that are conducted in RAN nodes [44]. The RAN node measurements are used for QoS verification that consists of for example, IP throughput and data volume measurement that can be conducted separately for both a downlink and uplink direction per QCI or per UE in an eNB [44]. The accessibility measurement refers to the logging details of the failed RRC connection establishment attempts and reporting the logs to the network after a successful connection

establishment [44]. Similarly, RLF reporting refers to the logging information of the connection failures experienced by the UE [59]. The connection failure can be a radio link or a handover failure which is triggered if the signal quality in the serving cell reaches an intolerable level, if a random access procedure fails or if the maximum number of Radio Link Control (RLC) retransmissions are sent [58]. Since the content of the accessibility and RLF reports can be similar to the MDT reports, they can be combined and correlated to obtain a comprehensive view of network coverage, capacity and quality.

It is expected that the MDT measurement procedure allows operators to gather huge amounts of field measurement data. However, this can easily overcrowd operator databases, and therefore, cost efficient and agile methods for processing the databases are needed in order to acquire information and knowledge from the data. Two essential problems with big databases are *information overflow* and the "*curse of dimensionality*". These problems must be addressed while analyzing and transforming raw measurements into meaningful information. Information overflow refers to a problem where the number of data samples is too big to be processed manually in a way that data analysis can provide useful knowledge. For example, in the case of network alarm floods, some alarms are ignored because it would be too time consuming to process them all. The curse of dimensionality refers to a problem where the dimensions of data samples are high and this makes accurate and efficient processing of such data cumbersome. Methods for addressing these problems are discussed in Chapter 4 and the applications where knowledge mining can be used to process the MDT databases are discussed in Chapter 5.

4. Means and Methods for Supporting Network Self-Organization

This chapter introduces the fundamental principles of knowledge mining and control theory that can provide means and methods for designing automated solutions that address the challenges of network self-organization. Some alternative theories for design principles can be found for example in [60].

4.1 Autonomic Control Function

In automation and control theory, the main principle is that control functions adjust a target system, i.e. network elements, based on references and a feedback loop in order to achieve the desired behavior [61]. This process is illustrated in Figure 9. By using incremental steps and a feedback loop, a control function can autonomously react to changes in the output of a target system. The changes can be normal due to the dynamic nature of the target system or they can be unexpected due to disturbance, uncertainty and noise. It is anticipated that the deployment of a reliable and robust self-organizing network requires intelligent control functions that can tolerate higher degrees of disturbance, uncertainty and noise as a result of the complexity of radio networks which was discussed in Chapter 3. Automation of such networks is challenging because:

- A desired system output can be achieved by tuning many different system parameters, but since control parameters can have intricate interdependencies, there is uncertainty with regards to how the chosen parameter combination affects overall system performance.
- Different SON functions that control one network element can have conflicting goals and this requires coordination between the SON functions to ensure robust behavior. However, coordination can limit control function behavior, thus resulting in suboptimal behavior and disturbance.
- Neighboring network elements also have complex dependencies. Hence, the control decisions in one network element can cause noise and disturbances in the desired behavior of the SON functions in its neighboring elements. Thus, coordination is also required between the SON functions inside one network element as well as between its nearest neighbors.

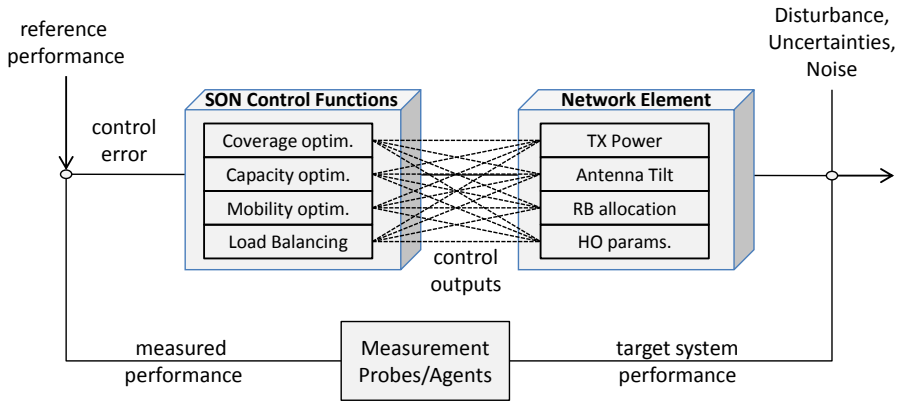

Figure 9: Block diagram for SON control process

These challenges makes it complex to decide which performance metrics should be measured and how often. There are several performance indicator alternatives to choose from and selecting the one that would reveal the effect of a control decision on network overall behavior in the most meaningful way is often difficult. This situation increases the monitoring complexity of automation and self-optimization.

It is envisioned that these challenges can be solved with autonomous computing where more intelligent control functions can monitor and analyze network elements to acquire *knowledge*, and thus, plan and execute control decisions with little or no human involvement. The concept of knowledge mining provides mathematical tools for converting measurements into knowledge that is based on learning from radio network behavior. Although the above-mentioned challenges are more related to the design of self-optimization control functions that operate in an online manner by adapting to the behavior of network elements, they also have an impact on the design of MDT and self-healing functions. For example, in the scope of MDT, knowledge mining can be used for efficient processing of big databases and for finding hidden non-trivial information patterns in the data. While efficient processing is a mandatory requirement as the amount of data increases, the hidden patterns can further help to improve network self-healing and fault management, thus resulting in:

- Earlier detection of network problems and anomalies;
- A lower detection rate of false alarms;
- More autonomous operation and data gathering.

Earlier detection of network problems with a lower false detection rate improves the reliability and robustness of the fault management process. Autonomous operation and data gathering plays an important role for example in helping to determine when enough data is gathered to create reliable alarm detection for a certain area.

4.2 Principles of Knowledge Mining

Knowledge mining is a concept that is used for extracting interesting, previously unknown and potentially useful information from a large amount of data [62]. The process of knowledge mining usually consists of several phases such as data cleaning, database integration, relevant data selection, data mining, and data pattern evaluation. Data cleaning, integration and selection are preprocessing phases where data is prepared for further analysis. Knowledge mining itself can consist of several different functionalities such as classification; clustering and association of data; dimensionality reduction and outlier detection to name a few [62]. In the pattern evaluation phase, information patterns are visualized and analyzed to see if novel and valid information can be extracted. It is worth highlighting that even if interesting information patterns are discovered, it does not mean that it is automatically usable or useful. Therefore, information patterns need to be validated. The following subsections describe in more detail the data mining methods that were used in [P1-P8].

4.2.1 Classification

Classification refers to a supervised learning process for determining a set of models that describe data classes. The purpose of using these models is to classify new data which class is unknown [62]. Sometimes classification is also used to determine missing values in new data by finding the best matching class which characteristics are used for predicting the missing values. The models for describing the classes can be presented in many ways. Often models such as decision trees, statistical models or mathematical models are used. For example, classification algorithms such as rough sets and classification and regression trees (CART), were used for performance measurement analysis in GSM networks in [63].

In this thesis, the decision tree-based approach was used in [P2] to classify radio link failures to coverage failures, interference failures and handover failures. The tree was deduced based on expert knowledge rather than by means of autonomous machine learning. In addition, a mathematical model of *k-Nearest Neighbors* (KNN) was used in [P5] to find similarities between labeled and unlabeled MDT measurements. A similar approach in principle was also applied in [P6] and [P7] for RF fingerprint positioning of MDT samples. The *k*-Nearest Neighbors classification consists of two steps as described in [62]. First, a set of data samples where the class label is known, i.e. *training samples*, are used to construct an *n*-dimensional training database. In the second step, all data samples where the class label is unknown, i.e. *testing samples,* are labeled by finding the *k* nearest training samples among all samples in the training data base. The complexity of the KNN depends on the number of samples in both the training and testing sets, as well as on the dimensionality of the data samples. The algorithm searches for the nearest neighbors because typically a distance metric is used to determine the similarity of the samples.

Various distance metrics for determining the nearest neighbors can be used. In [P5], the well-known Euclidean distance d_e between training sample $\mathbf{p}$ and the testing sample $\mathbf{q}$ was used and it is given as,

$$d_e(\mathbf{p},\mathbf{q}) = \sqrt{(\mathbf{q}-\mathbf{p})^T(\mathbf{q}-\mathbf{p})}, \tag{4.1}$$

where $\mathbf{p}$ and $\mathbf{q}$ are the k-dimensional column vectors in the embedded space that correspond to the diffusion distance between the $\mathbf{p}$ and $\mathbf{q}$ in high dimensional space. In [P6] and [P7], Mahalanobis distance and Kullback-Leibler Divergence (KLD) were employed to determine the nearest neighbors. Mahalanobis distance d_m is given as,

$$d_m(\mathbf{p},\mathbf{q}) = \sqrt{(\mathbf{q}-\mathbf{p})^T \boldsymbol{\Sigma}_\mathbf{p}^{-1}(\mathbf{q}-\mathbf{p})}, \tag{4.2}$$

where $(.)^T$ denotes the transpose operation and $(.)^{-1}$ denotes the matrix inverse. In (4.2), the distance is normalized based on the inverse of the covariance matrix $\boldsymbol{\Sigma}_\mathbf{p}$ to make it scale-invariant. Kullback-Leibler Divergence d_{kl} is a non-symmetric measure of the relative entropy between two probability distributions rather than distance and it is given as,

$$d_{kl}(\mathbf{p},\mathbf{q},) = \frac{1}{2}\left((\mathbf{q}-\mathbf{p})^T \boldsymbol{\Sigma}_p^{-1}(\mathbf{q}-\mathbf{p}) + tr\left(\boldsymbol{\Sigma}_q\boldsymbol{\Sigma}_p^{-1} - \mathbf{I}\right) - \ln\left|\boldsymbol{\Sigma}_q\boldsymbol{\Sigma}_p^{-1}\right|\right), \tag{4.3}$$

where $tr(.)$ denotes the trace operation, $|.|$ is the determinant operation and $\mathbf{I}$ is the identity matrix. One notable difference between d_m and d_{kl} is that in (4.3), the covariance matrix $\boldsymbol{\Sigma}_\mathbf{q}$ and inverse of the covariance matrix $\boldsymbol{\Sigma}_\mathbf{p}$ are used whereas in (4.2) only the inverse of the covariance matrix of training data $\mathbf{p}$ is employed. The final step in the KNN algorithm is to label the unknown sample based on the k nearest training samples. There are various ways to define the class based on the characteristics of nearest neighbors. One simple way for example, is to use the most common class among the k nearest training samples.

4.2.2 Clustering

Clustering refers to an unsupervised learning process where data is grouped into different *clusters*, i.e. classes without predefined labels, by maximizing the similarities among the samples within one cluster while minimizing the similarities with samples in other clusters [62]. In clustering, the purpose is to find methods for measuring similarity or dissimilarity between the samples in different clusters. For numerical variables, distance metrics such Euclidean distance, as in (4.1), can be used. For other variable types such as categorical data or a mixture of numerical and categorical data, more sophisticated similarity metrics are needed. For example, if data contains categorical values such as a type of failure, it is not self-evident how one can measure the dissimilarity between the different failure types. Moreover, in some applications, numerical variables must be unitless variables, i.e. s*tandardized*, to avoid the dependence of the chosen

measurement unit [62]. Hence, by standardizing the measurement, one attempts to weigh all of the different variables in the *n*-dimensional data set equally. For this purpose (4.2) can be used.

A heuristic method of *k*-means clustering has been applied in [P4] to find clusters for both normal and anomalous samples. The *k*-means algorithm partitions a set of numerical samples into *k* clusters where the center of the cluster is defined for example, as the mean value of all samples belonging to the cluster. In the beginning, randomly selected *k* samples present *k* different clusters and their centers. The remaining samples are assigned to different clusters one by one based on the distance to the center of the cluster. After finding the cluster with the shortest distance, the centers of the clusters are updated with new mean values that take the new sample into account. One of the drawbacks of the *k*-means clustering algorithm is that it is not suitable for detecting nonconvex shapes or clusters of very different sizes. In addition, it is sensitive to noise and outliers because a small number of such points can influence the value of the center of point [62].

4.2.3 Anomaly Detection

Anomaly detection or outlier detection refers to a use case for clustering where the purpose is to cluster samples into two groups. One group contains samples with consistent behavior and the other contains samples with inconsistent behavior. This procedure typically consists of two steps. The first step is to define a criterion for consistent and inconsistent data samples. This requires expertise and knowledge about the behavior of data. In the second step, an efficient method for detecting the samples that have similar characteristics as the inconsistent samples is employed. Several approaches for outlier detection can be found in the literature, for example statistical-based, distance-based, density-based and deviation-based outlier detection approaches [62], [64].

In the scope of cellular networks, the anomaly detection task could be to find anomalous network elements, for example eNBs, whose behavior is inconsistent and suspicious. Traditionally, the detection of suspicious behavior has been based on the network alarms which trigger when test statistics based on the event counts exceeds a predefined threshold [42]. There are at least two different fundamental principles for detecting anomalies in base station behavior. This was discussed in [42], [P5]. The anomalies can be detected:

- In time domain by explicit learning;
- In the network element domain by correlating.

In time domain detection, the behavior of a target base station is compared with its observed behavior earlier in time. For this reason, time domain profiles are created. However, anomaly detection in time domain can be tricky due to the seasonal or other cycling changes, and thus, the anomalies can be hidden in the trend, thus making detection more challenging [62]. Creating reliable time domain profiles can require long monitoring and data gathering periods.

On the other hand, inconsistencies can be detected in a base station domain by comparing the behavior of the target base station to the behavior of other similar base stations. The assumption is that base stations with similar characteristics, for example neighboring base stations, correlate on some level when they are operating as expected. Therefore, a lack of correlation would reveal suspicious behavior. In the latter case, more data is gathered in a shorter time period and long learning periods in time domain are not needed, but the data can be biased if the neighboring base stations behave differently, for example due to the slightly different parameterization. In [65], the correlation of the network load levels in neighboring base stations was studied based on empirical data from a 3G network. The study indicated surprisingly low correlation levels between the neighboring cells. Only 14% of the neighboring cells had a correlation that was higher than 0.5 when load statistics were collected with a granularity of one hour.

In [42], time domain and base station domain detection algorithms were introduced based on the observations of the loading levels in the base stations. In [43], a hierarchical fault detection framework for detecting faults in a base station on a sector and a carrier level was introduced. In the hierarchical detection framework, statistical hypothesis tests are used based on a combination of parametric and non-parametric test statistics. The difference is that the parametric statistical test can be used when the test statistics are drawn from known distributions whereas the non-parametric tests are employed when the distributions are unknown. In [66], [67] and [68], the anomaly detection is based on the statistical profiling in time domain. In [66], a general detection and diagnosis framework is introduced. The detection is based on creating statistical profiles of KPIs which are associated with faults. The framework has similarities with the *Case-Based Reasoning* methodology since the fault knowledge database is learned autonomously (or with expert assistance) from earlier fault situations. In [67], detection is improved by learning statistical profiles by constructing empirical distributions rather than by using normally distributed KPI statistics as in [66]. The improved detector is based on a common statistical primitive derived from the sample Kolmogorov-Smirnov test and its performance is validated by analyzing the amount of voice and data call establishments per cell in live 3G networks. In [68], the detection is also based on the uplink packets that are used for establishing data connections. However, in this case, a Kullback-Leibler Diverge metric is used for discriminating between the empirical distributions. In this thesis, particularly in [P4], [P5], anomaly detection relies on learning but the statistical apparatus and the test statistics are different.

The anomaly detection in [P4] is done jointly based on the distance and the density metrics of the test samples in low dimensional embedded space. It was observed that by using both metrics, anomaly detection is improved compared with a case where only a density metric is employed. Hence, a sample is an anomaly if it is far away from the group of common samples

and it does not have many similar samples nearby that indicate another undiscovered group of common samples. In [P4], the density of the samples is determined based on the *k*-dimensional ball. For each point in the embedded space, a *k*-ball with a certain radius is defined and the density is calculated based on the samples which lay inside the ball by using any normalized density function. Since the scale of each diffusion coordinate in the embedded space is different, the ball radius is scaled as well. The density ρ_m of the *m*th point is defined as,

$$\rho_m = \frac{\eta_m}{\sum_{i=1}^{M} |\eta_i|}, \tag{4.4}$$

where η_m is the number of points inside the ball and the sum in the denominator is norm-1 over all M points. If the density of a certain point is large in the embedded space then it has many neighbors nearby and it is considered to be regular. On the contrary, irregular points would have a small density. After obtaining the densities, *k*-means clustering was employed to search for the anomalous samples. The *k*-means algorithm used Euclidean distance metric to group the samples consisting of seven variables in the embedded space. That is, each sample consisted of the six most meaningful diffusion coordinates and the density variable.

In [P5], the anomaly detection is based on tracking the absolute standard score in the base station domain. First, a statistical model for network outage behavior for a set of base stations is constructed based on the observations during the learning phase. Later in the tracking phase, the absolute standard score, i.e. the anomaly score, for each base station is computed as,

$$z_i = \frac{|x_i - \mu_L|}{\sigma_L}, \tag{4.5}$$

where variable x_e is the number of outage samples associated with eNB i and variables μ_L and σ_L are the expected mean and standard deviation of the outage samples that characterize outage behavior in the eNBs local neighborhood during the learning phase. If z_i is much larger than one, then eNB i is expected to be an anomaly since the number of outage observations does not fit within the normal deviation of the outage observations.

4.2.4 Dimensionality Reduction

The goal of dimensionality reduction is to represent high dimensional data sets in a lower dimensional space in order to reduce the computational complexity of knowledge mining and to address the curse of dimensionality. The curse of dimensionality refers to various problems in classification, clustering and anomaly detection. Typically, using fewer variables or features in knowledge mining makes the mining process faster, less complicated and more robust. Widely used dimensionality reduction methods are for example, an attribute selection method and a data compression method. In attribute selection, one tries to select a minimum subset of attributes so

that the data mining result will be as close as possible to the result that would be obtained by using the all attributes [62]. The best attributes can be selected for example, based on expert knowledge or statistical significance, assuming that the attributes are independent from each other [62]. In data compression, encoding or transformations are used to obtain a compressed representation of data [62]. Principal Component Analysis (PCA) is a widely used linear data compression method where *k* most significant orthonormal vectors are used to project *n*-dimensional data onto a lower *k*-dimensional subspace while still providing a good approximation of the original data in the lower subspace.

In [P4] and [P5], a non-linear data compression method known as Diffusion Maps is used. Diffusion Maps is a dimensionality reduction method for finding meaningful geometrical descriptions of the high dimensional data sets. It is done by constructing diffusion coordinates and diffusion distance metrics that parameterize the original data set and provide a local preserving metric for the data [69], [70], [71], [72]. Parameterization is done by using a graph G and a weight function kernel W that measure the pairwise similarity of the points in a training set. If a proper kernel function is used, then W can be normalized into a Markov transition matrix. The diffusion is created by conducting a random walk to this transition matrix. The most significant eigenfunctions, i.e. the functions associated with largest eigenvalues, of the transition matrix provide a good low dimensional geometric embedding of the data in a way that Euclidean distance in the embedding space measures the meaningful diffusion metrics of the data. The expression of the diffusion distance $D_t^2(.)$ between data points x_i and x_j can be given as in [72],

$$D_t^2(x_i, x_j) = \sum_{l=1}^{k} \lambda_l^{2t} \left(\psi_l(x_i) - \psi_l(x_j) \right)^2, \tag{4.6}$$

where k is the number of the most significant eigenvectors, t represents the depth of the random walk and variable λ_l is the eigenvalue of the lth eigenvector. The variables $\psi_l(x_i)$ and $\psi_l(x_j)$ are the lth entries of the right eigenvectors of the transition matrix for points x_i and x_j. Moreover, the diffusion coordinates are constructed using k most significant right eigenvectors and eigenvalues as described in [72],

$$\Psi_t(x_i) = \left[\lambda_1^t \psi(x_i), \ldots, \lambda_k^t \psi(x_i) \right], \tag{4.7}$$

where the diffusion coordinates for ith data sample x_i can be obtained from m-by-k diffusion coordinate matrix Ψ_t. The column vectors of Ψ_t are the right eigenvectors of Markov transition matrix multiplied by the corresponding eigenvalue term λ_k as shown in (4.7). Moreover, the diffusion coordinates for a particular point x_i are found in the ith row vector of the diffusion coordinate matrix Ψ_t. As seen from (4.6) and (4.7), the diffusion distance for samples in the high dimensional space corresponds to the Euclidean distance of the samples in the embedded space.

5. Knowledge Mining Assisted Network Performance Improvements

This chapter walks readers through various knowledge mining assisted methods that improve the performance of cellular network. The motivation for using these methods comes from the fact that networks are getting denser and more complex, thus requiring efficient new ways to operate a network.

5.1 Coverage Optimization with Extended RLF Reports

As described in Section 3.2.3, RLF reporting provides a mechanism for a UE to indicate that it has encountered a connection failure. This is a strong indicator from a UE that something is wrong. By extending the RLF report to contain additional information, for example location, radio measurements and cell identification data, it becomes easier to analyze the root cause of the RLFs and learn how networks should be optimized to avoid the occurrence of similar problems. For this reason, coverage optimization of an irregular network layout was studied in [P2] with the assistance of extended RLF reports. It was anticipated that the irregular network layout provides a realistic simulation environment for studying coverage hole related problems due to diverse coverage and interference conditions [P1]. In addition to irregular topology, four artificial coverage holes with a radius of 180 meters were modeled in a system simulator to further emphasize the heterogeneity of the studied scenario. The coverage holes were placed in four different locations: two at the intersection of the border area of three sites with short and long inter-site distance; one between two sites and one at the center of a single sector. It is worth pointing out that the coverage and the interference conditions are quite different depending on the location of the coverage holes.

Coverage optimization was carried out by constructing a classification tree for discriminating between different types of RLFs. The structure of the classification tree was derived from the radio measurements and the number of identified cells reported along with the RLF reports. The structure of the classification tree is illustrated in Figure 10. It is expected that RLF is caused by a coverage problem if only the serving cell is identified and the RSRP threshold is below a predefined level of -120 dBm. If RSRP is above the threshold level, an interference problem is assumed be the cause of the problem. This is the case because downlink RSRP is acceptable, but no other neighbors are detected. If the UE can identify several neighbor cells in addition of the serving cell, the root cause of RLF can be classified as either a coverage problem or a mobility problem. Mobility problems are expected to occur due to the poor selection of

handover parameters or missing neighbor relations. In this study, RLF is classified as a mobility problem if an A3 event has been sent or if the RSRP difference between target cell and serving cell is negative prior to RLF. A negative RSRP difference indicates that the signal level in one of the neighbor cells is stronger compared to the serving cell.

Therefore, the neighboring cell is a better candidate for being a new serving cell and it is likely that a handover to this cell should have been done earlier. The classification and simulation results presented in [P2] suggest that the severity of the coverage problems depend on the location of the coverage hole whereas interference and mobility problems were caused mainly by network loading and handover parameterization. If larger offsets or longer time-to-trigger values are configured then the number of mobility related RLFs increase even if no artificial coverage hole exists. Specifically, Figure 6 in [P2] shows that the number of mobility related RLFs increase even in low loaded network if UE velocity is 30 km/h. However, the increase is relatively smaller compared with the RLFs that are observed with higher network loadings. It was concluded that classification of the extended RLF reports provides additional value to the MDT coverage optimization use case, since it can provide a better understanding of the root cause of RLFs with a rather low false alarm rate. It is worth highlighting that the tree was not constructed autonomously in this study. Instead, expert knowledge was used to develop the structure of the tree. Hence, it would have been interesting see the shape of the tree if machine learning would have been used.

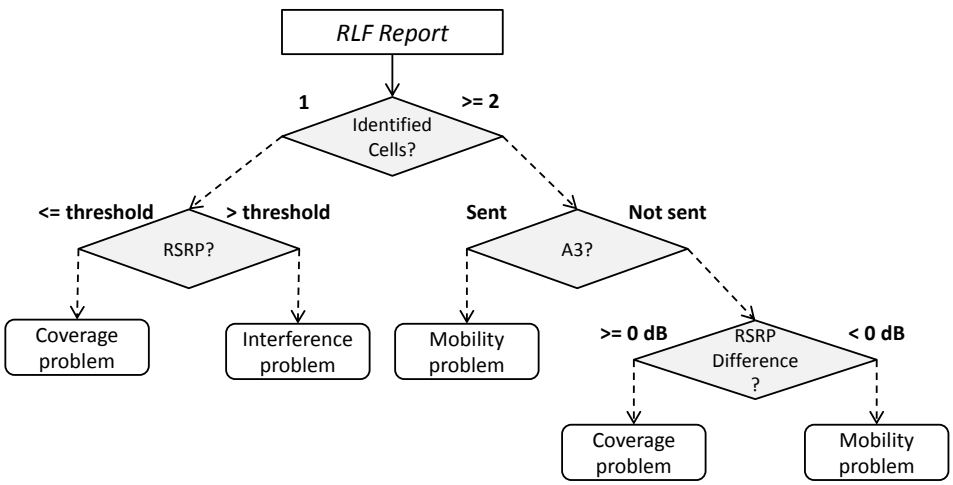

Figure 10: Classification tree for RLF problems

5.2 Smart Discrimination of Uplink Coverage Problems

It is worth noting that the classification tree shown in Section 5.1 does not take into account any uplink related coverage problems since the RLFs in [P2] were triggering only if downlink physical layer problems were detected. In fact, uplink coverage can be limited and cause severe QoS performance degradation without triggering downlink coverage problems. This can occur for example, if there is large imbalance between the downlink and the uplink link budgets due to a poor radio network plan or misconfiguration of the uplink radio parameters. Using MDT for uplink coverage optimization in LTE is supported by collecting UE Power Headroom Reports (PHR). The purpose of the PHR is to inform the eNB about the difference between the nominal UE maximum transmit power and the estimated power for the uplink shared channel (UL-SCH) transmission [73]. The PHR for *i*th subframe in decibel units (dB) is given in as described in [74],

$$PH(i) = P_{\mathrm{CMAX}} - \left\{10\log_{10}(M_{\mathrm{PUSCH}}(i)) + P_{\mathrm{O\_PUSCH}}(j) + \alpha(j)\cdot PL + \Delta_{\mathrm{TF}}(i) + f(i)\right\}, \quad (5.1)$$

where variable P_{CMAX} is the UE maximum transmission power and the variables inside the curly braces are the output of the LTE uplink power control procedure. The variable $M_{PUSCH}(i)$ is a number of Physical Resource Blocks (PRB) allocated for *i*th subframe. The variables $P_{0\_PUSCH}(j)$ and $\alpha(j)$ are uplink power control parameters that define minimum transmission power level per PRB and pathloss compensation factor for the measured downlink pathloss *PL*. The *j* depends on the transmission type i.e., whether a semi-persistent or a dynamically scheduled grant is provided. The variable $\Delta_{TF}(i)$ is the Modulation and Coding Scheme (MCS) dependent constant offset of *i*th subframe. The variable $f(i)$ is a function that provides relative, cumulative or absolute corrections to the closed loop power control mechanism. The PHR reporting range is from 40 dB to -23 dB. Although UE transmission power never exceeds the maximum transmission power, negative PHR values are reported if the content of the curly braces becomes larger than P_{CMAX}. This can occur for example if scheduled PRB allocation $M_{PUSCH}(i)$ is too large or if power control parameters $P_{0\_PUSCH}(j)$ and $\alpha(j)$ are not properly configured for the observed pathloss levels.

It is anticipated that, if PHR and MDT measurements are correlated when UE transmit power headroom becomes less than a threshold, operators can recognize insufficient uplink link budgets and predict achievable uplink throughputs [20]. Therefore, two types of uplink coverage problems were studied in [P3]. The first problem is a misconfiguration of the $P_{0\_PUSCH}(j)$ parameter and the second is a misconfiguration of the antenna downtilt angles. Both problems can results in uplink outage i.e., coverage problems where either received power or signal quality in uplink are close to their minimum acceptable levels for maintaining the connection to the network. The difference between the problems is that misconfiguration of $P_{0\_PUSCH}(j)$ only affects uplink performance in one eNB whereas downtilting antennas from 6 degrees to 12 degrees affects both uplink and downlink coverage. For evaluating the performances of two problem

scenarios, statistics for PHR, UL received power and UL signal to interference ratio were compared with the performance of the optimized reference scenario. In the reference scenario, the uplink power control parameters were configured according to a strategy where a scheduler aims to schedule one PRB UL-SCH allocation for UEs at the cell edge as discussed for example in [38]. This ensures that the UEs will allocate all available power to the single PRB at the cell edge, thus maximizing the received power per Hz and the uplink coverage. By adjusting the uplink power control parameters, more bandwidth at the cell edge can be provided. However, if $P_{0\_PUSCH}(j)$ is reduced too much in contrast to the chosen $\alpha(j)$, then uplink transmission may drown out in the noise, thus resulting in uplink coverage problems that cannot be not detected by observing PHR.

Table I and II gather the main results from the figures presented in [P3] and show the performance comparison between the studied scenarios for the three centermost base stations. These base stations are eNB-8, eNB-16 and eNB-18. In Table I, the performance indicators are for the simulated scenarios where a parameter for building penetration loss was set to 10 dB. The values in Table II correspond to the simulations where the building penetration loss was increased to 15 dB. The following conclusion was made based on the simulation results in [P3]. First of all, PHR behavior depends on the uplink power control parameterization and the scheduled allocation size. If one is confident that uplink coverage problems are not caused by misconfiguration of the power control parameters, then PHR condition exceeding a threshold can be used to detect uplink problems. This can be seen by observing the probability of PHR being less than 0 dB, thus meaning that all available power is used. In the coverage problem case that is caused by overtilted antennas, the probability of PHR exceeding the threshold is much higher than in the reference case. However, it is beneficial to scale the PHR with the allocation size before making any conclusion about uplink coverage problems in order to avoid unnecessary signaling over the air interface. It was observed in [75], that the probability of PHR exceeding the threshold is approximately 35% if PHR is not scaled whereas for the scaled PHR the corresponding probability was around 5%, thus indicating significantly less false alarms.

It was also observed that if the power control parameters are not configured properly, PHR do not necessarily trigger at all. This can be seen by comparing the probability of PHR being less than 0 dB in the reference and the misconfigured $P_{0\_PUSCH}(j)$ scenarios. By reducing the $P_{0\_PUSCH}(j)$, UEs would allocate less transmission power per PRB. This on the other hand results in larger PHR values which suggest that UE can support larger bandwidth allocations. In this case, *PHR_perPRB* do not exceed the threshold but the uplink received power (RXP) and the signal to interference and noise ratio (SINR) would be very poor, thus suggesting a severe uplink outage as show in Table I and Table II.

Table I: Uplink performance indicators for 10 dB building penetration loss scenarios [P3]

Building Penetration Loss is 10 dB	*Reference*			*Misconfigured P0*			*Overtilted antennas*		
	eNB-8	eNB-16	eNB-18	eNB-8	eNB-16	eNB-18	eNB-8	eNB-16	eNB-18
Pr(PHR_perPRB < 0dB)	5.0%	2.5%	5.0%	0.0%	3.1%	4.0%	20.0%	13.0%	9.0%
5%-ile UL SINR [dB]	-1.8	-1.3	-2.1	-14.2	-1.1	0	-3.5	-1.8	-1.8
5%-ile UL RXP [dBm]	-114	-113	-114	-124	-113	-114	-119	-116	-116

Table II: Uplink performance indicators for 15 dB building penetration loss scenarios [P3]

Building Penetration Loss is 15 dB	*Reference*			*Misconfigured $P_{0\_PUSCH}(j)$*			*Overtilted antennas*		
	eNB-8	eNB-16	eNB-18	eNB-8	eNB-16	eNB-18	eNB-8	eNB-16	eNB-18
Pr(PHR_perPRB < 0dB)	4.0%	1.9%	3.5%	0.0%	1.4%	3.8%	14.0%	8.2%	9.0%
5%-ile UL SINR [dB]	-3.8	-3.6	-3.6	-16.1	-3.7	-3.5	-5.9	-4.5	-4.2
5%-ile UL RXP [dBm]	-120	-119	-120	-130	-119	-120	-124	-122	-123

According to the link level simulation results and a link budget calculation, SINR and RXP threshold values of -5 dB and -123 dBm are reasonable values for the uplink outage. The dotted horizontal lines in [P3] resembles these thresholds. According to Table I and Table II, these threshold are not exceeded at the cell edge in the reference case. However, in case of the parameter misconfiguration, the thresholds are exceeded indicating uplink outage.

5.3 MDT assisted Sleeping Cell Detection

The purpose of self-healing is to provide functions which improve automatic control of cellular network operations for detecting and handling network failures. A sleeping cell is a special case of malfunctioning base station where the base station appears to be operable while its performance is degraded. One approach for detecting a sleeping cell is to monitor the changes in the base station's neighbor relation patterns as suggested in [76]. Another approach is to monitor network traffic and loading profiles and detect suspicious behavior from these profiles as discussed in [42], [65]. In [P4] and [P5], the goal is to study an alternative framework for detecting a sleeping cell with degraded downlink performance. The detection framework is based on employing the Diffusion Maps knowledge mining method to find hidden patterns from MDT databases. The research was carried out by conducting system simulations for gathering MDT reports and RLF reports. In the reference scenario, the network is in healthy state, coverage is optimized, and the RLF rate is low. In the problem scenario, the antenna line for eNB-8 is malfunctioning causing outage and higher RLF rates. Dominance areas for the reference and the problem scenario in [P5] are depicted in Figure 11. The dominance area indicates the area where a particular cell is the strongest serving cell. In the leftmost illustration in Figure 11, the dominance area of eNB-8 is shown with a turquoise color that covers less than 5% of the analyzed area. This is similar to the dominance areas of the other cells.

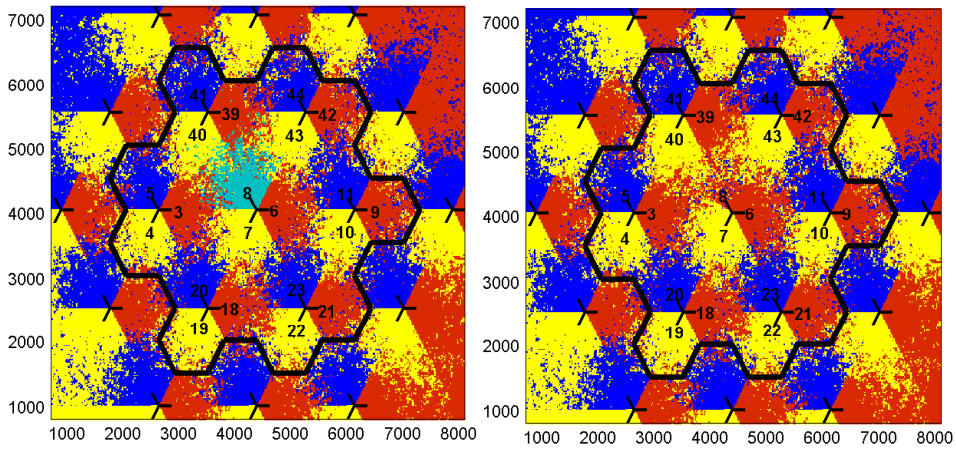

a) Optimized reference scenario *b) Sleeping cell scenario*

Figure 11: Simulated network dominance areas

In the rightmost illustration, eNB-8 is sleeping and it is not transmitting anything in a downlink direction. Therefore, the area is served by the neighboring cells. It is worth pointing out that detection of the sleeping cells based only on the RLF reports is not a straight-forward process for two reasons:

- Firstly, the neighbor base stations can partly cover the service area of the sleeping cell. Thus, the coverage can be weak but severe outage is not necessarily detected.
- Secondly, in multi-layer and multi-RAT radio networks, UEs can be handed over to overlapping layers on a different RAT before RLF triggers.

Hence, the number of RLFs can remain small and detection of outage or sleeping cells based only on the extended RLF reports become challenging. The motivation for finding hidden patterns from MDT databases was to identify periodical MDT reports that have similarities with RLF reports. This is anticipated to enable earlier outage detection even in a case where only an insufficient amount of RLF reports are observed.

5.3.1 Clustering based approach for Sleeping Cell Detection

In [P4], the purpose is to study how unsupervised *k*-means clustering method groups extended RLF reports and those MDT reports that are triggered by an A2[2] event. Clustering is done for the reports after transforming them into a low dimensional embedded space by using diffusion maps. The analyzed MDT and RLF reports contained RSRP and RSRQ radio measurements from the serving cell and the three strongest neighboring cells on the same frequency band. In addition, it

[2]A2 Event triggers when serving cell is less than a threshold.

is assumed that the eNB would incorporate the Wideband Channel Quality Indictor (WCQI) into the MDT and RLF reports. Thus, the high dimensional presentation of the MDT and RLF samples consisted of 9 numerical variables. The MDT reports from the reference simulation are used for training the Diffusion Maps algorithm to construct the presentation of the embedded space in a case where the network behavior is normal. After the training phase, all MDT and RLF reports from the problem scenario were transformed into this embedded space and the samples were clustered into two groups. The group with most of the sample is assumed to represent the *normal* group because it has similar behavior as the MDT reports in the reference simulation. The other group, the *anomalous* group, would contain the samples which are not similar to the samples in the normal group. It is expected that most of the RLFs and some of the A2 events which have similar characteristics with RLFs would fall into the anomalous group.

After clustering the samples, sleeping cell detection is done by finding the most probable dominance area for the anomalous samples by comparing their location, i.e. by using GNSS coordinates or RF fingerprint, with the operator's database of the dominance areas. This is illustrated in Figure 12. In this study, the availability of GNSS coordinates is assumed to be ideal, and therefore, the correlation between the location of the anomalies and the expected dominance areas was simple. The performance results indicated that the majority of the anomalies, i.e. more than 50%, fall into the dominance areas of eNB-8 and eNB-16 as illustrated in Figure 12. eNB-8 is the sleeping cell and eNB-16 is an adjacent cell to the sleeping cell. In addition, it was observed that approximately one-third of the anomalies associated with eNB-8 were MDT reports triggered by an A2 event, thus suggesting that sleeping cell detection would be possible to some extent based solely on the MDT reports without knowledge of RLFs.

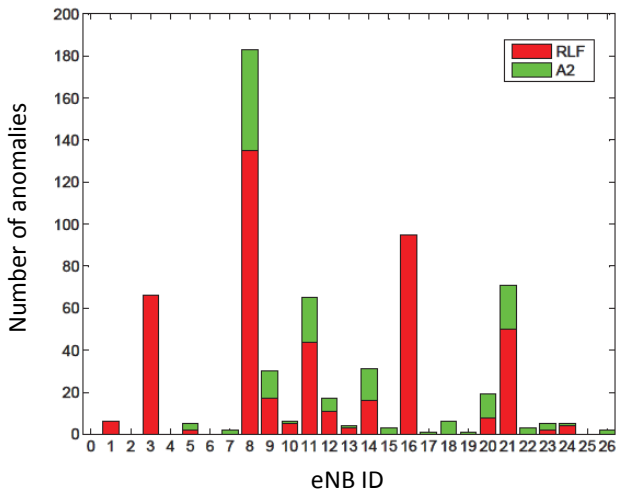

Figure 12: Number of anomalies per e-NB

It is worth highlighting that MDT reports with less accurate location information increase the probability of associating anomalies with the dominance area of wrong base station. According to the simulation results in [P7], two-thirds of MDT reports can be located with positioning error less than 276 meters if fingerprinting is used. However, if one of the cells is sleeping, the error of fingerprinting can be even more significant. It is expected that in such case the anomalous measurements are distributed among neighboring base stations. This increase the amount of MDT measurements that are needed to detect the problem. On the other hand, network can control which MDT samples are used to detect the anomalies. If enough measurements can be obtained with accurate location information then samples with less accurate location can be neglected.

5.3.2 Classification based Approach for Sleeping Cell Detection

In [P5], sleeping cell detection was improved by classifying all periodical MDT reports and extended RLF reports into three classes: *Periodical*, *Handover* and *Outage*. This was done by using the KNN classification algorithm based on the diffusion coordinates and distance. The motivation for classifying the periodically transmitted MDT reports is to detect areas which have similarities with the samples that belong to the outage category. This is different from [P4], where clustering is employed only for MDT reports that are triggered by an A2 event condition. The performance of the classification is verified by using 8-feature and 10-feature classifiers. The 8-feature classifier analyzes MDT and RLF reports that contain only RSRP and RSRQ radio measurements from the serving cell and the three strongest neighboring cells whereas the 10-feature classifier assumes that the serving eNB would include two additional measurements (WCQI and PHR) in the MDT and RLF reports before transmitting the trace records to the TCE for post processing.

The confusion matrices shown in Table III and Table IV illustrate the classification accuracy of the 8-feature and the 10-feature classifiers. The diagonal cells of the confusion matrices show the outcome of a *true-positive* test which indicates the likelihood that a sample is correctly labeled according to the class it belongs to. A *false-positive* test indicates the likelihood that samples are labeled incorrectly and have been assigned to the wrong classes. Table III shows the classification accuracy of MDT and RLF samples in the reference simulation. It can be seen that the true-positive probability is more than 80% for all class types regardless of the classifier that is used. The 10-feature classifier performs better but the performance of the 8-feature classifier is not much worse either. It is worth highlighting that we do not expect to achieve 100% classification accuracy, since it is quite likely that some of the periodical, handover and radio link failures would have similar characteristics in any case; this is especially true because the periodical reports are transmitted frequently. The reports preceding a handover or a radio link failure event are assumed

to have similar characteristics. The numerical value in parenthesis following the real class label in the tables indicates the total amount of analyzed samples in each class. After classifying the MDT reports based on either 8-feature or 10-feature classifiers, the detection of the sleeping cell is done by counting the number of suspicious MDT reports that have similar characteristics with samples collected from outage regions i.e., RLF samples. These samples are associated with eNBs based on the geographical location of the samples and the dominance areas of the eNBs. The relative number of outage samples that are associated with different eNBs in a case where a 10-feature classifier is used is shown in Figure 13.

Table III. Confusion matrices for reference simulation data

Real Class	8 features (only RSRP & RSRQ)			10 features (with CQI & PHR)		
	Per.	HO	RLF	Per.	HO	RLF
Periodical (148723)	96.4 %	2.9 %	0.7 %	96.6 %	2.9 %	0.5 %
Handover (698)	11.9 %	82.1 %	6.0 %	11.8 %	83.0 %	5.2 %
Radio Link Failure (138)	0.0 %	0.0 %	100 %	0.0 %	0.0 %	100 %

Table IV. Confusion matrices for problem simulation data

Real Class	8 features (only RSRP & RSRQ)			10 features (with CQI & PHR)		
	Per.	HO	RLF	Per.	HO	RLF
Periodical (148693)	96.0 %	2.9 %	1.1 %	96.2 %	2.9 %	0.9 %
Handover (683)	13.3 %	79.9 %	6.8 %	12.7 %	81.4 %	5.9 %
Radio Link Failure (210)	3.3 %	0.5 %	96.2 %	1.0 %	1.0 %	98.0 %

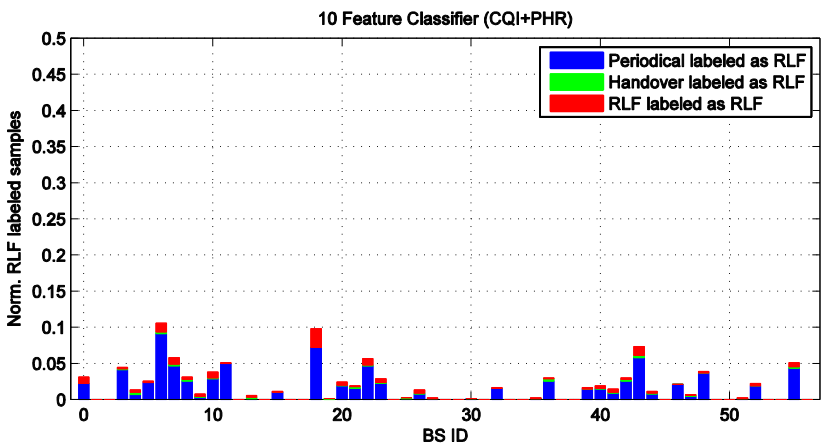

a.) Reference scenario

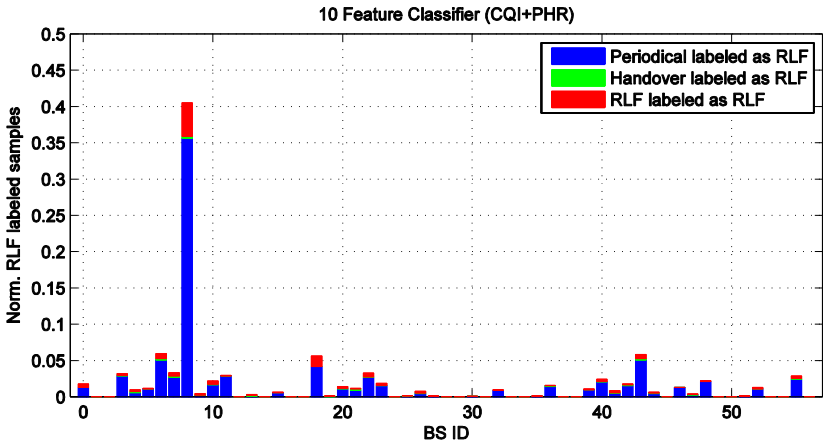

b.) Problem scenario

Figure 13: Relative number of different outage samples

Figure 13 shows that in the problem scenario, the increase in the number of outage samples is significantly larger for eNB-8. Almost 40% of all RLF labeled samples were associated with the eNB-8 dominance area whereas it was only 3% in the reference scenario. In addition, it was observed that a large amount of the periodical MDT samples in the dominance area of eNB-8 were classified as outage samples after triggering the problem. This suggests that by finding similarities between MDT and extended RLF reports:

- The detection of outages or weak coverage can be done even in cases where an insufficient amount of RLF reports are available for a particular area of interest.

In [P5], network alarms trigger if the number of outage samples associated with a particular eNB is different compared to the behavior of the outage samples in the neighboring eNBs. For triggering an alarm in eNB i, a base station specific anomaly score z_i is used. The figure in [P5] shows a distribution of the anomaly scores during the reference scenario which indicates that for the majority of the eNBs, the z_i remains below two. Only eNB-6, eNB-18 and e-NB 43 indicated some outage. However, when the sleeping cell problem is triggered in e-NB 8, the alarm score z_8 starts to increase remarkably. Figure 14 illustrates how much data and how long data collection period is needed to make reliable detection of sleeping cell in a case where the 10-feature classifier is used. Fast detection requires that enough anomalous data is obtained from UEs moving in the area of sleeping cell. Hence, the volume of the measurement data depends on the measurement configuration for collecting the MDT reports, amount of users and users' mobility patterns. In Figure 14, the y-axis indicates the anomaly score as shown in (4.5) and the x-axis indicates the amount of received MDT reports per eNB as the simulation advances in time. The scores are updated every five seconds using the mean and standard deviation values obtained from the

reference simulation. In the end of the problem simulation, the score for the eNB-8 increased to 26.2 for the 10-feature classifier and 25.2 for the 8-feature classifier. This indicates that both classifiers can detect anomalous network behavior because the scores were much larger than the scores that were observed during the reference scenario. However, already after receiving approximately 3000 MDT reports after triggering the problem, the anomaly score of the sleeping cell is increased to 20 times larger than the average score which is a clear indication of a sleeping cell.

The 10-feature classifier is able to better isolate the problem from the reference data. Isolation is better because the score is larger, thus indicating that more RLF labeled samples are associated with the malfunctioning eNB-8 while less false detections are done in other eNBs. This suggests that it is beneficial to include WCQI and PHR metrics in MDT reports in order to improve network coverage optimization and outage detection. However, a small constraint of the 10-feature classifier is that it requires assistance from the serving eNB. The 8-feature classifier is less accurate, but it does not require any additional network measurements, and therefore, it can be applied for MDT measurements that are obtained from frequency layers that are different than the serving frequency layer. This is an attractive feature since it is foreseen that in multi-layer and multi-RAT networks, UEs would be handed over to overlapping layers before RLF occurs in the serving layer.

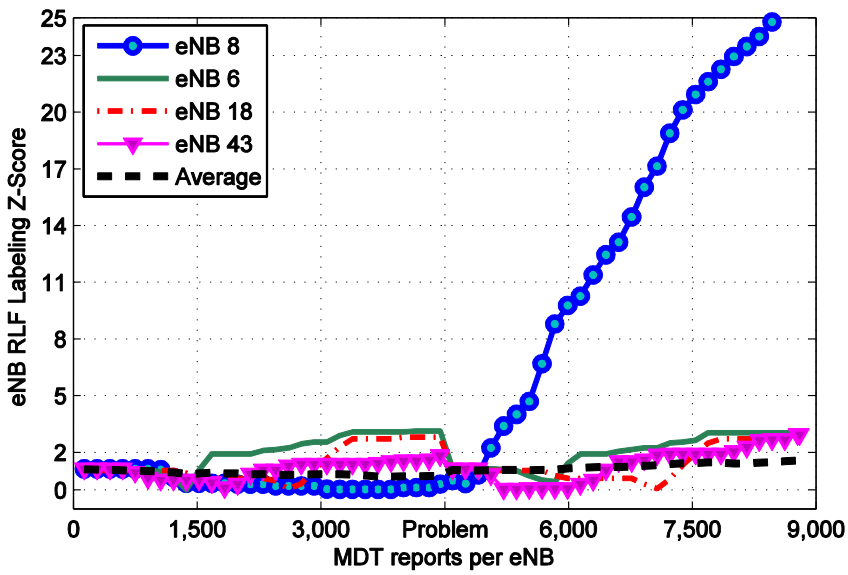

Figure 14: Anomaly scores in time before and after triggering the problem in eNB-8

5.4 Localization of MDT Radio Measurements

One goal in [P4] and [P5] was to associate the anomalous MDT reports with a base station to detect sleeping cells based on the geographical location of the anomalous MDT reports and the dominance areas. As described in Section 3.2, the MDT reports can be located based on the detailed location obtained from the GNSS receiver or by using RF fingerprinting. If the detailed location in an MDT report is obtained from the GNSS receiver then the correlation with the dominance areas is not an issue. However, if one cell is sleeping and it is not detectable, then positioning based on RF fingerprints can be challenging and can lead to the wrong conclusion because of missing neighbor measurements.

Typically, RF fingerprinting refers to a database correlation method where the position is estimated by comparing the radio measurements (the RF fingerprint) of the UEs with the training fingerprints in the correlation database [77]. The training fingerprints consist of radio measurements from several base stations that are used to provide a fingerprint of the radio conditions at a specific geographical location. Typically, this location is determined with an accurate positioning method, for example GNSS. One of the biggest challenges of RF fingerprinting is the burden of creating and maintaining the correlation database of the training fingerprints. Operators can maintain the correlation database by conducting extensive and expensive periodical drive test campaigns to collect the required measurements. In fact, one of the benefits of MDT is that it provides an efficient way to automate the collection of training fingerprints. Hence, the positioning framework for MDT reports that was developed in [P6] and [P7] is designed to understand how MDT reports can be located based on RF fingerprints in heterogeneous inter-frequency LTE networks. The framework is developed to study how LTE network heterogeneity and the number of monitored frequency layers affect RF fingerprint positioning performance in interference limited LTE deployments. It is anticipated that a synchronous LTE network is deployed using a frequency reuse 1 strategy, and therefore it is interference limited. This may restrict the ability of UEs to detect and measure the neighboring cells that have a negative impact on RF fingerprinting performance.

The RF fingerprinting framework consists of two phases: a training phase and an estimation phase. In the training phase, a correlation database is created by using MDT reports that contain detailed GNSS location information. These MDT reports form training fingerprints which are associated with a search grid that represents the area of interest. In this study, the grid consists of rectangular grid units of varying size, for example 10-by-10 meters or 40-by-40 meters. This allows RSRP measurements from different intra- and inter-frequency eNBs to be associated with different geographical locations. Later in the estimation phase, the locations of the unknown MDT reports are estimated by searching for a grid unit with the training fingerprint that gives the best match with the RF fingerprint that is obtained from the unknown MDT reports.

5.4.1 Performance in various intra- and inter-frequency network deployments

The motivation of [P7] was to study how RF fingerprint positioning accuracy behaves in urban, rural and heterogeneous LTE networks when fingerprint matching is based on either the Kullback-Leibler Divergence method or the Mahalanobis Distance (MAD) method. For rural and urban environments, only the serving frequency layer is measured and the RF fingerprints contained measurements from a serving cell and three neighboring cells. However, in the heterogeneous urban network, macro eNBs and small cells were deployed on different frequency layers and the RF fingerprints consisted of the measurements from four intra-frequency and three inter-frequency cells. Recent research in [78] suggested that KLD is a state of the art method for matching training and testing fingerprints in small cell WLAN environment. Hence, one goal of [P6] and [P7] was to evaluate its feasibility in heterogeneous LTE networks. A prime requirement of KLD method is to have invertible covariance matrices available for training and testing fingerprints. Collection of measurements for constructing training fingerprint covariance matrices can be obtained with periodical MDT measurement in LTE. However, existence of measurements for testing signature covariance matrices cannot be assumed always. Hence, MAD method is good alternative for KLD method since it uses similar measurements but it does not require covariance matrices for testing signatures.

Figure 15 illustrates the RF fingerprint positioning errors in both the urban and heterogeneous network deployments. In the urban environment, the 68% and 95% percentile errors for the MAD method are 53 meters and 154 meters whereas for the KLD method the corresponding errors are 38 meters and 137 meters. Moreover, in the heterogeneous network, the 68% and 95% percentile errors for MAD correspond to 35 meters and 113 meters whereas with the KLD method the respective errors are 21 meters and 95 meters. This indicates that KLD can improve the positioning accuracy in urban and heterogeneous environments compared to MAD.

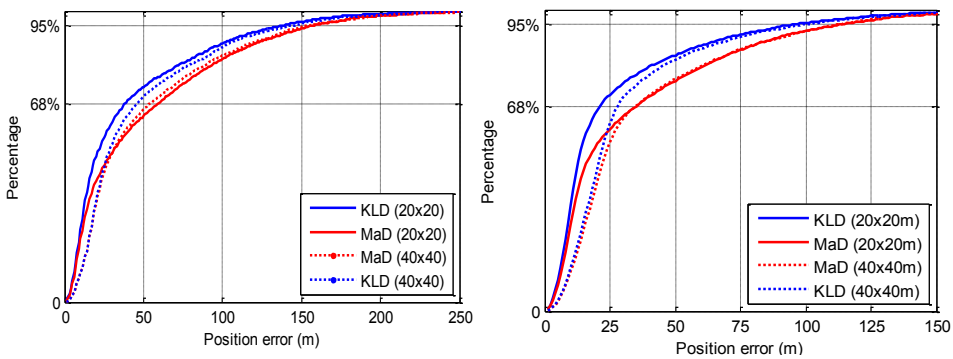

a.) Positioning error in urban intra-frequency deployment

b.) Positioning error in heterogeneous inter-frequency deployment

Figure 15: Cumulative distribution functions of RF fingerprinting position error

The results in [P7] indicate that the performance of KLD and MAD are similar in rural deployment. However, in urban and heterogeneous deployments, the KLD method shows better positioning accuracy compared to the MAD method. It is also noticed that when higher resolution grids were used, KLD can further improve positioning performance whereas such improvement is not observed for the MAD method. The performance improvement is highest in the heterogeneous network. This suggests that by exploiting the interdependencies of the received signal strengths from different base stations and by incorporating the corresponding covariance matrices into the RF fingerprints, a promising network-based method for locating MDT reports can be established.

5.4.2 Performance constraints by 3GPP cell detection performance requirements

In [P7], RF fingerprinting performance was evaluated with the assumption of ideal cell detection performance; all MDT reports always consisted of measurements from the 4 strongest intra-frequency and the 3 strongest inter-frequency eNBs regardless of the energy per symbol over interference plus noise (Ês/Iot) criteria. Such evaluation is a well justified way of comparing the performance of KLD with the MAD method. However, if ideal cell detection performance is assumed it can also produce positioning accuracies that are too optimistic. In [P6], the performance of RF fingerprinting is evaluated by comparing ideal cell detection performance with the practical cell detection performance. Practical cell detection was taking into account the -6 dB Ês/Iot criteria from 3GPP specifications [79]. In other words, a cell can only be detected and measured if Ês/Iot is above -6 dB and RSRP is above -127 dBm.

The performance evaluation is done for the heterogeneous small cell network scenario (Case0) and the sparse regular macro network scenario (Case4) as show in Figure 16. In both cases, the deployment is inter-frequency deployment that consists of two layers of eNBs which operate on adjacent carriers.

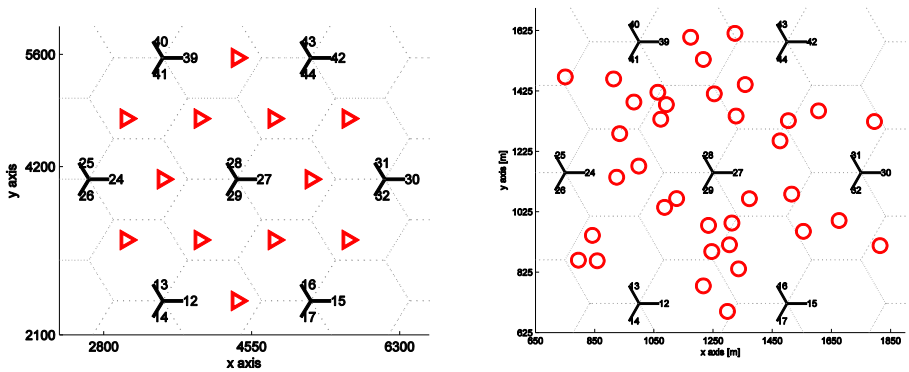

a.) Regular macro network *b.) Heterogeneous network*

Figure 16: Heterogeneous and regular macro network simulation scenarios

However, in the regular macro scenario, the sites in the denser frequency layer are deployed in a coordinated manner whereas in the heterogeneous scenario a random uncoordinated deployment of small cells is employed. Table V shows the positioning error percentiles for the KLD method, this is done with and without considering the Ês/Iot criteria. It was observed in [P6] that if Ês/Iot is taken into account, then the average number of detected cells was reduced significantly and the positioning error increases. In Case 4, a larger 40-by-40 meter grid unit setup resulted in the best positioning accuracy whereas in Case 0, a smaller 10-by-10 meter grid unit setup provides the best performance. Since KLD requires several MDT reports to construct covariance matrices, the grid units which contained only one MDT measurement cannot form signatures. Therefore, a large amount of training data was eventually left unused in 10-by-10 meter cases [P6].

With Case 4 in particular, the amount of used training data was not sufficient to cover the area of interest properly. This suggests that from a positioning accuracy perspective, the best choice for grid unit size depends on the number of MDT reports that can be used to form KLD signatures. Moreover, the results suggest that RF fingerprint performance can be improved by configuring UEs to gather radio measurements from several frequency layers. This is due to the fact that under the practical Ês/Iot constraints, the number of detected cells on the serving frequency layer is reduced. This results in low dimensional signatures and therefore RF fingerprinting positioning is more ambiguous, thus increasing the positioning error as seen in Table V. Observed positioning accuracies of RF fingerprinting in [P6] and [P7] are much lower than the accuracy of GNSS positioning in outdoors. On the other hand, if Cell-ID[3] based positioning would have been used in Case 0, then positioning errors would have been even larger since the 68% and 95% distances from user to serving cell were 208.6 meters and 310.2 meters, respectively. Comparison of positioning errors between trilateration based positioning (e.g., enhanced Cell-ID) and RF fingerprinting was not done during this thesis. However, the benefit of using RF fingerprinting algorithm is its simplicity. Signature matching can be easily applied to the practical process of position estimation whereas trilateration requires determining complex model for translating RF measurements to distances. Therefore the RF fingerprinting is currently more preferred than trilateration based positioning estimation [80].

However, it is worth highlighting that although the used system simulator is capable of modeling signal propagation and reception very accurately, some error sources which are expected to have a negative impact on the absolute accuracies of RF fingerprinting were not modeled. For example, the effects of UE orientation, type of the device, user body loss or building penetration loss in a case where the UE is indoors were not modeled. All of these would have an effect on the reported RSRP levels, thus making them vary more in a particular location.

[3]In Cell-ID based positioning, user location is approximated to correspond the location of serving cell.

Table V: KLD positioning performance [P6]

Scenario	Ês/Iot criteria	For 10-by-10 m grid unit		For 40-by-40 m grid unit	
		68% PE	95% PE	68% PE	95% PE
Case 4 (1750m)	n/a	127 m (-37%)	281 m (-28%)	106 m (-40%)	259 m (-28%)
	-6 dB	203 m	395 m	177 m	362 m
Case 0 (500m)	n/a	22 m (-55%)	63 m (-49%)	29 m (-42%)	65 m (-50%)
	-6 dB	49 m	124 m	50 m	131 m

5.5 MDT assisted Self-Optimization of UE Mobility State

As discussed in earlier sections, MDT reports can be used for self-healing in various ways, for example: detecting outage, weak coverage, sleeping cells and changes in dominance areas. In [P8], MDT measurement data is used to self-optimize the LTE Mobility State Estimation (MSE) procedure. The MSE that is defined in 3GPP is a procedure for optimizing the mobility performance of UEs that move at the higher velocities. It works by counting the number of handovers or reselections (N_{CR}) that the UE does during a sliding time window (T_{CRmax}), and it categorizes the UE into one of three mobility states: *Normal*, *Medium* or *High*. If the N_{CR} count is smaller than a threshold N_{CR_M}, then a UE's mobility state is Normal. However, if N_{CR} is greater than a threshold N_{CR_M} but smaller than a threshold N_{CR_H}, then a UE's mobility is Medium and if the N_{CR} count is greater than the threshold $N_{CR\_H,}$ then a UE is assumed be in a High mobility state. Therefore, the more handovers or reselections that a UE does during T_{CRmax}, the "faster" the UE is moving with regards to the cell size. Mobility state information is used to scale the UE mobility parameters, for example an idle mode reselection trigger or connected mode reporting triggers are used to improve UE mobility performance.

The purpose in [P8] is to use the GNSS location of the MDT reports to construct a statistical model of N_{CR} samples for three different mobility categories in order to learn how reselection and handover counts are related to UE velocity in a particular geographical area. The three distributions are parameterized by estimating mean and standard deviation values which are used to self-optimize the MSE thresholds. A threshold between two adjacent distributions is found by balancing z-score criterion as discussed in [P8]. By balancing the criterion, the threshold between two adjacent distributions is given as,

$$N_{TH} = \frac{\sigma_1 \mu_2 + \sigma_2 \mu_1}{\sigma_1 + \sigma_2}, \tag{5.2}$$

where variables μ_1 and σ_1 are the mean and standard deviation for the lower mobility distribution and μ_2 and σ_2 are the mean and standard deviation for the higher mobility distribution. By using (5.2), one can define the thresholds N_{CR_M} and N_{CR_H}. The validation of threshold selection is done

by simulating the behavior of the observed N_{CR} values for UEs that move with a velocity of 30 km/h, 60 km/h and 120 km/h in both sparse and dense heterogeneous networks. In the sparse scenario, 2 small cells were randomly deployed in every macro cell in the simulated area whereas in the dense scenario, 10 small cells were randomly deployed. Figure 17 illustrates the observed distributions for the three mobility classes in the sparse and the dense network for the case where T_{CRmax} is 120 seconds whereas

Table VI shows the corresponding sample means and standard deviations. The distributions indicate that the range of N_{CR} values is much smaller in the sparse network compared with the range of values in dense network. This suggests that if the same set of parameters were used in both environments it would lead to poor estimation accuracy of UE MSE.

Moreover, the distributions indicate that handover counts deviate quite much in each mobility case. In simulations, this deviation is mainly caused by random user path selection and spatial two dimensional slow fading which tend to increase the handover rates due to coverage islands. In addition, several non-idealities in real network deployments e.g., overshooting antennas and street canyons, can increase the handover rates even more. On one hand, such unidealities can make the reliable detection of the mobility state even more challenging since it is difficult to predict their impact on the handover counts. On the other hand, subscribers' mobility patterns can also be less random because their movement is limited by streets and buildings in real deployments. In fact, these local non-idealities emphasize the importance of using learning based approach for enhancing the MSE procedure. By using (5.2) with the simulated sample mean and standard deviation values presented in Table VI, the thresholds between the adjacent distributions can be determined. In the sparse network the N_{CR_M} was 13.0 and N_{CR_H} is 20.7 whereas in the dense network the N_{CR_M} is 18.4 and N_{CR_H} is 29.4. According to Figure 17, these thresholds are good for discriminating between N_{CR} samples that belongs to different distributions. It is worth highlighting that in the case of normal distributions, the thresholds balance the tail distributions. By using these thresholds, the classification accuracies of Normal, Medium and High mobility categories in sparse network is 80.7 %, 52.6 % and 83.2 %. In the dense network, the classification accuracies were 84.9 %, 66.6 % and 82.5 %, respectively. The accuracy of classifying fast moving UEs into the high mobility category is similar for example with the weight-based MSE approach as reported in [81]. This suggests that by optimizing the MSE thresholds, one can achieve reasonably good classification accuracy for discriminating between the different mobility categories in heterogeneous networks. However, if MDT reports with GNSS location are used to self-optimize the thresholds, the MSE parameters can be configured autonomously. It is also worth pointing out that the proposed self-optimization approach is applicable without needing to change the standards regarding UE behavior which makes it a backward compatible enhancement for MSE.

In this study, availability of accurate GNSS location was assumed. This can be slightly optimistic assumption e.g., in urban canyons, since the MDT reports do not include the GNSS velocity but instead the velocity is derived from a set of location measurements. The accuracy of these measurements can vary from centimeters to several tens of meters impacting also on the velocity estimation. On the other hand, velocity is used only to discriminate between three mobility categories and therefore certain amount of uncertainty can be tolerated.

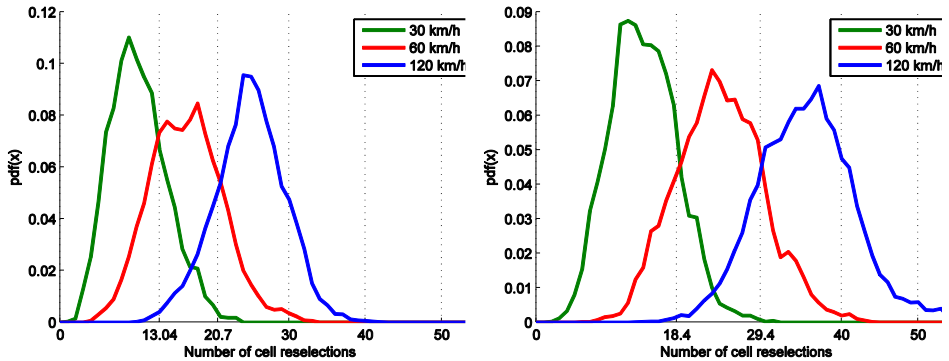

a.) sparse heterogeneous network *b.) dense heterogeneous network*

Figure 17: UE handover count distributions in a case where the sliding time window is 120s

Table VI: Sample means and deviations for handover distributions [P8]

TCR	Value	Sparse HetNet (2 small cells per macro)			Dense HetNet (10 small cells per macro)		
		X_{Normal}	X_{Medium}	X_{High}	X_{Normal}	X_{Medium}	X_{High}
120s	μ	10.3	16.5	24.8	14.0	24.1	35.3
	σ	3.7	4.7	4.6	4.4	5.7	6.3

6. Conclusion

6.1 Concluding Summary

In the first part of this thesis, the concept of a self-organizing network was introduced and the trends and challenges of operating a modern radio network were discussed. The challenge of operating a modern radio network comes from increased capacity demand which will lead to network densification that further increases network complexity. Without automation and self-organization, cost efficient operation of such a network is seen impossible. In the second part of the thesis, different *Knowledge Mining* methods were introduced for processing and analyzing field measurement data which is used to minimize an operator's need to conduct manual drive tests. From an operator's perspective, *Minimization of Drive Tests* is one of the most anticipated features of self-organizing radio networks because it can be used to reduce the operational expenditures that come from drive tests while also providing additional value to a network's self-organization functionality. However, it is foreseen that minimizing drive tests through autonomous data collection from user terminals produces an extensive amount of radio measurements. This data can overcrowd operator databases and must be processed efficiently by means of Knowledge Mining in order to acquire knowledge which provides additional value to the operators and eventually also to the network elements.

As a way to support coverage optimization, MDT measurements and extended RLF reports were used to construct a model that discriminates between different downlink and uplink coverage problems. In [P2], extended RLF reports were classified autonomously into coverage, interference and handover problems whereas uplink coverage issues due to the lack of coverage and power control misconfiguration were discussed in [P3]. The purpose of the discrimination was to acquire knowledge about the root cause of the problems. By knowing the root cause, one can make a faster decision with regards to the desired optimization strategy and act accordingly. Moreover, the feasibility of using MDT and extended RLF reports to detect sleeping cells was studied in [P4] and [P5]. The detection strategy was based on a novel concept for finding anomalous MDT reports in embedded low dimensional space and associating those with the eNB dominance areas by using detailed location information from MDT reports. This allows both weak coverage and sleeping cells to be detected even in a case where an insufficient amount of RLFs are reported. This is one of the main outcomes of this thesis. Such a case may occur for example when coverage is being verified during the pre-commercial phase of new frequency layers. This can be done by using inter-frequency radio measurements of commercial UEs operating on a different RAT or frequency than the new layer.

The positioning of MDT reports by means of RF fingerprinting in heterogeneous LTE networks was studied in publications [P6] and [P7]. The focus was on understanding how network heterogeneity and the number of monitored frequency layers affect the location estimates of the MDT reports. The results indicate that as the network gets denser, positioning errors decrease significantly. This suggests that in a dense heterogeneous small cell network, RF fingerprinting can provide an accurate way to locate MDT reports, although the GNSS location is not always available. In addition, a location estimation based on the Kullback-Leibler Divergence metric was found to perform better in dense networks compared with Mahalanobis Distance. The results also indicate that the number of measureable base stations decreases when the effect of the inter-cell interference in LTE is taken into account. This increases the ambiguity of the location estimate. Thus, it is proposed that radio measurements for MDT should be collected from several frequency layers, thus allowing for the detection of more base stations. This improves positioning accuracy and makes RF fingerprinting more usable.

In addition to using the MDT procedure for self-healing purposes, MDT reports were used to support self-optimization of the mobility state estimation parameters in LTE. The purpose of self-optimization was to learn about network behavior and to adapt the MSE configuration to fit the network topology in a particular geographical area. Learning was based on using MDT reports to construct statistical models for finding the relation between UE velocities and the number of handovers. The statistical models were used to determine and update the MSE thresholds N_{CR_M} and N_{CR_H} in an automated manner. The results indicated that by self-optimizing the threshold, the estimation accuracy increases in the heterogeneous networks in a way that is similar to the alternative MSE enhancements discussed for example in 3GPP. However, the self-optimization approach is a cost-efficient and backward compatible solution from a UE perspective whereas the other enhancements require changes to 3GPP specifications regarding UE behavior. It is expected that the studied approach is also applicable for configuring the MSE in rural and sub-urban areas, although the research in [P8] was only conducted in a heterogeneous small cell environment.

6.2 Future Work

During the years spent completing the research for this thesis, the concept of self-organization has clearly become a core concept on the way towards truly cognitive next generation radio networks. This supports the need for further development of the methods studied in this thesis. Although the research conducted for the thesis has thoroughly addressed various areas of self-organization, knowledge mining and minimization of drive tests, there are still research problems related to the work that should be addressed in the future work. From an industry point of view, future work is focused on implementing the developed algorithms and validating them in the field. This requires setting up an application that is able to access MDT data in the Trace Collection

Entities by using the available interfaces. To achieve this, collaboration work with network vendors or operators using the User and Equipment Trace functionality is anticipated. From an academia point of view, future work can address using MDT data in MDT use cases other than coverage optimization; improvements in RF fingerprinting; and extending MSE self-optimization so that it addresses more parameters than just handover thresholds. For example, most of the simulation results in this thesis focused on detecting a lack of coverage based on MDT reports. However, the applicability of correlating the anomalous MDT reports with the dominance areas for detecting sleeping cells was not considered in a case where detailed location is not available. This is clearly an area of future research.

The work regarding the RF fingerprinting of MDT reports is still in its infancy. Validation of the concept was limited because it only considered training and testing data that is always collected outdoors. Performance degradations due the various error sources, for example the ambiguities in a case where indoor measurements are correlated with training data that was only obtained from outdoor locations, were not addressed at all. This is clearly one area of future research. Moreover, novel methods for using RF fingerprints to optimize network performance were not studied and this is another potential area for future work. For example, currently an operator can determine which MDT reports are obtained from outdoors, but a novel method is needed for discriminating between indoor and outdoor MDT measurements. Furthermore, a novel way of autonomously verifying network coverage indoors is also needed.

Self-optimization of MSE parameters only adjusts handover and reselection thresholds. However, by using MDT functionality to obtain an eNB velocity profile, one can further optimize MSE performance. It is expected that the scaling factor and the length of the sliding time window can be better optimized by learning the typical velocity profile of UEs in a particular area. It is expected that if the MSE parameters are not self-optimized, operators will not put effort and money into optimizing and using the MSE feature, even though it improves the mobility performance of high velocity UEs.

The aforementioned aspects are the short-term areas of future research. However, in the long-term, future work should address changes in the evolution of cellular networks. It is foreseen that networks will merge towards more heterogeneous small cell networks that provide seamless and coordinated radio access through various technologies. One particular aspect of MDT functionality is based on how it can support coverage optimization and integration with 3GPP and Non-3GPP radio technologies. Furthermore, it is important to find out what role MDT plays in concepts such as RAN sharing, Authorized Shared Access or Software Defined Networks. These concepts are currently being discussed and are expected to be trends in the next generation of networks.

Appendix A: Dynamic System Simulator

A big part of the thesis work consisted of testing MDT functionalities with a proprietary dynamic system simulator known as *Freac*. This appendix gives a brief introduction to the simulator and modeling aspects of MDT measurements. The aim of the system simulator is to model the effect of a large number of users on a system's overall performance. Simulators can be categorized as follows: static, quasi-static and dynamic simulators. The dynamic system simulators are the most sophisticated because they model system behavior and user mobility over time whereas the other system simulators assume that user mobility behavior is stationary. For complexity reasons the system simulators use simplified link performance models to evaluate whether or not a packet is received. This is different from link simulators that focus on evaluating transmitter and receiver functionalities, and their performance in a radio channel on a more detailed level.

A Freac simulator models an E-UTRAN system in a downlink and an uplink direction by incorporating detailed implementations of various LTE functionalities such as radio resource management, link adaptation, scheduling, radio link detection and monitoring, radio measurements for mobility management, and various models for user mobility and traffic profiles. Since the users are moving in a simulated world, modeling of the radio propagation and slow fading in a spatial domain needs special care. In Freac, the LTE system is modeled in Orthogonal Frequency-Division Multiplexing (OFDM) symbol resolution in time domain and in subcarrier resolution in frequency domain. The simulator maps a link level SINR for an effective system level performance by following the methodology in [82]. This allows for an accurate estimation of packet error rates for different modulation and coding schemes. The simulator is configurable in various ways. Most of the time the system configuration follows the 3GPP simulation assumptions in [83] and [84] that are based on the modeling of radio propagation, antenna characteristics, slow fading and fast fading.

A simulation architecture is depicted in Figure 18. Before a simulation begins, it is initialized. During the initialization step, a simulation world is created where the configuration and location of network elements and users are determined. When the simulation is running, the network elements and users are called to do a simulation step. In Freac, one simulation step corresponds with a time duration of 1/14000 seconds. During the simulation step, a user's spatial location is recalculated and their radio conditions are updated. By default the UEs monitor the radio link quality of all eNBs. Typically, the strongest eNB is the serving eNB and other eNBs interfere with the connection between the UE and the serving cell.

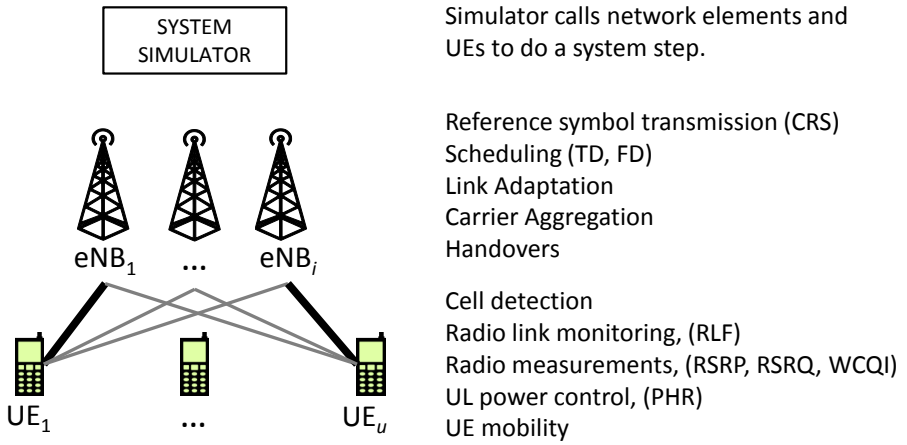

Figure 18: System simulator architecture

From an MDT modeling point of view, the most interesting aspect is how RSRP and RSRQ measurements are modeled, as they are the core part of an MDT as discussed in Chapter 3. RSRP measurement refers to Reference Signal Received Power measurement and it is defined as the linear average over the power contributions of the resource elements that carry cell-specific reference signals (CRS) within the considered measurement bandwidth [85]. In LTE, transmitted energy is divided into subcarriers in frequency domain and OFDM symbols in time domain. One subcarrier and one OFDM symbol forms a resource element in LTE. Moreover, 12 adjacent subcarriers and 14 consecutive OFDM symbols form a physical resource block. During the simulations the measurement bandwidth was configured to consist of the six centermost PRBs.

In Freac, RSRP and RSRQ modeling begins by determining a radio link between eNB and UE. The radio link is antenna specific and it is given as,

$$l_e^{iu} = \frac{pl_{iu}(d_{iu}) \cdot sf_{iu} \cdot \left| ff_{iu}(e_{s,sc}) \right|^2}{g_i(\varphi_{iu}, \theta_{iu})}, \tag{A.1}$$

where l_e^{iu} is the radio link between eNB i and UE u for one resource element $e_{s,sc}$. The total attenuation of the radio link is a product of pathloss $pl_{iu}(d_{iu})$ depending on the distance d_{iu}; log-normal slow fading factor sf_{iu} depending on UE's spatial location; average power of complex fast fading factor $|ff_{iu}(e_{s,sc})|^2$ varying for each resource element e indexed by the OFDM symbol s and subcarrier sc; and antenna gain $g_i(\varphi_{iu},\theta_{iu})$ depending on the angular difference of the UE and the eNB antenna direction in horizontal plane φ_{iu} and vertical plane θ_{iu}. The radio link is used to determine the received power per resource element. The received power per resource element rx_e^{iu} is given as,

$$rx_e^{iu} = \frac{tx_e^i}{l_e^{iu}}, \tag{A.2}$$

where rx_e^{iu} is the received power and tx_e^i is the transmitted power per resource element from eNB i. For calculating an instantaneous RSRP denoted by *rsrp(t)*, the received power is averaged over the resource elements in the measurement bandwidth containing CRS symbols for antenna port 0. In Freac, the default measurement bandwidth consisted of the six centermost PRBs and the measurement period for the instantaneous RSRP is one subframe that consists of 14 OFDM symbols. The six PRBs contain 48 resource elements that transmit the CRS symbols. These resource elements are distributed in frequency and time domain. A set S={1,4,7,11} denotes the indexes of OFDM symbols that carry CRS symbols for antenna port 0 whereas a set RS_s^N denotes the indexes of subcarriers that contain the CRS symbol on the measurement band during the OFDM symbol s. The linear average of instantaneous RSRP for tth subframe is given as,

$$rsrp(t) = \frac{1}{Ns \cdot Nrs_N} \sum_{s \in S} \sum_{sc \in RS_s^N} rx_e^{iu}, \tag{A.3}$$

where Nrs_N equals to 12 and it is the total number of subcarriers per OFDM symbol that transmit the reference symbols for antenna port 0 on the measurement bandwidth of six PRBs. The variable Ns is 4 and this corresponds to the size of S i.e., the number of OFDM symbols containing reference symbols per subframe. For calculating a layer one RSRP denoted by $rsrp_{L1}$, the instantaneous *rsrp(t)* is measured once in 40 milliseconds. The $rsrp_{L1}$ is the linear average of five consecutive measurements of *rsrp(t)* given as,

$$rsrp_{L1} = \frac{1}{Nw} \sum_{w=0}^{Nw-1} rsrp(t - w\Delta t) + \varepsilon_m, \tag{A.4}$$

where Nw is five, which is the number of samples used for calculating the $rsrp_{L1}$ and Δt is the sampling period of instantaneous RSRP (40 milliseconds). In addition, a random measurement error ε_m is added to the measurements. The error is drawn from a random distribution in a way that the measurement accuracy is in line with the 3GPP technical requirements specified in [79]. Finally, for calculating the layer three RSRP which is denoted by $rsrp_{L3}$, the following formula is used as specified in [58],

$$rsrp_{L3} = (1-a) rsrp_{L3\_prev} + a \cdot rsrp_{L1}, \tag{A.5}$$

where new layer 3 measurement $rsrp_{L3}$ depends on the previous layer 3 measurement $rsrp_{L3\_prev}$, a fresh layer 1 measurement $rsrp_{L1}$ and the coefficient $a=1/2^{(k/4)}$ as defined in [58]. The variable a depends on the configurable filter coefficient k. Note that if k is configured to 0, layer 3 filtering is not done. It is also worth noting that layer three RSRP is the measurement quantity that is reported by the UE to the eNB and used in the MDT analysis.

The Principle of measuring the RSRQ is similar to the one used when measuring RSRP. The RSRQ measurement refers to Reference Signal Received Quality measurement and the averaged instantaneous RSRQ for *t*th subframe is defined as,

$$rsrq(t) = \frac{N \cdot rsrp(t)}{rssi(t)}, \tag{A.6}$$

where N is corresponds to the number of physical resource blocks of the E-UTRAN carrier Received Signal Strength Indicator (RSSI) measurement bandwidth [85]. The RSSI measurement comprises of the linear average of the total received power observed in the OFDM symbols that contain CRS symbols for antenna port 0, over N number of resource blocks from all sources, including co-channel serving and non-serving cells, adjacent channel interference and thermal noise [85]. The averaged instantaneous RSSI for *t*th subframe is defined as,

$$rssi(t) = \frac{1}{Ns} \sum_{s \in S} \sum_{sc \in SC} \left(\eta_0 + \sum_{i=1}^{Nbs} rx_e^{iu} \right), \tag{A.7}$$

where the set SC consists of the subcarrier indexes of all resource elements in the measurement bandwidth. The variable Nbs corresponds with the total number of radio links between the UE and eNBs and the variable η_0 is the thermal noise per resource element. Layer one and layer three RSRQ samples are obtained in a similar way as the $rsrp_{L1}$ and $rsrp_{L3}$ in (A.4) and (A.5).

An instantaneous wideband CQI is also used in MDT analysis, for example in [P4] and [P5]. In Freac, the instantaneous WCQI is the linear average of the signal to interference ratio that is obtained from all resource elements that transmit the CRS symbols for antenna port 0 during one subframe. Hence, for a 10 MHz LTE system that consists of the transmission bandwidth of 50 PRBs the WCQI is defined as,

$$wcqi(t) = \frac{1}{Ns \cdot Nrs_W} \sum_{s \in S} \sum_{sc \in RS_s^W} \frac{rx_e^{iu}}{\eta_0 + \sum_{j \neq i}^{Ntx} rx_e^{ju}}, \tag{A.9}$$

where the set RS_s^W contains the subcarrier indexes for the subcarriers transmitting the reference symbols during OFDM symbol s over the whole 10 MHz bandwidth. The size of the set RS_s^W is 100 denoted by Nrs_W. It is worth highlighting that $rsrp(t)$, $rsrq(t)$ and $wcqi(t)$ are all in the linear unit scale whereas the reported L3 values in the MDT logs were converted to the decibel unit scale. Moreover, the specifications state that the reported RSRP and RSRQ values in dBm and dB units are quantized before they are reported. However, this quantization was not done in Freac during the MDT simulations. Thus, the measurements were reported with higher precision than what can be obtained in practical implementations.

Bibliography

[1] Viestintävirasto, “Viestintämarkkinat Suomessa - vuosikatsaus 2011”, 8.6.2012.

[2] IDATE, “Mobile traffic forecast 2010-2020 report”, in *UMTS Forum Report#44*, May 2011.

[3] Parkvall S. et al, "LTE advanced - Evolving LTE towards IMT-advanced", in *Proc. of 68th IEEE Vehicular Technology Conference*, September 2008.

[4] Hwang I., Song B. and Soliman S.S., “A holistic view on hyper-dense heterogeneous and small cell networks,” *IEEE Commun. Mag.*, vol. 51, no. 6, pp. 20–27, Jun. 2013.

[5] Lempiäinen J. and Manninen M., “Radio interface system planning for GSM/GPRS/UMTS”, ISBN: 978-0-7923-7516-6, Kluwer Academic Publishers, 2001.

[6] Lempiäinen J. and Manninen M., “UMTS radio network planning, optimization and QoS Management”, ISBN: 978-1-4020-7640-4, Kluwer Academic Publishers, 2003.

[7] Next Generation Mobile Networks, “A deliverable by the NGMN alliance: NGMN top OPE recommendations,” Version 1.0, September 2010, available at http://www.ngmn.com.

[8] Sesia S., Toufik I. and Baker M., “LTE - the UMTS long term evolution: From theory to practice”, 2nd edition, ISBN: 978-0-470-66025-6, John Wiley & Sons, 2012.

[9] Gavish B. and Sridhar S., “Economic aspects of configuring cellular networks”, in *Wireless Networks*, Vol. 1, No. 1, pp. 115-128, February, 1995

[10] Johansson K., Furuskär A., Karlson P., and Zander J., “Relation between base station characteristics and cost structure in cellular systems”, in *Proc. 15th IEEE International Symposium on Personal, Indoor and Mobile Radio Communications*, September 2004.

[11] Johansson K., Zander J., and Furuskar A., "Cost efficient deployment of heterogeneous wireless access networks", in *Proc. of IEEE 65th Vehicular Technology Conference*, 2007.

[12] Mölleryd B. G., Markendahl J., Werding J. and Mäkitalo Ö., “Decoupling of revenues and traffic – Is there a revenue gap for mobile broadband?”, in *Proc. of 9th Conference on Telecommunications Internet and Media Techno Economics*, June 2010.

[13] Ericsson Business Review, “Mobile broadband – busting the myth of the scissor effect”, No. 2, 2010.

[14] Olsson M., Sultana S., Rommer S., Frid L. and Mulligan C., “EPC and 4G packet networks – Driving the mobile broadband revolution”, 2nd edition, ISBN:978-0-12-394595-2, Academic Press, 2013.

[15] Hämäläinen S., Sanneck H., Sartori C., "LTE self-organising networks (SON): Network management automation for operational efficiency", ISBN:1119970679, John Wiley and Sons, 2011.

[16] Niemelä J., “Aspects of radio network topology planning in cellular WCDMA”, Doctor of Technology Thesis, Tampere University of Technology, September 2006.

[17] Kreher R., “UMTS performance measurements. A practical guide to KPIs for the UTRAN environment”, ISBN: 978-0-470-03249-7, Wiley, September 2006.

[18] Kreher R. and Gaenger K., “LTE signaling: troubleshooting and optimization”, ISBN:0470977671, John Wiley & Sons, 2010.

[19] Laiho J., Wacker A. and Müller S., “Measurement based methods for WCDMA radio network design verification”, *in Proc. 10th Communications and Networking Simulation Symposium*, March 2007.

[20] 3GPP TR 36.805, “Study on minimization of drive-tests in next generation networks”, v.9.0.0, December 2009, available at http://www.3gpp.org.

[21] 3GPP TS 32.421, "Subscriber and equipment trace: Trace concepts and requirements", ver. 11.6.9, March 2013, available at http://www.3gpp.org.

[22] Barco R. et al., “Automated troubleshooting of mobile networks using Bayesian networks”, in Proc. *International Conference Communications Systems and Networks*, 2002.

[23] Schmelz L.C. et al., ”Self-configuration, -optimization and –healing in wireless networks”, in *Wireless World Research Forum Meeting 20*, April, 2008.

[24] Magnusson P. and Oom J., “An architecture for self-tuning cellular systems”, *Journal of Network and System Management*, Vol. 10, No. 2, 2002.

[25] Prehofer, C. and Bettstetter, C., “Self-organization in communication networks: principles and design paradigms”, in *IEEE Communications Magazine*, Vol. 43, no. 7, 2005.

[26] Eisenblätter A. et al., “Final report on automatic planning and optimisation”, IST MOMENTUM Deliverable, D4.7, 2003, available at http://momentum.zib.de/.

[27] Altman Z., “Final system definition and validation”, Celtic GANDALF Deliverable, D2.3, 2007, available at http://www.celtic-gandalf.org

[28] Kürner T. et al., “Final report on self-organisation and its implications in wireless access networks”, SOCRATES Deliverable, D5.9, 2010, available at http://fp7-socrates.org.

[29] Nawrocki M., Aghvami H. and Dohler M., “Understanding UMTS radio network modelling, planning and automated optimisation: Theory and practice”, ISBN:978-0470015674, John Wiley & Sons, 2006.

[30] Next Generation Mobile Networks, “Next generation mobile networks beyond HSPA & EVDO”, white paper, version 3.0, December, 2006, available at http://www.ngmn.com.

[31] Next Generation Mobile Networks, “NGMN use cases related to self-organizing network; Overall description”, version 2.02, December, 2008, available at http://www.ngmn.com.

[32] 3GPP TS 32.500, “Telecommunication management; Self-organizing networks (SON); Concepts and requirements”, version 11.1.0, December 2011, available at http://www.3gpp.org

[33] 3GPP TS 36.902, “Self-configuring and self-optimizing network (SON), Use cases and solutions”, version 9.3.1, April 2011, available at http://www.3gpp.org

[34] 4G Americas, “Self-Optimizing Networks: The Benefits of SON in LTE”, white paper, 2011, available at http://www.4gamericas.org

[35] Amirijoo M. et al., “Use case, requirements and assessment criteria for future self-organizing radio access networks”, COST 2100 Technical document, TD-08616, 2008.

[36] Feng S. and Seidel E., “Self-organizing networks (SON) in 3GPP long term evolution”, Nomor Research white paper, May 2008, available at http://www.nomor.de.

[37] Nihtilä T. and Turkka J., “Performance of LTE self-optimizing networks uplink load balancing”, in *Proc. 73rd Vehicular Technology Conference*, May 2011, Budapest, Hungary.

[38] Turkka J. and Nihtilä T., “Performance of LTE SON Uplink Load Balancing in Non-regular Networks”, in *Proc. 22nd IEEE International Symposium on Personal, Indoor and Mobile Radio Communications*, September 2011, Toronto, Canada.

[39] Amirijoo M. et al., “Cell outage management in LTE networks”, in *Proc. 6th international conference on Symposium on Wireless Communication Systems*, 2009, Siena, Italy.

[40] Amirijoo M., Jorguseski L., Litjens R., Nascimento R., "Effectiveness of cell outage compensation in LTE networks," in *Proc. IEEE Consumer Communications and Networking Conference*, Las Vegas, USA, January 2011.

[41] Asghar M.Z., Hamalainen S. and Ristaniemi T., "Self-healing framework for LTE networks", in *Proc. IEEE 17th International Workshop on Computer Aided Modeling and Design of Communication Links and Networks*, September 2012.

[42] Cheung B., Kumar G.N. and Rao S., "Statistical algorithms in fault detection and prediction: Toward a healthier network", in *Bell Labs Technical Journal*, vol. 9, no. 4, pp. 171-185, February 2005.

[43] Rao S., "Operational fault detection in cellular wireless base-stations", in *IEEE Transactions on Network and Service Management*, Vol. 3, No 2., April 2006.

[44] 3GPP TS 37.320, "Radio measurement collection for minimization of drive tests", v.0.7.0, June 2010, available at http://www.3gpp.org.

[45] 3GPP TS 32.422, "Subscriber and equipment trace; Trace control and configuration management", v.11.0.1, September 2011, available at http://www.3gpp.org.

[46] Lähteenmäki J., Kyriazakos S., Fournogerakis P. and Laitinen H., "Using mobile location techniques for network planning and handover optimisation", in *Proc. 3G Infrastructures and Services Symposium*, July 2001.

[47] Ahonen S., Lähteenmäki J., Laitinen H. and Horsmanheimo S., "Usage of mobile location techniques for UMTS network planning in urban environment", unpublished, 2002.

[48] Horsmanheimo S. Jormakka H. and Lähteenmäki J., "Location-aided planning in mobile network-trial results", in *Journal of Wireless Personal Communications*, Vol. 30 No: 2-4, pp. 207 - 216, September 2004.

[49] AarnæS E. and Holm S., "Tuning of empirical radio propagation models effect of location accuracy" in *Journal of Wireless Personal Communications*, Vol. 30, No: 2-4, pp. 267-281, September 2004.

[50] Khan A.A., Adda M. and Khan T.K., "LRFP: An RF coverage reporting protocol for LTE systems", in *IEEE Wireless Communications*, Vol. 18, No. 6, December 2011.

[51] Wuri A. et al., "Minimization of Drive Tests Solution in 3GPP", in *IEEE Communications Magazine*, Vol. 50, No. 6, June 2012.

[52] Van De Beek J. et al., "How a layered REM architecture brings cognition to today's mobile networks", in *IEEE Wireless Communications*, Vol. 19, No. 4, pp. 17-24, August 2012.

[53] Galindo-Serrano A. et al., "Automated coverage hole detection for cellular networks using radio environment maps", in *Proc. of 9th international workshop on wireless network measurements*, May, 2013.

[54] Galindo-Serrano A. et al., “Harvesting MDT data: Radio environment maps for coverage analysis in cellular networks”, in *Proc. of 8th international conference on cognitive radio oriented wireless networks*, July 2013.

[55] Chernogorov F., Ristaniemi T., Brigatti K. and Chernov S., “N-gram analysis for sleeping cell detection in LTE networks”, in *Proc. IEEE International Conference on Acoustics, Speech and Signal Processing*, May 2013.

[56] Chernogorov F. and Nihtilä T., “QoS verification for minimization of drive tests in LTE networks”, in *Proc. 75th IEEE Vehicular Technology Conference*, May 2012.

[57] Johansson J., Hapsari W.A, Kelley S. and Bodog G., “Minimization of drive tests in 3GPP release 11”, in *IEEE Communications Magazine*, Vol. 50, No. 11, pp. 36-43, November 2012.

[58] 3GPP TS 36.331, “Evolved Universal Terrestrial Radio Access (E-UTRA); Radio Resource Control (RRC); Protocol specification”, ver.11.5.0, September 2013, available at http://www.3gpp.org.

[59] 3GPP TS 36.300, "Evolved Universal Terrestrial Radio Access (E-UTRA) and Evolved Universal Terrestrial Radio Access (E-UTRAN); Overall description", ver.11.7.0, September 2013, available at http://www.3gpp.org.

[60] Mahmoud Q.H., “Cognitive networks: Towards self-aware wetworks”, ISBN:978-0-470-06196-1, John Wiley & Sons, 2007.

[61] —, “Discussion with A.J. Mäki, an experienced automation engineer and a graduate student of TUT”, Tampere University of Technology, September 2013.

[62] Han J. and Kamber M., “Data mining: concepts and techniques”, ISBN:1-55860-489-8, Academic Press, 2001.

[63] Vehviläinen P., “Data mining for managing intrinsic quality of service in digital mobile telecommunications networks”, Doctor of Technology Thesis, Tampere University of Technology, March 2004.

[64] Zhang W., Yang Q. and Geng Y., “A survey of anomaly detection methods in networks”, in *Proc. International Symposium on Computer Network and Multimedia Technology*, January 2009.

[65] Asghar M.Z., Fehlmann R., Ristaniemi T., “Correlation-based cell degradation detection for operational fault detection in cellular wireless base-stations”, in *Proc. 5th International Conference on Mobile Networks and Management*, September 2013.

[66] Szilagyi P. and Novaczki S., “An Automatic Detection and Diagnosis Framework for Mobile Communication Systems”, IEEE transactions on Network and Service Management, Vol. 9, No: 2, June 2012.

[67] Novaczki S., “An improved anomaly detection and diagnosis framework for mobile network operators”, in Proc. *9th International Conference on the Design of Reliable Communication Networks*, March 2013.

[68] D’Alconzo A., Coluccia A., Romirer-Maiehofer P., “A distribution-based approach to anomaly detection and application to 3G mobile traffic”, in *Proc. IEEE Global Telecommunications Conference*, November 2009.

[69] Coifman R.R. et al., “Geometric diffusion as a tool for harmonic analysis and structure definition data: Diffusion maps”, In *Proc. National Academy of Science*, vol. 102, no. 21, May, 2005.

[70] Coifman R.R. and Lafon S., “Diffusion maps”, in *Applied and Computational Harmonic Analysis: special issues on Diffusion Maps and wavelets*, Vol. 21, No. 1, pp. 5-30, July 2006.

[71] Nadler B., Lafon S. and Coifman R.R, “Diffusion Maps, Spectral Clustering and Eigenfunctions of Fokker-Planck Operators”, *in Proc. Advances in Neural Information Processing Systems 18*, 2005.

[72] Schclar A., “A Diffusion Framework for Dimensionality Reduction”, in *Soft Computing for Knowledge Discovery and Data Mining*, pp. 315-325, ISBN: 978-0-387-69934-9, Springer US, 2008.

[73] 3GPP TS 36.321, “Medium access control (MAC) protocol specification”, ver.9.3.0, June 2010, available at http://www.3gpp.org.

[74] 3GPP TS 36.213, “Physical Layer Procedures”, ver.9.3.0, October 2010, available at http://www.3gpp.org.

[75] R2-097031, "MDT uplink coverage optimization", Nokia and NSN contribution, 3GPP TSG-RAN WG2 Meeting #68, Korea, November 2009.

[76] Müeller C. M., Kaschub M., Blankenhorn C. and Wanke S., “A Cell Outage Detection Algorithm using Neighbor Cell List Reports”, *in Proc. 3rd International Workshop on Self-Organizing Systems*, 2008, Vienna, Austria.

[77] Zekavat R. and Buehrer R., “Handbook of position location: Theory, practice and advances”, pp. 487 -520, ISBN: 978-0-470-94342-7, Wiley-IEEE Press, 2012.

[78] D. Milioris et al., “Low-dimensional signal-strength fingerprint-based positioning wireless LANs”, Ad Hoc Networks, 2012, doi:10.1016/j.adhoc.2011.12.006.

[79] 3GPP TS 36.133, “Requirements for support of radio resource management”, version 11.4.0, March 2013, available at http://www.3gpp.org.

[80] S. Das, T. Teixeira and S.F. Hasan, “Research issues related to Trilateration and fingerprinting”, Int. J. Res. Wireless Systems 1, 33-35, 2012.

[81] R2-131422, “Enhanced Mobility State Estimation”, Nokia Siemens Networks, 3GPP TSG-RAN WG2 Meeting #81bis, April 2013, available at http://www.3gpp.org.

[82] Brueninghaus K. et al., “Link performance models for system level simulations of broadband radio access systems”, in *Proc of the Personal, Indoor and Mobile Radio Communications (PIMRC’05)*, vol. 4, September 2005, Berlin, Germany.

[83] 3GPP TR 25.814, “Physical layer aspect for evolved Universal Terrestrial Radio Access (UTRA)”version 7.1.0, October 2006, available at http://www.3gpp.org.

[84] 3GPP TR 36.814, “Further advancements for E-UTRA physical layer aspects”, version 9.0.0, March 2009, available at http://www.3gpp.org.

[85] 3GPP TS 36.214, “Evolved Universal Terrestrial Radio Access (E-UTRA); Physical layer; Measurements”, version 11.1.0, December 2012, available at http://www.3gpp.org.

Original Papers

Publication 1

Non-regular Layout for Cellular Network System Simulations

by
Jussi Turkka and Andreas Lobinger

In *Proc. of 21st IEEE International Symposium on Personal, Indoor and Mobile Radio Communications (PIMRC)*, Istanbul, Turkey, September 2010.

Publication 2

Coverage Optimization for Minimization of Drive Tests in LTE with Extended RLF Reporting

by

Jani Puttonen, Jussi Turkka, Olli Alanen and Janne Kurjenniemi

in *Proc. of 21st IEEE International Symposium on Personal, Indoor and Mobile Radio Communications (PIMRC)*, September 2010, Istanbul, Turkey.

Publication 3

Using LTE Power Headroom Report for Coverage Optimization

by

Jussi Turkka and Jani Puttonen

in *Proc. of 72nd IEEE Vehicular Technology Conference (VTC-fall)*, September 2011, San Francisco, United States.

Publication 4

Detection of Sleeping Cells in LTE Networks Using Diffusion Maps

by

Fedor Chernogorov, Jussi Turkka Tapani Ristaniemi and Amir Averbuch,

in *Proc. of International Workshop on Self-Organizing Networks (IWSON)*, May 2011, Budapest, Hungary.

Publication 5

An Approach for Network Outage Detection from Drive Testing Databases

by

Jussi Turkka, Fedor Chernogorov, Kimmo Brigatti, Tapani Ristaniemi and Jukka Lempiäinen,

In *Journal of Computer Networks and Communications*,
Vol. 2012, No. 163184, 13 pages, doi:10.1155/2012/163184, September 2012.

Hindawi Publishing Corporation
Journal of Computer Networks and Communications
Volume 2012, Article ID 163184, 13 pages
doi:10.1155/2012/163184

Research Article

An Approach for Network Outage Detection from Drive-Testing Databases

Jussi Turkka,[1,2] Fedor Chernogorov,[2] Kimmo Brigatti,[2] Tapani Ristaniemi,[2] and Jukka Lempiäinen[1]

[1] *Department of Communications Engineering, Tampere University of Technology, 33720 Tampere, Finland*
[2] *Department of Mathematical Information Technology, University of Jyväskylä, 40014 Jyväskylä, Finland*

Correspondence should be addressed to Jussi Turkka, jussi.turkka@tut.fi

Received 18 March 2012; Revised 24 September 2012; Accepted 25 September 2012

Academic Editor: Sayandev Mukherjee

A data-mining framework for analyzing a cellular network drive testing database is described in this paper. The presented method is designed to detect sleeping base stations, network outage, and change of the dominance areas in a cognitive and self-organizing manner. The essence of the method is to find similarities between periodical network measurements and previously known outage data. For this purpose, diffusion maps dimensionality reduction and nearest neighbor data classification methods are utilized. The method is cognitive because it requires training data for the outage detection. In addition, the method is autonomous because it uses minimization of drive testing (MDT) functionality to gather the training and testing data. Motivation of classifying MDT measurement reports to periodical, handover, and outage categories is to detect areas where periodical reports start to become similar to the outage samples. Moreover, these areas are associated with estimated dominance areas to detected sleeping base stations. In the studied verification case, measurement classification results in an increase of the amount of samples which can be used for detection of performance degradations, and consequently, makes the outage detection faster and more reliable.

1. Introduction

Modern radio access networks (RAN) are complex infrastructures consisting of several overlaying and cooperating networks such as next-generation high-speed-packet-access (HSPA) and long-term evolution (LTE) networks and as such are prone to the impacts of uncertainty on system management and stability. Classical network management is based on a design principle which requires knowledge of the state of all existing entities within the network at all times. This approach has been successfully applied to networks of limited scale but it is foreseen to be insufficient in the management of future complex networks. In order to maintain a massive multivendor and multi-RAN infrastructure in a cost-efficient manner, operators have to employ automated solutions to optimize the most difficult and time-consuming network operation procedures. Self-organizing network concept [1] has emerged in the last years, with the goal to foster automation and to reduce human involvement in management tasks. It implies autonomous configuration, optimization, and healing actions which would result in a reduced operational burden and improve the experienced end user quality-of-service (QoS). One of the downsides of the SON concept is the necessity to gather larger amounts of operational data from user equipment (UE) and different network elements (NE).

To guarantee sufficient coverage and QoS for subscribers in indoor and outdoor environments, mobile operators need to carry out various radio coverage measurements. In the past, manual drive tests have been employed for this purpose. However, there are some challenges and limitations in manual drive testing that could be improved. Firstly, manual drive testing is a resource-consuming task requiring a lot of time, specialized equipment, and the involvement of highly qualified engineers. Secondly, it is impossible to capture the full coverage data from every geographical location by using manual drive testing, since most of the UE generated traffic comes from indoor locations, while drive testing is limited mainly to roads. The cost and reachability limitations of manual drive testing prompts the research

towards automated UE-assisted data gathering solutions which can minimize the need for manual drive testing and allow gathering of more comprehensive databases. If UEs measure the radio coverage periodically and provide the measurements together with location and time information to the network, then large radio environment databases with user-perceived coverage experience can be built to support the RAN operation and optimization. However, essential problems with these large databases are the information overflow and a "curse" of dimensionality. Those problems need to be addressed while analyzing and transforming the raw measurement data in these huge operational databases into meaningful information. This paper describes an approach to the above-mentioned problems by proposing a data-mining framework for the analysis of the UE-reported radio measurements. This approach allows the detection of the coverage problems in a cellular network on the basis of learning the network's prior operational behavior. The proposed framework is validated with simulations by using *Renesas Mobile Europe's* state-of-art LTE system simulator to construct large MDT measurement databases.

The article is organized as follows: Section 2 describes the Minimization of Drive Tests concept which can be used to gather and build the UE measurement report databases for HSPA and LTE networks with the focus on coverage aspects. Section 3 describes the data-mining framework which is used for the analysis of the MDT databases, and finally, Section 4 describes simulation scenarios and the performance evaluation results of outage detection caused by a specific type of network failure known as "*sleeping cell*."

2. Minimization of Drive Tests

Minimization of Drive Testing use cases for self-organizing networks were introduced by the operators alliance Next Generation Mobile Networks (NGMN) during 2008 [2] and at the time of writing this, the MDT solutions are researched by the network vendors and operators in the 3rd Generation Partnership Project (3GPP) [3, 4]. The goal of the MDT research in 3GPP is to define a set of measurements, measurement reporting principles and procedures which would help to collect coverage-related information from UEs. MDT feasibility study phase [3] started at late 2009 and during 2010 it focused on defining the reported measurement entities and MDT use cases for example, coverage optimization and QoS verification. Coverage optimization use case targets for the detection of such network problems as coverage holes, weak coverage, pilot pollution, overshoot coverage, and issues with uplink coverage, as described in [3]. After the feasibility study, the research focused on defining MDT measurement, reporting and configuration schemes for LTE release 10 during 2011 [4]. The MDT measurement and reporting schemes are *immediate MDT* and *logged MDT*. The immediate MDT scheme extends Radio Resource Control (RRC) measurement reporting to include the available location information to the measurement reports for UEs which are in connected mode [4]. In the logged MDT scheme, the UEs can be configured to collect measurements in idle mode and report the logged data to the network later [4]. After the release 10, the main focus of MDT work will be on enhancements in the availability of the detailed location information and improvements in QoS verification [5].

2.1. MDT Measurement Configuration. MDT measurements can be configured in LTE either by using management based or signaling-based configuration procedures [4, 6]. In the *management-based configuration*, the base stations are responsible for configuring all selected UEs in a particular area to do the immediate or logged MDT measurements [4, 6]. The *signaling-based MDT* is an enhancement to a signaling-based *subscriber and equipment trace* functionality [6] where the MDT data is collected from one specific UE instead of a set of UEs in a particular area. Detailed signaling flows for activating MDT measurements are described in [6].

The MDT measurement functionality allows operators to collect measurements either periodically or at an instance of a trigger such as a network event [3, 4]. The measurement report consists of the available location, time, cell-identification data and radio-measurement data. There are different mechanisms for estimation of user locations. The most coarse location info is the serving Cell Global Identification (CGI) and in the best case the detailed location is obtained from the Global Navigation Satellite System (GNSS). The cell identification info consists of the serving-cell CGI or Physical Cell Identifications (PCI) of the detected neighboring cells. The radio measurements for the serving and neighboring cells include the reference signal received power (RSRP) and reference signal received quality (RSRQ) for LTE system and common pilot channel received signal code power (RSCP) and received signal quality (E_C/N_0) for HSPA system [3, 4].

2.2. Logged MDT. The logged MDT measurement and reporting scheme enables data gathering from the UEs which are camped normally in RRC idle state. The logged MDT configuration is provided to the UEs via RRC signaling while UEs are in RRC connected mode. Logged mode configuration parameters are listed and described with more details in [4]. When the UE moves to the RRC idle state, MDT measurement data that is, time, location info and radio measurements, are logged to UE memory. The network can ask UEs to report the logged data when UE returns back to RRC connected state. Currently there can be only one RAT specific logged MDT configuration per UE which is valid only for the RAN providing the configuration. If an earlier configuration exists it will be replaced by newer one [4]. Since the logged MDT mode is an optional feature for UEs, this paper focuses more on the immediate MDT which will be a tool for operators to gather the measurements from LTE release 10 and onwards.

2.3. Immediate MDT. Immediate MDT is based on the existing RRC measurement procedure with an extension to include the available location information to the measurement reports. LTE release 10 RRC specifications [7] allow

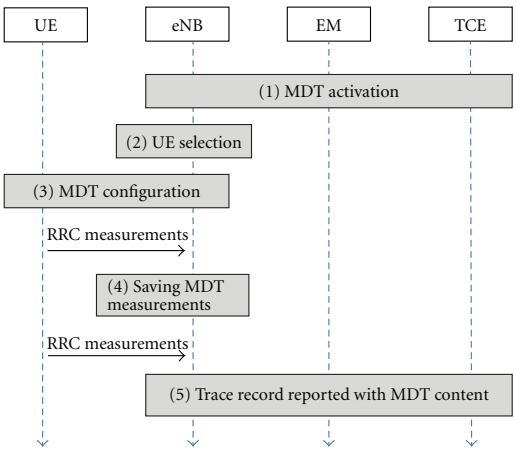

Figure 1: Immediate MDT reporting.

operators to configure RRC measurements in a way that RSRP and RSRQ measurements are reported periodically from the serving cell and intrafrequency, interfrequency and inter-RAT neighboring cells with the available location information. The immediate MDT measurement reporting principles are depicted in Figure 1 as described in [6].

Before the immediate MDT reporting can be started, a base station—E-UTRAN NodeB (eNB) is activated and configured to collect immediate MDT measurements. In step 1, an element manager (EM) sends a cell trace session activation request to the eNB including MDT configuration so that the eNB can later report the trace records back to the trace element (TCE). After the cell traffic trace activation, the eNB selects the UEs for MDT while taking into account the user consent that is, users permission for an operator to collect the MDT measurements. The eNB sends the RRC measurement configurations to the selected UEs for example, reporting triggers, intervals, and list of intrafrequency, interfrequency and inter-RAT measurements with a requirement that UEs include the available location information into the measurement reports as specified in the RRC specification information element (IE) *ReportConfigEUTRA* field [7].

When the RRC measurement condition is fulfilled for example, a periodical timer expires or a certain network event occurs, the UE sends available RSRP and RSRQ measurements to the eNB with the available *LocationInfo* IE added to the measurement report [7]. If detailed location information is available, then the latitude and the longitude are included into the measurement report. If the detailed location information is obtained by using GNSS positioning method then the UE shall attach time information to the report as well [4]. This GNSS time information is used to validate the detailed location information. Note that in case of the immediate MDT, the UE does not send the absolute time information as it does in case of logged MDT. The eNB is responsible for adding the time stamp to the received MDT measurement reports when saving the measurements to the trace record.

2.4. MDT Database. The MDT database is constructed by collecting the MDT measurements from the network. In our study the MDT database consists of periodical measurements, as well as measurements collected at the time instance of A3 (A3 event is E-UTRAN RRC measurement event which triggers when neighboring cell becomes an offset better than the serving cell) events preceding successful intra-LTE handovers (HO) and radio link failures (RLF). It is assumed that each measurement sample in the analyzed database consists of 22 features as described in Table 1.

The MDT measurement samples consist of the latitude, longitude, serving cell, and neighboring cell radio measurements reported by the UE. In addition, time information, serving-cell wideband channel quality indicator (WCQI) and uplink power headroom report (PHR) values were added by the eNB. Moreover, a label of the report condition is always appended to a measurement sample, that is, eNB knows if the MDT data sample is a periodical, A3 event-triggered measurement report or UE RLF report [4]. Currently, the release 10 MDT specifications do not support the feature of collecting detailed location for A3 events. However, this feature is to be included to MDT in release 11. Therefore, the structure of the MDT measurement sample described in Table 1 is assumed to be common for all of these three types of MDT reports.

3. Outage Detection Data-Mining Framework

It is known that the SON framework includes three functionalities, namely self-configuration, self-optimization, and self-healing. Self-configuration is related to the initial steps of the network setup. Self-optimization is concentrated on monitoring the network state and automatic parameter tuning for achievement of the highest possible network performance without compromising the robustness of its operation. In case of a network failure or malfunction, the self-healing tries to autonomously detect problems, diagnose root causes, and compensate or recover from the malfunctioning state back to normal operation. A good example of self-healing is the cell-outage management [8, 9] use case in LTE networks, which aims to improve the offline coverage optimization process by detecting and mitigating outage situations automatically. For this purpose, the self-healing algorithm requires several key performance indicator (KPI) measurements from both eNBs and UEs. The KPIs such as cell load, RLF counters, handover failure rate or, UEs neighboring cell RSRP measurements may be used as indicators of the network outage [8]. In [9], the condition for the outage was based on predefined thresholds of received signal strength and quality. However, deployment of several self-organizing functionalities can increase significantly the number of measured and reported KPIs thus increasing the complexity of the network and SON architectures. This may result in new challenges for network engineers as well. Firstly, high-dimensional KPI databases of network measurements

Table 1: Structure of the MDT measurement.

Feature No.	Feature	Description
1	Time	Time stamp
2-3	Location	Latitude and longitude
4	Serving-cell info	CGI
5	RSRP	Serving-cell RSRP in dBm
6	RSRQ	Serving-cell RSRQ in dB
7–13	Three strongest intra-LTE neighbors	CGI and RSRP for each neighbor
14–20	Three best quality intra-LTE neighbors	CGI and RSRQ for each neighbor
21	Serving-cell wideband CQI	Indicator of wideband signal quality
22	Power headroom report	Available uplink transmission power

are created, making expert-driven manual data analysis for identifying the right KPI/fault-associations a complicated task. The KPI/fault-associations are needed for developing good algorithms. Secondly, since the networks are complex and dynamic in nature, it is not obvious which KPIs should be measured and how often. For example, how to select from among several performance indicators, those which are going to reveal a certain feature of the network behavior in the most meaningful and effective manner?

It is envisioned that the above-mentioned challenges can be solved with advanced machine learning and data-mining algorithms which rely on autonomous learning of network behavior and efficient processing of the high dimensional databases consisting of wide range of KPIs. The data-mining can be used for extracting interesting, previously unknown and potentially useful information patterns from the large databases [10]. Usually the data mining process consists of several phases such as data cleaning, database integration, task relevant data selection, data mining, and data-pattern evaluation [10]. Data cleaning, integration, and selection are data preprocessing phases where data is prepared for further analysis [10, 11]. The data mining itself can consist of several different functionalities such as classification of data, association of data, clustering of data, dimensionality reduction, and anomaly detection [10]. In the pattern evaluation phase, the information patterns are visualized and analyzed to see if novel and valid information can be extracted from them. Even if interesting information patterns are discovered, it does not mean that it is automatically usable or useful from the data mining problem point of view, and therefore, information patterns need to be validated.

Within the family of cell-outage use cases included into self-healing of cellular radio networks there is a specific problem called *sleeping cell*. The sleeping cell is a compound term, which includes erroneous network behavior ranging from performance degradation to complete service unavailability. A specific characteristic of sleeping cell is that the network performance is degraded but this degradation is not easily visible to network operators and thus detection of this problem with traditional alarming systems is a complicated and slow process as described in [12]. There is no definition of a certain network failure which would cause appearance of a sleeping cell, as there can be several reasons. One type of sleeping cell could be malfunction of eNB RF unit where the eNB transmission and reception capabilities degrade slowly to a point where transmission, reception, or both are not working anymore. This results in an outage situation where eNB cannot provide service for the UEs in the coverage area of the sleeping cell. Indicators which could reveal sleeping cells are degradation in handover activity, low call setup rates and low cell loading. Different kinds of indicators are needed to detect sleeping cells in live networks since networks consist of several overlapping frequency layers and radio access technologies. In [13], a sleeping cell is detected by using statistical classification techniques for graphs constructed from UE reported neighboring cell patterns. Changes in the neighboring cell patterns are used as indicators of outage.

One of the main goals of the research into the minimization of drive test is the development of algorithms which make operation of the networks more robust and efficient, so we developed a data-mining framework which detects coverage problems, such as sleeping cells, by using the high-dimensional MDT measurement databases. The data-mining framework described in this paper relies on dimensionality reduction which allows simplifying the anomaly detection and data classification processes. Motivation of using the dimensionality reduction is to make the framework robust and easily extendable with new numerical KPIs. On the other hand, the motivation of classifying MDT measurement reports to periodical, handover, and outage categories is to detect areas where periodical reports collected from certain frequency layer starts to show assumptions of outage. It is worth of noting that periodical MDT measurements can be collected from intra- and interfrequency layers simultaneously [4]. Therefore, some measurements for classification are available even if UE is connected on different frequency layer than the sleeping cell. This can happen in live networks where operators have deployed several overlapping frequency layers for capacity and coverage. If UE starts to experience outage on one frequency layer then it is handed over to another frequency layer before radio link failure occurs.

3.1. Data Mining Framework. The data-mining framework consists of learning and problem-detection phases. In the learning phase, the MDT database is constructed by collecting UE reported measurements from the network as depicted in Figure 2.

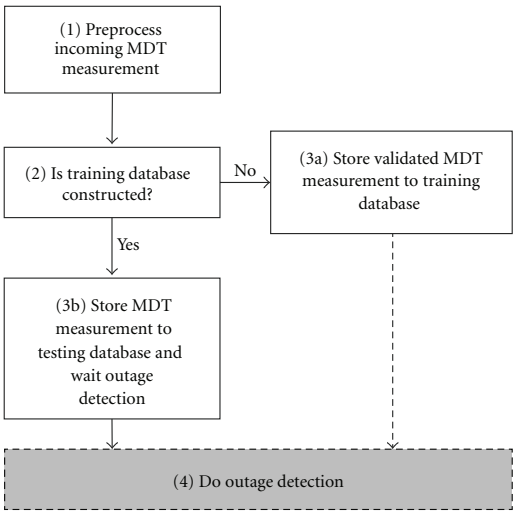

Figure 2: Data-mining learning phase description.

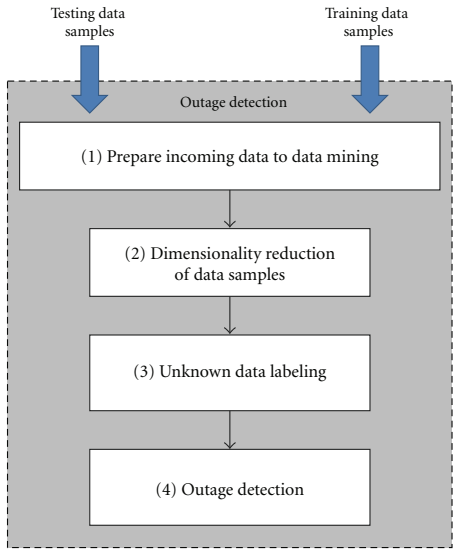

Figure 3: Data-mining outage detection-phase description.

The first step during the learning phase is preprocessing of the arriving MDT measurements which are labeled as periodical, HO-triggered, or RLF-triggered. Labeling is necessary because problem detection in step 4 relies on *supervised learning* from the labeled training samples. Labeling could be done at the eNB before the samples are sent to the TCE. The second step is to check whether or not a proper training database exists. In our case, the requirement is that a sufficient amount of periodical measurements and HO-triggered measurements are gathered from the network during its normal operation. In addition, some RLF samples from previous outage situations are gathered. A training database is created from the preprocessed MDT measurements which characterize normal network behavior without any outages. When the training database is constructed, all new measurement samples are put into the testing database. The operator needs to validate the training database and make sure it really resembles the needed network characteristics for example, the network behavior during its normal operation. The validation could be done by using anomaly detection and unsupervised learning techniques as described in [12].

In the problem-detection phase, recently received MDT measurements in the testing database are compared with the training data to detect anomalous behavior in the system, as depicted in Figure 3. The first step in the outage detection process is to prepare the data in the training and the testing set. Depending on the problem and the applied data mining algorithms, this preprocessing phase may contain several kinds of actions such as data cleaning, data integration, data transformation and data scaling. In our framework, each MDT measurement, as described in Table 1, is cleaned by splitting a single measurement to the header part and the data part. The header part contains information for post-processing of the outage detection results, like visualization and location correlation, but it is not used by the data-mining algorithm. The data part for ith measurement sample is a vector x_i consisting of 10 numerical features as follows:

$$x_i = \{\mathrm{RSRP}_S, \mathrm{RSRP}_{N1}, \ldots, \mathrm{RSRP}_{N3}, \mathrm{RSRQ}_S, \mathrm{RSRQ}_{N1}, \ldots, \mathrm{RSRQ}_{N3}, \mathrm{WCQI}, \mathrm{PHR}\}, \quad (1)$$

where RSRP_S and RSRQ_S are the serving cell measurements and RSRP_{Nj} and RSRQ_{Nj} are the jth strongest neighbor cell measurements, $j = \{1, 2, 3\}$. WCQI is the serving cell wideband CQI measurement and PHR is the serving cell power headroom report. RSRP and RSRQ measurements are given in a logarithmic scale as specified in [14]. Note that in our studies the WCQI and PHR measurements are not exactly the same as in 3GPP specifications. First of all, the CQI represents the downlink wideband signal-to-interference ratio and it is expressed using a dB scale. Moreover, the PHR metric is scaled by the allocation size resulting in a PHR per physical resource block metric as proposed in [15] since it was seen to improve the detection of uplink coverage problems and uplink power control parameterization problems. Thus, the high-dimensional data classifier consisted of 10 features. In addition, the performance of the 10-feature classifier was compared to an 8-feature classifier since the availability of the WCQI and PHR measurements depends on the eNB implementation. The 8-feature classifier uses only UE reported RSRP and RSRQ measurements.

3.2. Dimensionality Reduction. The next step in the outage detection framework is the dimensionality reduction step. The target of the dimensionality reduction is to represent

high-dimensional data sets in a lower dimensional space making the data mining faster and less complicated. By having the dimensionality reduction step employed to the framework, the outage detection framework is more robust and can be extended easier with new numerical KPIs. Dimensionality reduction techniques, such as principal component analysis (PCA) are widely used in machine learning.

In our framework, the testing and training data set dimensionality is reduced by using a nonlinear diffusion maps methodology [16–19]. The diffusion maps method allows finding meaningful data patterns in the high-dimensional space and represents them in the lower dimensional space using diffusion coordinates and diffusion distances while preserving local structures in the data. The diffusion coordinates parameterize the high-dimensional data sets, and the diffusion distance provides a local preserving distance metric for the data. In the following, we shortly describe the used dimensionality reduction method originally proposed in [19]:

(i) The data set X is used to construct a unidirectional graph G, where the graph vertices are the data points x and the edges between the data points are defined by a kernel weight function w_ε.

(ii) The diffusion is created by doing a random walk on the graph. The random walk is done from the Markov transition matrix $\mathbf{P}$ which can be obtained by normalizing kernel weight matrix $\mathbf{W}$ with a diagonal matrix $\mathbf{D}$.

(iii) Finally, if $\mathbf{P}$ exists then the Eigen decomposition of the $\mathbf{P}$ can be used to derive the diffusion coordinates $\Psi_t(x_i)$ in the embedded space and the diffusion-distance metric $D_t(x_i, x_j)$.

The kernel weight matrix $\mathbf{W}$ measures the pairwise similarity of the data points in the graph and it must be symmetric, positive, and fast decaying [19]. One common choice for the kernel is:

$$W_{i,j} = w_\varepsilon\left(x_i, x_j\right) = \exp\left(\frac{-\left\|x_i - x_j\right\|}{\varepsilon}\right). \tag{2}$$

If the weight $w_\varepsilon(x_i, x_j)$ between sample x_i and x_j is small it means that points are similar. On the other hand, if the weight is large then the points are different in nature. Variable ε can be used to scale the kernel weight function which on the other hand scales the size of the local neighborhood. In principle, any weight function form of $f(\|x_i - x_j\|)$ fulfilling the above-mentioned criteria could be used to estimate the heat kernel and thus used with the diffusion process [19]. The Gaussian kernel in (2) is scalable and it decays fast, that is, faster than plain Euclidean distance, and therefore it was chosen. Next, the diagonal matrix $\mathbf{D}$ is derived from $\mathbf{W}$ according to

$$D_{i,i} = \sum_{j=1}^{n} w_\varepsilon\left(x_i, x_j\right). \tag{3}$$

If a proper kernel is used, then the matrix $\mathbf{W}$ can be multiplied from left with matrix $\mathbf{D}^{-1}$ to get the normalized Markov transition matrix $\mathbf{P}$:

$$\mathbf{P} = \mathbf{D}^{-1}\mathbf{W}. \tag{4}$$

In the Markov matrix, the $P_{i,j}$, describes the probability to move from sample x_i to sample x_j in the graph with one step. The random walk in the graph is obtained by raising the Markov transition matrix $\mathbf{P}$ to the tth power $\mathbf{P}^t$. This gives the probability to move from sample x_i to sample x_j in the graph with t steps. Finally, the eigen decomposition of $\mathbf{P}^t$ provides tools to define the high-dimensional data set in $\mathbb{R}^n$ in the embedded space $\mathbb{R}^k$ by constructing an estimate of $\mathbf{P}^t$ by using only k largest eigenvectors:

$$\mathbf{P}^t = \sum_{l=1}^{k} \lambda_l^t \psi_l \phi_l^T, \tag{5}$$

where the variables ψ_l and φ_l are right and left eigenvectors, and the variable λ_l is the eigenvalue of the lth eigenvector. Moreover, the diffusion distance D_t^2 and diffusion coordinates Ψ_t can be constructed by using the eigenvalues and the right eigenvectors as proven in [19]:

$$D_t^2\left(x_i, x_j\right) = \sum_{l=1}^{k} \lambda_l^{2t}\left(\psi_l(x_i) - \psi_l\left(x_j\right)\right)^2, \tag{6}$$

where the diffusion distance D_t^2 is the Euclidean distance between the measurement x_i and x_j in the embedded space by using the diffusion coordinates. The diffusion coordinates are constructed using k most significant right eigenvectors and eigenvalues as given in [19]:

$$\mathbf{\Psi}_t(x_i) = \left[\lambda_1^t \psi_1(x_i), \lambda_2^t \psi_2(x_i), \ldots, \lambda_k^t \psi_k(x_i)\right], \tag{7}$$

where the diffusion coordinates $\mathbf{\Psi}_t(x_i)$ for measurement x_i can be obtained from the m-by-k diffusion coordinate matrix $\mathbf{\Psi}_t$. The column vectors of $\mathbf{\Psi}_t$ are the right eigenvectors of $\mathbf{P}^t$ multiplied by the corresponding eigenvalue term λ_l^t as shown in (7). Moreover, the diffusion coordinates for measurement x_i are found in the ith row vector of the diffusion coordinate matrix $\mathbf{\Psi}_t$. As seen from (6) and (7), the diffusion distance for samples in the high-dimensional space corresponds to the Euclidean distance of the samples in the embedded space.

3.3. Data Classification. The third step in our outage detection framework is data classification used to learn the characteristics of the testing data. In our earlier paper, we considered unsupervised learning techniques to detect sleeping cells [12] by incorporating *k means clustering* without taking into account the periodical MDT measurements. In this paper, we are describing the application of the supervised learning classification algorithm known as *nearest neighbors search* (NNS). Difference between the supervised learning and the unsupervised learning techniques is that in the supervised learning we know labeling for the training data

and based on the training data characteristics we try to label unknown testing data samples. In our approach the training data consists of samples which belong to one of three class types, labeled as periodical, handover, or RLF samples, and the target is to classify all unknown testing data samples to those three known category types. Motivation of classifying testing data to these three class types is to detect periodical MDT measurements which have similarities with samples belonging to the outage category. By doing the classification, early outage detection can be done even in cases that only insufficient amount of RLF reports are available.

The fundamental idea of NNS is to find a set S_i of nearest neighbors from the training database for each unknown sample x_i in the testing database. One method of determining S_i is to calculate a distance from x_i to all points in the training database. Therefore, the complexity of the NSS depends on the size of training and testing sets as well as the dimensionality of the data samples. In our work, the nearest neighbors search is done in embedded low dimensional space based on the Euclidean distances. This is equally the same as classifying samples in high dimensional space according to the diffusion distances. The set S_i is used to define the labeling for all the unknown samples. There can be a wide range of vendor specific algorithms to determine the label for the unknown samples based on the S_i but here a simple algorithm was used and the class label is chosen based on the largest class in terms of number of samples present in the set S_i.

3.4. Anomaly Detection. The final step of the outage detection framework is anomaly detection. By this stage, the testing database is already labeled and this information is used to detect possible outage or sleeping-cell problems in the network. There are two different principles for detecting anomalous base-station behavior. On one hand, anomalies can be detected in time domain by comparing target base-station behavior in time to the behavior observed earlier. This requires long observation times and data-gathering periods per base station for creating reliable time domain profiles. On the other hand, anomalous base-station behavior can be detected in base station domain by comparing target base-station behavior to the neighboring base stations. In the latter case, more data is gathered in a shorter time period but the data can be biased if the neighboring base stations behave differently, that is, due to the different parameterization. In our framework, the common assumption for all base stations is that during normal operation the amount of RLF samples is small. Thus, the data classification should not result in many periodical MDT samples which are considered to belong to the RLF class. On the other hand, when the network is in outage, many periodical MDT measurements should be similar to the RLF samples. Since the anomaly detection criterion that is, increase of the number of periodical MDT measurements which have similar characteristics as the RLF samples, assumes similar behavior of the base stations during normal operation, the outage detection is based on the base-station domain analysis.

In our framework, the anomaly detection is done by counting the number MDT reports labeled as RLF samples for each eNB and comparing this with the network normal operation in time and base-station domain. The detection is based on the well-known standard score metric which describes how similar an observation of a particular eNB is compared with the normal behavior of a set of neighboring eNBs taking into account the normal deviation of the observations. Standard score z_e for eNB e is defined as,

$$z_e = \frac{|x_e - \mu_x|}{\sigma_x}, \tag{8}$$

where variable x_e is the number of RLF-labeled samples for eNB e and variables μ_x and σ_x are expected mean and standard deviation of the number of RLF-labeled samples in the eNBs local neighborhood. If z_e is much larger than one, then eNB e is probably an anomaly since the amount of RLF-labeled observations do not fit within the normal deviation of the RLF observations.

4. Simulation Results

4.1. Simulation Configuration. Our outage detection approach was verified with the dynamic LTE system simulator which was used to collect a large MDT measurement database. The simulator is capable to simulate E-UTRAN LTE release 8 and beyond in downlink and uplink with several radio resource management, scheduling, mobility, handover, and traffic-modeling functionalities. The simulation scenario consists of a regular hexagonal network layout of 19 sites and 57 base stations with inter site distance of 1750 meters. The 7 center sites are normal cells where the UEs are placed to gather MDT measurements and the outer tier of 12 sites are used only to generate interference. The users were moving in the scenario with velocity of 3 km/h and handover parameters were chosen in a way that the performance during normal operation was assumed to be good. On the other hand, the radio link monitoring values were chosen to trigger the RLF slightly faster than normally to ensure that some RLF samples are gathered during the normal operation of the network. The simulation assumptions are based on the 3GPP macro case 3 specifications [20] defining the used bandwidth, center frequency, network topology, and radio environment as listed in Table 4.

The simulation campaign consisted of a reference and problem simulations. The reference simulation was used to gather training data during the normal operation of the network and the simulated MDT database consisted of 148723 periodical measurement samples, 698 handover samples, and 138 RLF samples. The periodicity of sending MDT measurement reports was 0.5 seconds. In the problem scenario, one eNB was attenuated completely since the target was to model a sleeping cell where the uplink and the downlink are malfunctioning. The outage was created by adding 50 dBi antenna attenuation to the eNB 8. Since all sites were operating on the same band and overlaying interfrequency layer didn't exist, the eNB 8 was in outage. This enlarged the dominance areas of the neighboring cells

as depicted in the Figure 4. The dominance area indicates the area where a particular cell is the strongest serving cell. In the left figure, the eNB 8 dominance area is shown with turquoise color, and the size of the area is similar to the other cells. In the right figure, the eNB 8 is sleeping and the area is served by the neighboring cells. Note that the eNB 8 covers less than 5% of the overall area where the UEs are distributed during the simulation.

The described dominance area problem is easy to understand, and therefore, it is interesting to see how our approach is able to detect the change in the dominance areas. The MDT database gathered from the reference simulation provides the basis of the training database which defines the statistical structure and the characteristics of three classes. Since the MDT database from the reference simulation was large only a fraction of this data was used in the actual training data set. The training data set was constructed from 3000 periodical samples using random undersampling [21], all HO samples, and all RLF samples. Moreover, the size of the RLF data set was oversampled by a factor of 4 in order to have roughly the same amount of HO and RLF samples in the training data set. Even though oversampling leads to a certain degree of overfitting, and consequently might lead to a degradation of classification accuracy [22], it can also enhance the classifier performance as shown in [11]. All MDT data gathered from the problem simulation is used to construct the unknown database, and each sample in this database is labeled as either periodical, handover, or RLF class as earlier explained in Section 3.

4.2. Simulation Data Mining Results. To be able to detect the anomalous network behavior, all MDT measurement samples in the unknown database was labeled by using the training data set classifier. Labeling of unknown samples was done based on 7 nearest neighbors since this was found to perform reasonably well. The nearest neighbors in the training set were always chosen based on the Euclidean distance in the embedded space which is the same as the diffusion distance in the original space. Classification accuracy of the NNS algorithm applied to MDT data is shown in Tables 2 and 3. The classification accuracy is evaluated with confusion matrices showing the probability of *true-positive* labeling and *false-positive* labeling. Different confusion matrices are shown for 10-feature and 8-feature classifiers. The 10-feature classifier uses all 10 features including WCQI and PHR for the dimensionality reduction as described in (1), whereas the 8-feature classifier uses only UE reported RSRP and RSRQ values. Diagonal cells of the confusion matrices show the true-positive probability indicating the likelihood that a sample is correctly labeled to the same class it belongs. The false-positive likelihood indicates the probability for the samples to be labeled to a wrong class. This kind of comparison is easy to do since we know the real labels of the data. The number inside the parenthesis of the real class column indicates the total amount of the different sample types in simulations and confusion matrices showing how these samples were labeled by the different classifiers.

Table 2 shows the reference simulation labeling accuracy for all MDT samples. It can be seen that the true-positive-labeling likelihood of the reference data is more than 80% for all class types regardless of the used classifier. The 10-feature classifier performs better but the performance of 8-feature classifier is not much worse either. One should note that we do not try to achieve 100% classification accuracy since it is quite likely that some of the periodical, handover, and radio link failure samples would have similar kind of characteristics in any case. Periodical samples are collected in a periodical manner, and therefore, the samples preceding a handover or a radio link failure event are assumed to have similar kind of characteristics. It is worth noting that handovers occur at the cell edge, and depending on the handover parameters and the slow fading conditions some handovers can have similarities with radio link failures.

Classification quality of the MDT samples from the problem and reference simulation is approximately the same as shown in Table 3. Classification accuracy of the 10-feature classifier remains better in the problem scenario as well. There is a small change of 0.8% in handover false-positive labeling but that is negligible since the number of handover samples is only 683 meaning 8 samples were classified differently. A small change in periodical sample false-positive-labeling probability is observed as well. In the problem simulation, the 10-feature classifier labels 0.9% of the periodical samples to radio link failures. This is almost two times higher than in the reference simulation. However, this small difference of 0.4% is significant since the number of periodical samples in the problem simulation MDT database is huge that is, 148693 samples. This means that 1338 additional RLF-like samples were found from the set of periodical MDT samples indicating outage. This is 537% more samples than the 210 true RLFs detected in the problem scenario. If the 8-feature classifier is used the difference is same. However, the classification accuracy is slightly lower, and therefore the total number of RLF-labeled samples is higher in the reference and the problem simulation. On the other hand, the 8-feature classifier can be applied to the interfrequency measurements directly, since it does not use CQI or PHR measurements for the outage detection.

The final goal in the outage detection is to associate RLF-labeled samples with base stations. Generally, MDT samples with detailed location information are reported with latitude and longitude values and rest of the samples can be located based on the RF fingerprint of the MDT measurement. Recall that if only GCI of the serving cell would be used, the detected samples in the dominance area of malfunctioning eNB would be associated with neighboring cells leading to misjudgments. Our assumption is that majority of samples can always be located at least with the accuracy of the dominance area for example, an estimate of the strongest serving cell is known for each sample based on the operators estimate of the dominance areas. In urban network deployments, the definition of dominance areas can become ambiguous due to buildings, street layout, and slow fading. However, since the MDT is used to enhance the network coverage maps, it is assumed that dominance area estimates can be improved in urban environment as well. Therefore, it is

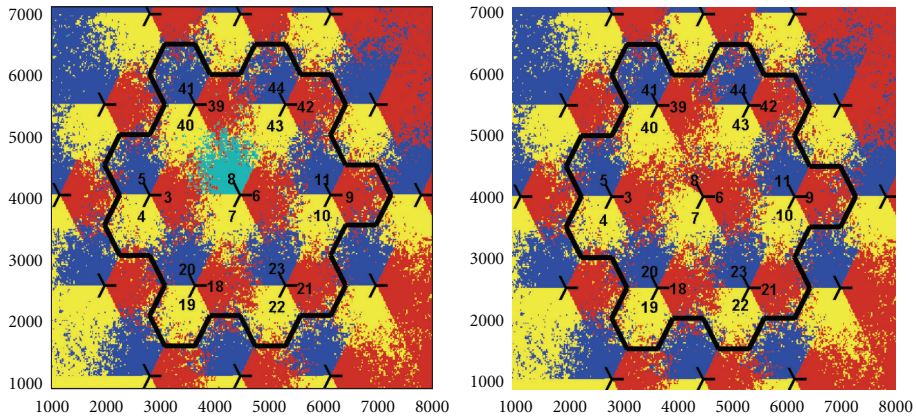

(a) Reference simulation (b) Problem simulation

Figure 4: Network dominance areas.

Table 2: Reference simulation confusion matrices.

Real class	8 features (only RSRP and RSRQ)			10 features (with CQI and PHR)		
	Per.	HO	RLF	Per.	HO	RLF
Periodical (148723)	96.4%	2.9%	0.7%	96.6%	2.9%	0.5%
Handover (698)	11.9%	82.1%	6.0%	11.8%	83.0%	5.2%
Radio link failure (138)	0.0%	0.0%	100%	0.0%	0.0%	100%

assumed that if the MDT measurements bear the detailed location, the correlation with the dominance areas is not an issue. However, if one of the cells is missing, the positioning and correlation with the RF fingerprint databases could be challenging and even lead to wrong conclusions. In this paper, the inaccurate RF fingerprint positioning is not taken into account, and the results rely on the availability of the MDT reports with detailed location information, that is, latitude and longitude. In Figure 5, the normalized RLF-labeling results from the reference simulation are depicted for all base stations. The RLF-labeled samples are associated with the base stations according to the estimated dominance areas. Blue color refers to periodical samples, green color refers to handover samples, and red color refers to RLF samples which are labeled as radio link failures. The results are normalized with the total number of RLF-labeled samples in the reference scenario. There are a few radio link failures occurring in the reference scenario and only 3% of all RLF-like samples were detected to occur at the dominance area of the eNB 8. These RLFs in the reference scenario are due to the long intersite distances between the base stations and slow-fading effect especially in eNBs 6, 18, and 43.

Based on all RLF-labeled samples, a standard score for each base station is calculated by using (8). The standard score can be used as a simple indicator to detect if eNB behavior is normal or not since it takes into account the statistical variability of the RLF-labeled samples per base station during normal network operation. In Figure 6, standard-score distributions in reference scenario are shown

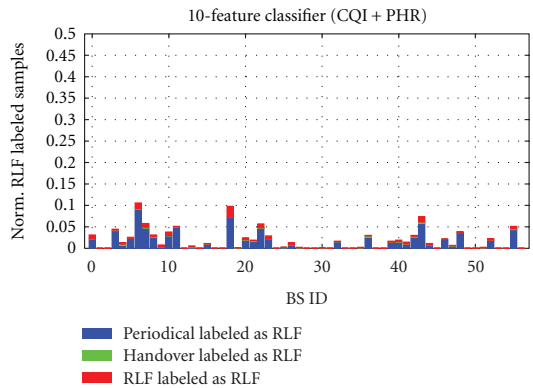

Figure 5: RLF-labeled samples per base station in reference simulation.

for 8-feature classifier with turquoise line and 10-feature classifiers with black-dashed line. Distributions are similar for both classifiers, and 95% of the eNBs have a standard score smaller than two.

The RLF-labeling results in the problem simulation are normalized in a same way as the reference simulation results. After triggering the sleeping-cell problem, the increase in the number of RLF-labeled samples is significant. Figure 7 shows that almost 40% of all RLF-labeled samples were associated

Table 3: Problem-simulation confusion matrices.

Real class	8 features (only RSRP and RSRQ)			10 features (with CQI and PHR)		
	Per.	HO	RLF	Per.	HO	RLF
Periodical (148693)	96.0%	2.9%	1.1%	96.2%	2.9%	0.9%
Handover (683)	13.3%	79.9%	6.8%	12.7%	81.4%	5.9%
Radio link failure (210)	3.3%	0.5%	96.2%	1.0%	1.0%	98.0%

Table 4: Simulator parameters.

Parameter	Notes	Value
3GPP macrocell scenario	Regular cell layout	57 sectors/19 BSs
Intersite distance		1.75 km
Distance-dependent path loss	Macro cell model [20]	$128.1 + 37.6 \log_{10}(R_{\text{km}})$
BS Tx power		46 dBm
Slow-fading standard deviation		8 dB
Slow-fading correlation		Site 0.5/Sector 1.0
Fast-fading profile		Typical Urban
UE velocity		3 km/h
UE placement	Uniformly distributed	7 centremost sites
RSRP/RSRQ Measurements	RSRP measurement period	40 ms
	L1 averaging window size	200 ms
	L3 filter coefficient	4
MDT reporting	Periodicity	500 ms
Handover parameters	A3 event threshold	3
	A3 event time to trigger	160 ms
	Handover preparation time	50 ms
Radio link failure monitoring	Qout threshold	−8 dB
	Qin threshold	−6 dB
	T310 timer	600 ms
Number of calls per simulation		4200
Base-stations loading	Full loading in all cells	100% RBs loaded
Diffusion parameter epsilon in (8)	Scales the size of local neighborhood	8
Embedded space dimension	Number of right eigenvectors	6

with the eNB 8 dominance area whereas it was only 3% in the reference scenario. Moreover, it was observed that the total number of RLF-labeled samples is higher for the 8-feature classifier since more periodical samples are labeled as RLFs due to slightly worse classification accuracy. Only 36% of the all RLF-labeled samples were associated with eNB 8 in this case. This indicates that both classifiers detect periodical measurements which are similar with the radio link failures. Moreover, eNB 8 standard score is 26.2 for the 10-feature classifier and 25.2 for the 8-feature classifier. This means that both classifiers detect anomalous network behavior since the standard score is much larger than two-indicating outage. However, the 10-feature classifier is able to isolate the problem from the reference simulation better since the standard score is larger and more RLF-labeled samples were associated with the malfunctioning eNB 8. This indicates that by using CQI and PHR metrics in the classification the outage detection can be improved. On the other hand, the 8-feature classifier can also detect the problem but since it does not depend on the CQI and PHR it can be applied to the interfrequency measurements as well. However, the verification of the interfrequency layer outage is not done in this paper.

Note that UEs in the problem scenario would not detect the presence of the eNB 8. Hence, the existence of the location information and correlation with the dominance information helps to build a better understanding of the root cause and location of the problem. The locations of the RLF-labeled samples in the map grid are illustrated in Figure 8. The simulation area was divided to 42×48 meters rectangular map grid points. The number of the RLF-labeled samples were counted for each grid point, and a heat map was used to visualize the likelihoods of the RLF-labeled samples in the estimated dominance area

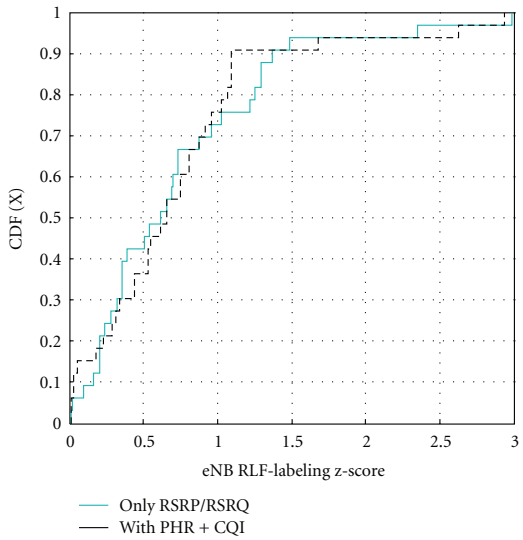

Figure 6: Standard-score distributions for reference simulation.

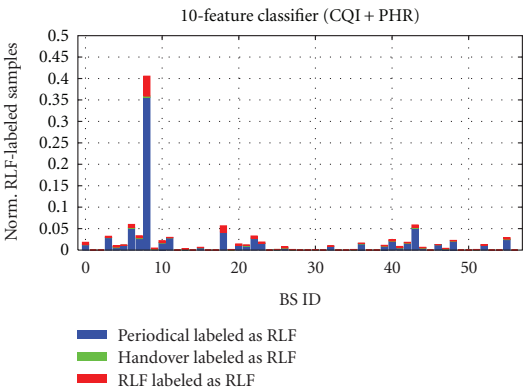

Figure 7: RLF-labeled samples per base station in problem simulation.

map. A gray color indicates areas in the heat map which might have some outage for example, when approaching a coverage hole, and a bright red color indicates areas where outage is detected. Figure 8(a) shows the heat map for the reference simulation together with estimated dominance areas, and it can be seen that some outage regions at the cell edges do exist due to the slow fading and large ISD between the sites. Figure 8(b) shows the heat map for problem simulation indicating clearly higher likelihood for the outage on the eNB 8 area compared with the reference simulation. It can be seen that the increased likelihood of RLF-labeled samples indicates the change on the dominance areas.

4.3. Anomaly Detection Time. Since anomaly detection is based on the increase in the number of periodical measurements classified as RLF samples, the detection time was analyzed by observing amount of reported samples instead of actual detection time. The amount of reported samples is a better metric, since time needed to gather a sufficient amount of samples for detection depends on the number of active users, user distribution, and MDT configuration, for example, periodicity of the measurements. Average base-station specific z-score metric before and after occurrence of the problem in eNB 8 is depicted in Figure 9.

In Figure 9, the colored curves depict how z-score metric behaves during system simulations in case 10-feature classifier is used. The x-axis indicates the average number of all received MDT reports per eNB, while the simulations advance. The y-axis indicates the eNB z-score as in (8). The z-score values were updated every five seconds but mean and standard deviation values were kept constant according to the reference simulation. Figure 9 indicates that if the observation window is too short, then anomalous base stations are not detected. In the reference simulation before the problem, approximately 3000 MDT samples per eNB are needed until some minor outage is detected. Solid green curve and dotted red curve indicate some outage in eNB 6 and eNB 18. The detection time in this case would depend on the average number of UEs per eNB, their movements in the eNB dominance area, and the periodicity of the MDT reports. For example, if 10 uniformly distributed UEs are sending MDT reports with periodicity of 0.5 second, then the detection for example, reception of 3000 samples, would take 2.5 minutes. The problem triggers after 4500 MDT reports per eNB are received. The eNB z-scores are cleared, and detection is restarted as well. Shortly after triggering the problem, eNB 8 starts to stand out from the statistics. Blue curve indicates that the z-score for eNB 8 is already more than 10 after reception of 1500 MDT reports per eNB. Moreover, purple curve shows that eNB 43 z-score increases from 2 to 3 due to the sleeping cell. This indicates that outage increases slightly in the dominance area of eNB 43 due to the problem in eNB 8. For the eNBs 6 and 18, the outage remains similar.

5. Conclusion

This paper described a data-mining framework which is capable of detecting network outage and sleeping cells in a cellular network by using drive testing databases. The framework is cognitive since it adapts to the deployed network configuration and topology by learning the network characteristics while gathering the training data for the problem classifier. In addition, the described outage detection framework works in a self-organizing manner since it uses the E-UTRAN minimization of drive testing functionality to gather the training and testing databases. The essence of the method is to label unknown data by finding similar characteristics from the previously known network data. For this purpose, diffusion maps dimensionality reduction and nearest neighbors data classification methods were utilized.

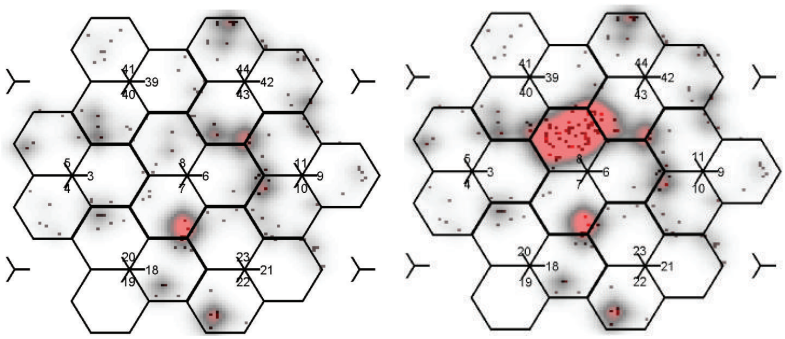

(a) Reference simulation (b) Problem simulation

Figure 8: RLF-labeled samples on the map grid.

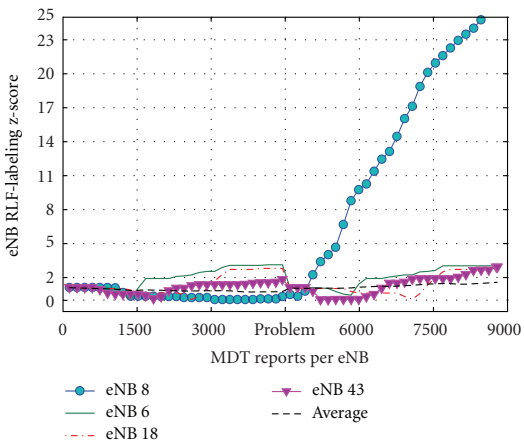

Figure 9: Average eNB z-score before and after problem triggering in eNB 8.

The presented approach is robust since the same principle utilized here can be used for a wide range of different network problems where the problem data can be isolated and used later as known problem classifiers.

In the case of the sleeping cell problem, the detection is based on finding periodical measurements which have similarities with the radio link failures. In the studied verification case, the algorithm gains 537% in the number of samples which can be used for the outage detection in addition to the real radio link failure reports. This makes detection more reliable and possibly faster compared with the algorithms which are based purely on the reported RLF events. Although our approach clearly helps to detect the outage situations by taking into account the periodical samples, there are still some drawbacks in this framework which needs to be solved in the practical deployments. First of all, our approach detects sleeping cells based on the outage present in the dominance areas of the sleeping cell. However, in denser networks, the outage might be less severe and the neighboring base stations can serve the users in the dominance area of sleeping base station without a significant increase of the radio link failures. Moreover, since the typical live networks consist of several overlapping frequency layers, then radio link failures in one layer can be avoided by handing UEs over to another frequency layer. In such situations, the framework could be extended to take into account additional features such as loading level of the cells, the handover activity, or the interfrequency layer measurements. These features together with the change in dominance areas could eventually result in a more comprehensive solution to the sleeping-cell problem. However, one advantage of the presented framework is indeed the robustness due to the dimensionality reduction step. This is a stepping stone for future research allowing an easy inclusion of new features in case of different anomaly detection studies.

Acknowledgments

The authors would like to thank Amir Averbuch and Gil David from Tel Aviv University for their support with the knowledge mining. Moreover, they would like to thank *Renesas Mobile Europe* for use of their system simulator since the work could not have been done without it. In addition, constructive criticism, comments, and support from the colleagues at Magister Solutions Ltd., University of Jyväskyläm and the Radio Network Group at Tampere University of Technology were extremely valuable during the work.

References

[1] 3GPP TS 36.902, "Evolved Universal Terrestrial Radio Access Network (E-UTRAN), Self-Configuring and Self-Optimizing Network (SON) Use Cases and Solutions," v.9.3.1, March 2011.

[2] NGMN Alliance, "Next Generation Mobile Networks Use Cases related to Self Organising Network, Overall Description," v.2.02, December 2008.
[3] 3GPP TR 36.805, "Study on minimization of drive-tests in Next Generation Networks," v.9.0.0, December, 2009.
[4] 3GPP TS 37.320, "Radio measurement collection for Minimization of Drive Tests," v.0.7.0, June 2010.
[5] 3GPP RP-111361, "Enhancement of Minimization of Drive Tests for E-UTRAN and UTRAN—Core Part Approval," Nokia Siemens Networks, Nokia, MediaTek, 2011.
[6] 3GPP TS 32.422, "Subscriber and equipment trace, Trace control and configuration management," v.11.0.1, September 2011.
[7] 3GPP TS 36.331, "Evolved Universal Terrestrial Radio Access (E-UTRA), Radio Resource Control (RRC), Protocol specification," v.10.4.0, December 2011.
[8] M. Amirijoo, L. Jorguseski, T. Kürner et al., "Cell outage management in LTE networks," in *Proceedings of the 6th International Symposium on Wireless Communication Systems (ISWCS '09)*, pp. 600–604, Siena, Italy, September 2009.
[9] M. Amirijoo, L. Jorguseski, R. Litjens, and R. Nascimento, "Effectiveness of cell outage compensation in LTE networks," in *Proceedings of the IEEE Consumer Communications and Networking Conference (CCNC '11)*, pp. 642–647, Las Vegas, Nev, USA, January 2011.
[10] J. Han and M. Kamber, *Data Mining: Concepts and Techniques*, Morgan Kaufmann, 2000.
[11] S. B. Kotsiantis, D. Kanellopoulus, and P. E. Pintelas, "Data Preprocessing for Supervised Learning," *International Journal of Computer Science*, vol. 1, no. 2, pp. 111–117, 2006.
[12] F. Chernogorov, J. Turkka, T. Ristaniemi, and A. Averbuch, *Detection of Sleeping Cells in LTE Networks Using Diffusion Maps*, VTC Spring, Budapest, Hungary, 2011.
[13] C. M. Mueller, M. Kaschub, C. Blankenhorn, and S. Wanke, "A cell outage detection algorithm using neighbor cell list reports," in *Proceedings of the International Workshop on Self-Organizing Systems*, pp. 218–229, 2008.
[14] 3GPP TS 36.214, "Evolved Universal Terrestrial Radio Access (E-UTRA); Physical Layer; Measurements," v.10.1.0, March 2011.
[15] J. Turkka and J. Puttonen, "Using LTE power headroom report for coverage optimization," in *Proceedings of 74th IEEE Vehicular Technology Conference (VTC '11-Fall)*, San Francisco, Calif, USA, September 2011.
[16] R. R. Coifman, S. Lafon, A. B. Lee et al., "Geometric diffusions as a tool for harmonic analysis and structure definition of data: diffusion maps," *Proceedings of the National Academy of Sciences of the United States of America*, vol. 102, no. 21, pp. 7426–7431, 2005.
[17] R. R. Coifman and S. Lafon, "Diffusion maps," *Applied and Computational Harmonic Analysis*, vol. 21, no. 1, pp. 5–30, 2006.
[18] B. Nadler, S. Lafon, and R. R. Coifman, "Diffusion maps, spectral clustering and eigenfunctions of fokker-planck operators," in *Advances Neural Information Processing Systems*, vol. 18, pp. 955–962, 2005.
[19] A. Schclar, "A diffusion framework for dimensionality reduction," in *Soft Computing For Knowledge Discovery and Data Mining*, chapter IV, pp. 315–325, 2008.
[20] 3GPP TS 36.814, "Further advancements for E-UTRA physical layer aspects (Release 9)," v.9.0.0, March 2010.
[21] H. He and E. A. Garcia, "Learning from imbalanced data," *IEEE Transactions on Knowledge and Data Engineering*, vol. 21, no. 9, pp. 1263–1284, 2009.
[22] R. C. Holte, L. Acker, and B. W. Porter, "Concept learning and the problem of small disjuncts," in *Proceedings of the International Joint Conference on Artificial Intelligence*, pp. 813–818, 1989.

Publication 6

Positioning in Heterogeneous Small Cell Networks using MDT RF Fingerprints

by

Riaz Uddin Mondal, Jussi Turkka, Tapani Ristaniemi and Tero Henttonen,

in *Proc. of the First IEEE International Black Sea Conference on Communications and Networking*, July 2013, Batumi, Georgia, (Invited paper).

Publication 7

Performance Evaluation of MDT Assisted LTE RF Fingerprinting Framework

by

Riaz Uddin Mondal, Jussi Turkka, Tapani Ristaniemi and Tero Henttonen,

in *Proc. of 7th International Conference on Mobile Computing and Ubiquitous Networking (ICMU2014),*
January 2014, Singapore.

Publication 8

Self-optimization of LTE Mobility State Estimation Thresholds

by

Jussi Turkka, Tero Henttonen and Tapani Ristaniemi

In *Proc. of IEEE International Conference on Wireless Communications and Networking, Workshop on Self-Organizing Networks (SONET)*,
April 2014, Istanbul, Turkey.

Tampereen teknillinen yliopisto
PL 527
33101 Tampere

Tampere University of Technology
P.O.B. 527
FI-33101 Tampere, Finland

ISBN 978-952-15-3332-7
ISSN 1459-2045